Intracellular *rols7* mRNA localization and the importance of Barren for mitosis in the embryonic myogenesis of *Drosophila melanogaster*

Dissertation

zur

Erlangung des Doktorgrades

der Naturwissenschaften

(Dr. rer. nat.)

dem

Fachbereich Biologie

der

Philipps-Universität Marburg

vorgelegt von

Matthias Philipp Florian Jacobs

aus Marburg an der Lahn

Marburg / Lahn 2018

Vom Fachbereich Biologie der Philipps-Universität Marburg als Dissertation angenommen am 09.04.2018

Erstgutachterin: Prof. Dr. Renate Renkawitz-Pohl

Zweitgutachter: Prof. Dr. Christian Bökel

Tag der mündlichen Prüfung: 24.04.2018

Parts of this study were published in:

A. Rudolf, D. Buttgereit, M. Jacobs, G. Wolfstetter, D. Kesper, M. Pütz, S. Berger, R. Renkawitz-Pohl, A. Holz and S. Önel:

Distinct genetic programs guide *Drosophila* circular and longitudinal visceral myoblast fusion.

BMC cell biology, 15:27, 2014. doi:10.1186/1471-2121-15-27.

Zusammenfassung

Die Körperwandmuskulatur der Larve von *D. melanogaster* ist ein hochgradig geordnetes System von quergestreiften Muskelfasern, die durch die Fusion von Myoblasten entstehen, ähnlich den Skelettmuskelfasern der Wirbeltiere. In der vorliegenden Arbeit wird die Embryonalentwicklung dieser Muskeln als genetisches Modellsystem für Myogenese, Muskelregeneration und verwandte Prozesse genutzt.

Rols7 ist ein wichtiges Protein in der Signalkette, die die zur Myoblastenfusion notwendige Verzweigung der Aktinfilamente steuert. In den somatischen Muskelgründerzellen ist die *rols7*-mRNA in einem oder mehreren Flecken nahe der Zelloberfläche lokalisiert.

Die vorliegende Arbeit zeigt, dass zur Lokalisation des rols7-Transkriptes der 3'-untranslatierte Bereich notwendig ist. Eine Reporter-mRNA, die sowohl diese Trailer-Region als auch den 5'-untranslatierten Bereich trägt, wird selbst in Abwesenheit von nativem *rols*-Transkript in einer Weise intrazellulär lokalisiert, die identisch mit dem wildtypischen Muster zu sein scheint.

Es wird gezeigt, dass die *rols7* mRNA auch in den Gründerzellen der zirkulären und longitudinalen visceralen Muskeln intrazellulär lokalisiert wird; in letzteren sammelt sie sich in Flecken in der Nähe der Spitzen der spindelförmigen Zellen, nahe den zu erwartenden Fusionspunkten. Zumindest für diesen Zelltyp kann daher vermutet werden, dass die Lokalisierung der *rols7* mRNA die Lokalisierung des Rols7-Proteins und damit die Myoblastenfusion vorbereitet.

Auf der Suche nach neuen myogeneserelevanten Faktoren wird der Muskelphänotyp der EMS-induzierten Mutante E831 analysiert. Als Grund für die chaotische Anordnung der embryonalen Körperwandmuskeln der Mutante wird eine Nonsens-Mutation der Condensin-Untereinheit *barren* identifiziert. *Cap-G*, eine andere Condensin-Untereinheit, zeigt einen sehr ähnlichen Phänotyp.

Während sowohl Gründerzellen als auch fusionskompetente Myoblasten in einer *barren*-Mutante offenbar korrekt determiniert werden, ist das Expressionsmuster der Muskelidentitätsgene in einer Weise gestört, die mit den chaotischen Störungen der Muskelanordnung korreliert.

Der Condensin-Komplex erfüllt in jeder Zelle eine Reihe unterschiedlicher essentieller Aufgaben. Um zu klären, ob der Muskelphänotyp mit der regulatorischen Rolle von Condensin während der Interphase oder mit seiner Funktion bei der Chromosomentrennung während der Zellteilung zusammenhängt, muss der Zeitpunkt bestimmt werden, an dem das Barren-Protein in der Muskulatur benötigt wird. Zu diesem Zweck wird ein *barren*-Rettungskonstrukt mit dem Gal4-UAS-System exprimiert.

Gal4-Treiber retten den Phänotyp nur, wenn sie Barren deutlich vor der letzten Zellteilung exprimieren, bei der die Muskelgründerzellen entstehen. Dieses Ergebnis legt nahe, dass der Phänotyp durch einen mitotischen Defekt bedingt ist. Der Mechanismus, der den Identitätsverlust der Muskeln auslöst, erinnert an die genomische Instabilität von Krebszelllinien.

Summary

The body wall musculature of the *D. melanogaster* larva is a highly ordered assembly of striated myotubes that are formed by fusion of myoblasts, much like the skeletal muscle fibres of vertebrates. In this study, the embryonic development of this musculature is used as a genetic model system for myogenesis, muscle regeneration and related processes.

Rols7 is a crucial protein in the signal transduction chain that controls the Actin filament branching necessary for myoblast fusion. In somatic muscle founder cells, the *rols7* mRNA shows intracellular localization into one or more patches near the cell surface. This thesis demonstrates that the *rols7* transcript's 3' untranslated region is necessary for its localization. A reporter mRNA with this trailer region as well as the 5' untranslated region gets intracellularly localized in a way seemingly identical to the wild type pattern, even in the absence of native *rols* transcripts.

The *rols7* mRNA is shown to be intracellularly localized in the circular and longitudinal visceral muscle founder cells as well; in the latter it forms spots close to the tips of the spindle-shaped cells, near the expected sites of cell-cell fusion. At least for this latter cell type it can be suspected that *rols7* mRNA localisation facilitates protein localisation and eventually myoblast fusion by preforming the Rols7 protein's distribution pattern.

In search of previously unknown factors involved in myogenesis, the muscle phenotype of the EMS-induced mutant line E831 is analyzed. As the cause for the disturbed arrangement of the embryonic body wall musculature a nonsense mutation of the Condensin subunit *barren* is identified. *Cap-G*, another Condensin subunit, is found to show a phenotype very similar to that of *barren*.

While in a *barren* mutant both muscle founder cells and fusion competent myoblasts seem to get specified, muscle identity genes are expressed irregularly in a manner that corresponds to the perturbation of the muscle pattern.

In every cell, the Condensin complex fulfills a variety of essential functions. To help clarify whether the muscle phenotype is connected to Condensin's regulatory role during interphase or its function in chromosome segregation during mitosis, the time point at which Barren is needed in the musculature has to be identified. To this end, the Gal4-UAS system is used to express a *barren* rescue construct.

Gal4 drivers are found to rescue the phenotype only if they express Barren considerably before the final cell division that gives rise to the muscle founder cells. This finding suggests that the muscle phenotype is caused by a mitotic defect. The mechanism behind the loss of muscle identity appears to be a phenomenon related to the genomic instability of cancer cell lines.

Contents

Chapter 1

Introduction

D. melanogaster is a convenient model organism for genetic research due to its simple and inexpensive cultivation, short generational time, numerous offspring and compact, low-redundancy genome in only 4 chromosomes. An additional advantage is the long tradition of *Drosophila* use in genetic research; a large collection of mutants is available, including "balancer" chromosomes that carry large inversions, suppressing meiotic crossing over and thus allowing recessive lethal alleles to be kept as stable stocks. *Drosophila* was the first metazoon whose germ line could be genetically modified (Rubin and Spradling 1982; Spradling and Rubin 1982). The sequence of the *Drosophila* genome was published in 2000 (Adams et al. 2000; Myers et al. 2000).

Drosophila embryos are accessible in their eggs with relative ease and develop from egg laying to hatching within a day. Morphological and anatomical changes during development are easily visible under a microscope; this allows to define developmental stages numbered from 1 to 17, with the egg usually beeing layed around stage 5 and the larva hatching after completion of stage 17 (see Appendix C, p. 136).

The highly regular, segmentally repeated pattern of larval body wall muscles makes deviations and alterations of the musculature easy to spot in the fly embryo; the developing musculature can be made visible for example with an antibody stain against β3Tubulin, a protein that is expressed quite specifically in muscles (Fig. 1.1).

Like the skeletal muscle fibres of vertebrates, *Drosophila* body wall ("somatic") myotubes are striated, multi-nucleated syncytia, arising from the fusion

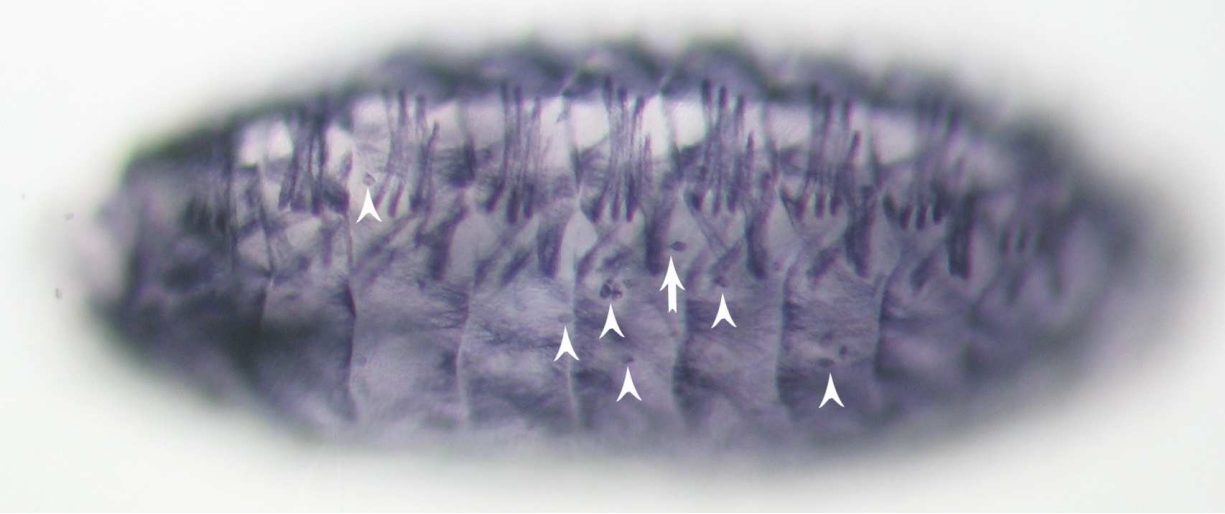

FIGURE 1.1. An immunohistochemical stain using anti-β3Tubulin antibody visualizes the somatic musculature of this early stage 17 embryo. Myogenesis is drawing to a close, with most muscles attached to their apodemes and only a few unfused myoblasts left (arrowheads); one can be seen stretching its filopodium towards a myotube (arrow). Every segment has the same muscle pattern, with little variation in the three thoracic segments and the first abdominal segment, and no variation in the abdominal segments 2–7. All embryos are depicted in standard orientation: anterior is to the left, dorsal is up.

of myoblasts. The process of myogenesis and muscle regeneration in vertebrates has been shown to share many of the components and mechanisms involved in *Drosophila* myogenesis (WAKELAM 1985; MAQBOOL AND JAGLA 2007; SRINIVAS ET AL. 2007; MOORE ET AL. 2007). However, while a vertebrate muscle is comprised from several myotubes, a larval *Drosophila* muscle is made up from only one myotube.

These traits and the aforementioned advantages make *Drosophila* a valuable model system for studying the mechanisms of myogenesis, helping to understand vertebrate development and human diseases like muscle dystrophies.

1.1 Embryonic myogenesis in *Drosophila*

1.1.1 Determination of myoblasts

On the ventral surface of the early embryo, the prospective mesoderm is designated by expression of the transcription factors *twist*, *snail* and *Mef2* (Simpson 1983; Anderson and Nüsslein-Volhard 1984; Boulay et al. 1987; Thisse et al. 1988; Nguyen et al. 1994). These ventral cells invaginate during gastrulation, first forming a tube along the embryo, then loosing their epithelial character; then they reassemble into a monolayer under the ectoderm (Leptin and Grunewald 1990).

This mesodermal cell layer is then further subdivided along the dorsoventral axis by the dorsal expression of *decapentaplegic (dpp)*, and along the anterior-posterior axis by the segmentally repeated expression of segment polarity genes (see Fig. 1.2). Domains with little *dpp* and *even-skipped (eve)*, but high levels of *sloppy-paired (slp)* retain strong *twist* expression, resume *Mef2* expression and develop into somatic musculature (Nguyen et al. 1994; Lilly et al. 1994; Baylies and Bate 1996; Riechmann et al. 1997).

From stage 10 on, Dpp and the *wingless (wg)* pathway in cooperation with various muscle identity genes (reviewed in Tixier et al. 2010) trigger *lethal of scute (l'sc)* expression in cell clusters in the high-Twist domains of each segment (Carmena et al. 1995, 1998). This expression of *l'sc* then gets narrowed down by the EGFR-Spitz pathway (Buff et al. 1998) until one muscle progenitor cell is singled out from the cluster via the Notch-Delta pathway (Baker and Schubiger 1996; Rusconi and Corbin 1998); all other cells become fusion competent myoblasts (FCMs).

FCMs are characterized by expression of the transcription factor *lame duck (lmd)* (Duan et al. 2001). Some of them undergo a final mitosis at stage 12-13 before beginning to fuse (Beckett and Baylies 2007). They present the Immunoglobin super family (IgSF) proteins Sticks and Stones (SNS) and Hibris (Hbs) on their membrane (Bour et al. 2000; Dworak et al. 2001; Artero et al. 2001).

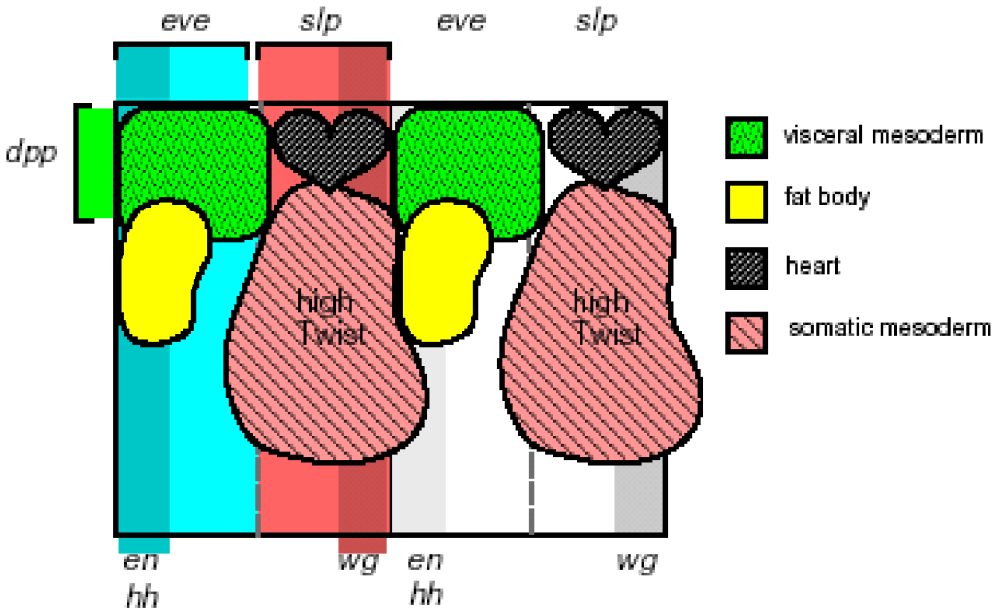

FIGURE 1.2. Subdivisions of the mesoderm at stage 9–10, in schematic lateral view; dorsal is up, anterior to the left. High levels of Slp in combination with low levels of Dpp and Eve specify segmental domains of high Twist expression, which give rise to the somatic musculature. Modified after RIECHMANN ET AL. 1997

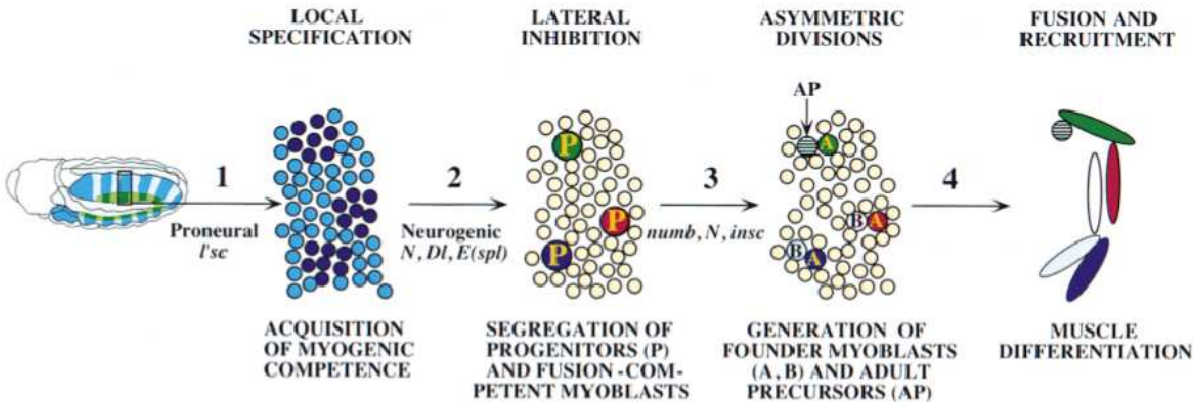

FIGURE 1.3. **1** In the segmental domains of high Twist expression (blue) the Wingless pathway, Dpp and various muscle identity genes trigger groups of cells to express lethal of scute (l'sc, dark blue). **2** Lateral inhibition via the "neurogenic" Notch-Delta pathway singles out progenitor cells from the competence clusters; all other myogenic cells become fusion-competent myoblasts (FCMs). The progenitor cells are already committed to form one specific muscle. **3** The progenitor cells go through one final wave of mitosis, giving rise to the founder cells (FCs). In one daughter cell, the Numb-Inscutable pathway modifies the previous cell fate; the other cell retains its preconceived identity. **4** The FCs fuse with FCMs and form muscles. Modified after BAYLIES ET AL. 1998.

The prospective musculature is patterned by intersecting expression domains of muscle identity genes: Each muscle progenitor cell expresses a characteristic individual subset (reviewed in Tixier et al. 2010).

At stage 12, the progenitor cells go through a final round of mitosis, during which Inscutable (Carmena et al. 1998) anchors Numb (Ruiz-Gómez et al. 1997) to the mitotic spindle so that only one cell inherits all Numb protein. Numb then inhibits the Notch pathway, modifying the expression of muscle identity genes; the other cell retains the set of muscle identity genes that the progenitor cell previously expressed.

In some cases, one daughter cell retains a high level of *twist* expression; these adult precursor cells remain dormant, undergo proliferation later in larval life and give rise to adult musculature (Bate et al. 1991).

All other daughter cells of the muscle progenitors give rise to embryonic musculature; each one of them is programmed to form one specific muscle. They are called muscle founder cells (FCs). Even if all other steps of myogenesis fail, the founder cells will still form so-called "mini-muscles" and try to attach to their respective apodemes; they carry all information necessary to form their muscle (Bate 1990; Carmena et al. 1998).

Every abdominal segment from A2 to A6 contains 30 muscle founder cells on each side.

1.1.2 Myoblast fusion

After determination, the founder cells loose *twist* expression and begin to fuse with FCMs. These fusions, however, only add cell mass; after fusion, FCM nuclei start to express the same genes as the original founder cell nucleus, and all nuclei in the myotube become indiscernible (Rushton et al. 1995; Carmena et al. 1995). In the end of the fusion process, the largest muscle contains up to 25 nuclei, the smallest 3–4 (Bate 1990).

The fusion of the nascent myotube with FCMs happens in two waves: At stages 12–13, a first wave of fusion events produces "muscle precursors" with two or three nuclei; the final number of up to 25 nuclei is reached in a second wave of fusions complete by stage 15. These two steps of accretion employ a slightly different set of genes.

Both the FCMs and the founder cells form filopodia to establish contact with each other (Bate 1990; Fig. 1.1). The chemoattraction of FCMs to the founder cells and nascent myotubes depends on Sticks and Stones (SNS) on the FCM's surface (Bour et al. 2000), and on the expression of the IgSF proteins Dumbfounded / Kin of Irregular Chiasma (Duf/Kirre) (Ruiz-Gómez et al. 2000; Dworak et al. 2001; Chen and Olson 2001) and Roughest / Irregular Chiasma C (Rst/IrreC) (Strünkelnberg et al. 2001) on the founder cell side.

The FCMs also express Rst. FCM Rst engages Rst proteins on the nascent myotube's membrane, while SNS binds both Rst and Duf (Ruiz-Gómez et al. 2000; Strünkelnberg et al. 2001).

Besides IgSF adhesion proteins, the myoblasts also present N-Cadherin (CadN) on their surface. N-Cadherin mutants do not show an aberrant muscle phenotype; however, mutants of *schizo / loner (siz)*, a negative regulator of CadN, have a massive fusion defect that is ameliorated in *siz,cadN* double mutants (Dottermusch-Heidel et al. 2012).

After cell adhesion is established, the interacting IgSF proteins clear the center of the circular contact surface between the two cells, forming a ring (Kesper et al. 2007). CadN must probably also be excluded or removed from the central part to allow fusion (Dottermusch-Heidel et al. 2012).

Upon engaging their counterparts on the opposed cell membrane, the intracellular domains of the IgSF proteins recruit Dreadlocks (Dock), an SH2/SH3 adaptor protein. Duf in the nascent myotubes additionally recruits Rolling pebbles / Antisocial (Rols/Ants) (Chen and Olson 2001; Menon and Chia 2001; Rau et al. 2001) and Siz (Bulchand et al. 2010), while SNS in the FCM also binds the SH2/SH3 adaptor protein Crk.

These proteins are the starting point of a cytoplasmic signal transduction cascade that triggers the branching of Actin filaments (Fig. 1.4).

Inside the FCM, under the circular contact surface, a dense plug of Actin filaments is formed; on the myotube side, a thinner sheet of Actin appears in the opposing position (Kesper et al. 2007; Schäfer et al. 2007; Kim et al. 2007; Massarwa et al. 2007; Richardson et al. 2007).

This circular adhesive structure with its spatially localized signal transduction chain is called the fusion-restricted myogenic adhesive structure (FuRMAS); it

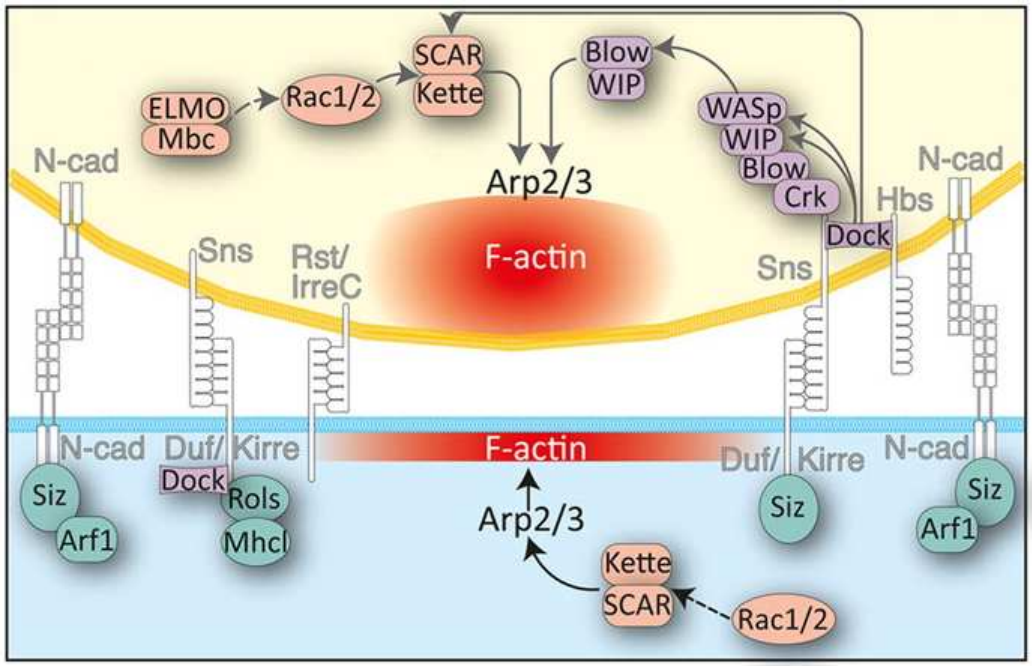

FIGURE 1.4. Signal cascades and interactions that trigger Actin filament branching, leading to myoblast fusion. Cell adhesion molecules in white. Illustration from ÖNEL ET AL. 2014.

resembles vertebrate immunological synapses, podosomes and synapses (KESPER ET AL. 2007; ÖNEL ET AL. 2014).

In the course of the fusion event, the FuRMAS widens from 1 μm to 5 μm, the diameter of an FCM KESPER ET AL. 2007; ÖNEL AND RENKAWITZ-POHL 2009. From the Actin plug on the FCM side, finger-like, Actin-filled membrane protrusions dig into the nascent myotube (SENS ET AL. 2010; DHANYASI ET AL. 2015; HAMP ET AL. 2016).

In some TEM images, electron-dense vesicles can be seen associated with the opposing membranes in both cells, aligning pairwise across the two cell membranes into what has been called the "prefusion complex". In presumably later stages of the process, the membranes take the form of electron-dense plaques (DOBERSTEIN ET AL. 1997).

It is unclear weather it is membrane stress around the Actin-filled membrane protrusions pushing into the myotube, some unknown fusogen perhaps carried in the electron-dense vesicles, or a combination of both that brings by the ultimate membrane breakdown. Some experiments imply the latter possibility:
In cultured *Drosophila* S2R$^+$ cells transfected with the *Caenorhabditis elegans*

fusogen Eff-1, which fuse at a low rate, cotransfection with *sns* or a chimeric fusion of *duf* and *Wasp-interacting protein (WIP)* triggers the formation of actinous protrusions and enhances fusion efficiency considarably (Shilagardi et al. 2013). In this experimental system, both Eff-1 and SNS localize towards the tips of the podosome-like, Actin-filled membrane protrusions, but do not strictly colocalize, remaining in separate, neighboring patches instead. Eff-1 appears as electron-dense plaques.

It is not yet known which proteins could be the native fusogens in *Drosophila* myoblast fusion; the only protein that is reckoned to be part of classical vesicle fusion machinery and that causes a fusion defect when mutant is the MARVEL-domain protein Singles Bar (Sing) (Estrada et al. 2007).

TEM images of sections of chemically fixed materials show the membrane between FCM and myotube vesicularizing at multiple sites or dissolving (Doberstein et al. 1997); newer studies, however, point out that this might be a fixational artefact, as it can also be found in juxtaposed membranes of cell types that are believed to never fuse. In sections of high pressure frozen material, seemingly only one large fusion pore per podosome-like protrusion appears (Sens et al. 2010; Dhanyasi et al. 2015; Hamp et al. 2016).

In the present study, two genes with a relevance for myogenesis are analyzed. The mechanism behind the intracellular localisation of the mRNA of *rols7* is elucidated; furthermore, a fly mutant line with a severe embryonic muscle phenotype is identified as a *barren* allel, and the role that this Condensin subunit plays in myogenesis is analyzed.

1.2 Intracellular *rols* mRNA localization

The Rolling Pebbles (Rols) protein is a central hub in the signal transduction for myoblast fusion; it is also part of the Z discs in mature myotubes (Kreisköther et al. 2006). Overexpression of the mammalian orthologue of *rols* , TANC1, is thought to be the cause of human Rhabdomyosarcoma, a cancer of myoblasts that fail to differentiate and fuse (Avirneni-Vadlamudi et al. 2012).

Rols is an intracellular adaptor protein that appears in two isoforms: Rols6, with 1670 amino acids, and Rols7, with 1900 amino acids (Rau et al. 2001).

Rols6 has 79 specific amino acids on its N terminus, which are coded by the first two exons. It is expressed in the endoderm, the Malpighian tubules and the apodemes.

rols7 has six downstream exons in common with *rols6*, plus two unique upstream exons. The second of the latter codes for 308 *rols7*-specific N-terminal amino acids. Rols7 is found in the musculature (Rau et al. 2001). In founder cells and nascent myotubes, the Rols7 protein is localized in the FuRMAS; it interacts with Duf, helping to transduce the signal for Actin sheet formation.

The *rols7* mRNA is localized in patches near the surface of the founder cells (Kesper 2005). A two kbp region including and upstream of the first exon of *rols7* is sufficient to let a reporter gene reproduce the somatic musculature expression pattern of *rols7* (Kesper 2005); however, the intracellular localization pattern of the *rols7* mRNA is not reproduced by such a construct (Kesper, personal communication).

Intracellular localization of transcripts often depends on a tertiary structure fold in the mRNA's 3' untranslated region (3' UTR); in *Drosophila* this is known for example from *hairy* (Bullock et al. 2003), *fs(1)K10* (Serano and Cohen 1995) and *bicoid* (MacDonald 1990; Macdonald and Struhl 1988). In some cases, however, localization is mediated by folding sequences in other parts of the mRNA, as in the *gurken* transcript, whose localization depends upon parts of its 5' UTR, coding region and 3' UTR at different time points (Saunders and Cohen 1999; Thio et al. 2000; Van De Bor et al. 2005).

In this study, the 3' UTR of the *rols7* transcript is assayed for its localizing activity in somatic founder cells. Furthermore, the founder cells of the visceral musculature are analyzed for *rols* transcript localization using improved *in situ* hybridisation methods.

1.3 SMC complexes and their functions

1.3.1 The SMC complexes Condensin and Cohesin

The E831 *Drosophila* mutant line, which is showing a disarrayed embryonic musculature, is speculated to host a *barren* mutant (Jacobs 2006). Barren is a member of the Kleisin protein family and a subunit of the Condensin I complex.

Condensins, as well as the closely related Cohesins, are DNA-binding protein complexes that are characterized by a core dimer of elongated SMC (Structural Maintenance of Chromosomes) proteins. These 50 nm (Hirano 2005) to 59 nm (Anderson et al. 2002) long proteins have a "hinge" domain located centrally in their polypeptide chain; to both sides of the hinge the chain forms α-helices and folds back on itself, forming an antiparallel coiled-coil stalk, bringing the N- and C-termini of the protein together to form a globular ATPase "head" that resembles an ATP binding cassette (ABC) transporter domain (Larionov et al. 1985; Notarnicola et al. 1991; Strunnikov et al. 1993; Saka et al. 1994; Saitoh et al. 1994; Michaelis et al. 1997; Melby et al. 1998). SMC proteins dimerize hinge to hinge and head to head (see Fig. 1.5, p. 22; 1.7, p. 33; Hirano and Mitchison 1994; Strunnikov et al. 1995; Hirano et al. 1997; Losada et al. 1998; Yoshimura et al. 2002; Anderson et al. 2002; Haering et al. 2002).

This SMC dimer alone can already fulfill certain functions. For other functions, a larger holocomplex must be formed: A Kleisin family protein (named for greek "kleisimo" for "closure") binds at or near the dimerized head domains, and additional non-SMC subunits bind usually to the Kleisin (Hirano et al. 1997; Losada et al. 1998; Anderson et al. 2002; Schleiffer et al. 2003).

SMC holocomplexes bind to DNA strands in a non-sequence-specific manner, likely by closing around them (Gruber et al. 2003; Ivanov and Nasmyth 2005). However, they often use a loading factor that confers a degree of sequence specifity. It consists of Scc2 and Scc4, and is sometimes called Kollerin (Michaelis et al. 1997; Furuya et al. 1998; Tóth et al. 1999; Ciosk et al. 2000; Watrin et al. 2006; Chao et al. 2015). Scc2 and most of the non-SMC non-Kleisin subunits and regulatory factors are characterized by HEAT-repeats and form a protein family defined by general structural similarity (Wells et al. 2017).

The SMC complexes and their associate proteins are fairly ubiquitous among organisms from bacteria to humans. The names they are called by have varied over time and from species to species; the nomenclature preferred in most contemporary texts is mainly derived from that of *Saccharomyces cerevisiae*. For easier understanding of the literature referenced here, some of the various synonyms are listed in Table 1.1.

Several more variants of SMC complex exist beside the already mentioned: The Condensin-like Dosage Compensation Complex of *C. elegans*, the homodimeric bacterial SMC complexes, the eukaryotic SMC5-SMC6 complex with non-SMC subunits that resemble the bacterial ones, and the Rad50 DNA repair complex, which matches the general structure of a SMC complex but has a differently built "hinge". All these will be omitted here, as they are beyond the scope of this study.

TABLE 1.1. Homologues and Synonyms of SMC complex components and associated proteins in various species

General name in this text	**Protein class**	**Drosophila Ortholog (abbreviated)**	**Other synonyms**	**Obsolete names**
Scc2	SMC loader / Kollerin component – HEAT repeat	Nipped B	NIPBL, DeLangin	
Scc4	SMC loader / Kollerin component		Mau2	
SMC2	Condensin SMC subunit		Cap-E	Sc2
SMC4	Condensin SMC subunit	Gluon (Glu)	Cap-C	
Cap-H	Condensin I non-SMC subunit – γ-Kleisin	Barren (Barr)		
Cap-G	Condensin I non-SMC HEAT-repeat subunit			

General name in this text	*Protein class*	*Drosophila Ortholog (abbrev.)*	*Other synonyms*	*Obsolete names*
Cap-D2	Condensin I non-SMC HEAT-repeat subunit			
Cap-H2	Condensin II non-SMC subunit – β-Kleisin			
Cap-G2	Condensin II non-SMC HEAT-repeat subunit			
Cap-D3	Condensin II non-SMC HEAT-repeat subunit			
Topo II	Topoisomerase type II	Top2		Sc1
SMC1	Cohesin SMC subunit		Cap-C	
SMC3	Cohesin SMC subunit	Cap		SMC2
Scc1	Mitosis specific Cohesin non-SMC subunit – α-Kleisin	Verthandi (Vtd)	Mcd1, Rad21	
Rec8	Meiosis specific Cohesin non-SMC subunit – α-Kleisin			
Scc3	Cohesin regulator – HEAT repeat	Stromalin/ Stromalin2 (SA/SA2)	STAG1/STAG2	
Pds5	Cohesin regulator – HEAT repeat			
Wapl	Cohesin regulator – helical repeat	Wings apart-like (Wapl)	Wpl1, WAPAL	
Sororin	Cohesin regulator	Dalmatian		
Shugoshin (Sgo)	Cohesin regulator	Shugoshin-like (Sgol)		

1.3.2 The Condensin complex

Molecular composition and DNA binding mechanism

Condensins are pentameric complexes that are characterized by the SMC proteins SMC2 and SMC4 (Saitoh et al. 1994; Hirano et al. 1997). This SMC dimer alone is called 8S Condensin, referring to its sedimentation coefficient of 8 Svedberg (Hirano et al. 1997). It is able to bind both single stranded DNA (ssDNA) and double stranded DNA (dsDNA), probably with its "hinge" region (Yoshimura et al. 2002; Sakai et al. 2003).

The SMC dimer can bind a Kleisin protein and two other non-SMC subunits at its "head" region to form 13S Condensin (Hirano et al. 1997; Anderson et al. 2002; Yoshimura et al. 2002). This holocomplex associates with DNA probably by closing around the strands and encircling them, with the two SMCs topologically forming a "ring" (Cuylen et al. 2011).

However, in electron microscopic and atomic force microscopic images, Condensin appears more rod-shaped than ring-like, probably because of the elongated SMC subunits being straight and oriented in parallel in the complex (Anderson et al. 2002). Moreover, seemingly the SMCs' coiled-coil regions can bend around, possibly bringing the hinge region into contact with the head (Fig. 1.5; Yoshimura et al. 2002; Anderson et al. 2002).

It is not clear whether the SMC complex loading factor Scc2-4 is necessary to load Condensin onto DNA. In Scc2-4 mutants, overall levels of Condensin binding to chromosomes are reduced by about 50%; however, Condensin binding still happens, and no physical interaction between Scc2-4 and Condensin could be proven (D'Ambrosio et al. 2008b).

The longest-known form of the complex, Condensin I, contains the non-SMC subunits Cap-D2, Cap-G, and the Kleisin Cap-H, which is called Barren (Barr) in *Drosophila*. A second SMC2-SMC4 complex, Condensin II, has first been identified in HeLa cells and was shown to exist in many metazoans (Ono et al. 2003; Yeong et al. 2003). It is formed with the subunits Cap-D3, Cap-G2 and the Kleisin Cap-H2.

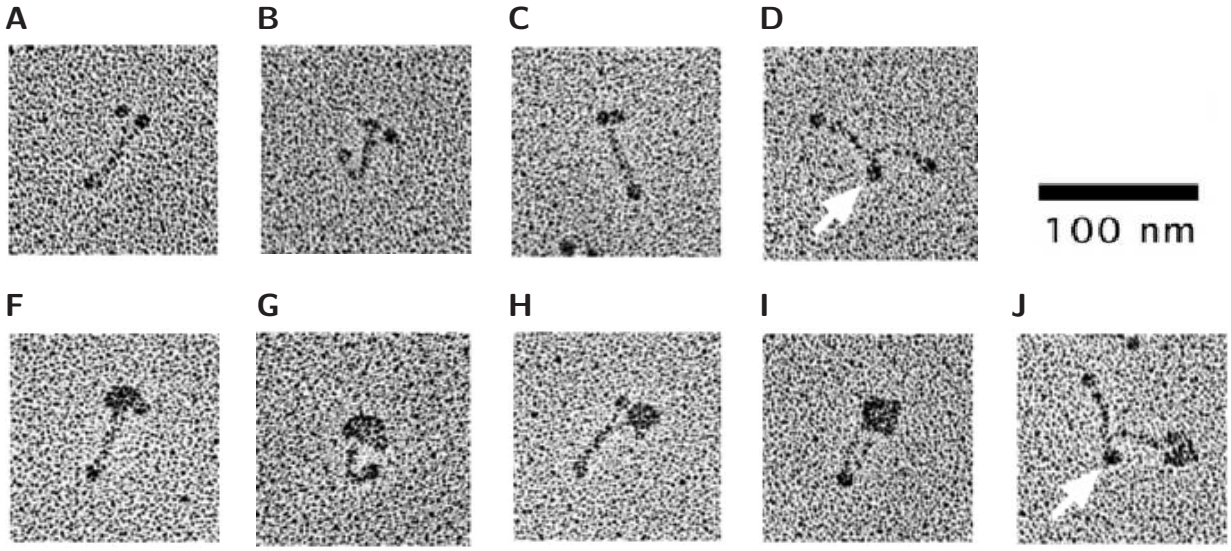

FIGURE 1.5. Electron micrographs of human Condensin, modified from ANDERSON ET AL. 2002. **A**–**D** show what presumably are SMC2-SMC4 dimers, **F**–**J** can be assumed to be pentameric holocomplexes. Shown configurations are sorted from the more abundant (left) to the less abundant (right). Frequencies of different configurations might be skewed by preparational artefacts. **A** 44% of SMC dimers split at the head end. **B** Many of these complexes bend in the coiled-coil regions. **C** 32% form a compact rod. Many of these also are bent in their coiled-coil region (not shown). **D** 12% form an open "V" shape with the SMCs seemingly only interacting at the hinge (arrow), and another 12% of the complexes split along the coiled-coils, remaining connected at both the head and hinge domains (not shown). **F** 49% of pentameric Condensin holocomplexes show a compact rod configuration. **G** About a third of the latter show a sharply bent coiled-coil region. **H** 27% show what seems to be one of the SMC heads dissociating from the rest of the complex. About a third of these also have a sharp bend in their coiled-coil stalk (not shown). **I** 21% split along the stalk, remaining connected at both the head and hinge domains. **J** 3% of the holocomplexes show one SMC dissociating almost completely, remaining connected only at the hinge region (arrow).

For *Drosophila*, the existence of a functional Condensin II complex has been disputed, as no Cap-G2 gene could be identified and other putative Condensin II components do not seem to interact with each other (Herzog et al. 2013).

C. elegans, on the other hand, seems to lack a classical Condensin I, expressing only a homologue of Condensin II (Hirano 2005).

Enzymatic activities of Condensin

8S Condensin has a strong activity of reannealing denatured DNA without ATP hydrolysis (Sutani and Yanagida 1997). DNA binding relies on the hinge region, and reannealing works even when one of the SMC head domains is deleted (Yoshimura et al. 2002; Sakai et al. 2003).

Phosphorylation of the 13S Condensin non-SMC subunits by Cdk I activates positive DNA supercoiling activity in the presence of Topoisomerase I (Kimura et al. 1998, 1999). The mechanism behind this seems to be that a single 13S Condensin complex can introduce two positive writhes into a DNA molecule, consuming 2 ATP in the process; this probably happens by physically wrapping two loops of about 92bp each through (or around) the "head" side of the Condensin complex. Topoisomerase then removes the corresponding negative supercoils, effecting a net change in linking number (Bazett-Jones et al. 2002; Strick et al. 2004).

Condensin interacts directly with Topoisomerase II (Bhat et al. 1996) and might be necessary for the latter's recruitment to DNA and activation (Coelho et al. 2003).

In regard to its biological function, Condensin plays a confusing multitude of roles. The common principal behind them seems to be the looping and unlooping of DNA that Condensin mediates in cooperation with Topoisomerase II. The looping activity seems to be the functional basis for chromosomal condensation during heterochromatinization and mitosis, as well as for long-distance regulatory sequence interaction and transcriptional insulation; the presumptive reverse capability to dissolve DNA loops may be behind the disentangling of chromosomes at anaphase and the cytophysiological "antipairing" activity of Condensin that acts as a repulsive force between chromatids.

Condensin in chromosomal condensation and segregation

SMCs were first isolated as a protein component of condensed chromosomes; together with Topoisomerase II, SMCs in mitotic HeLa cells comprise at least 40% of non-histone chromosomal proteins, and up to 7% of total chromosomal protein (Lewis and Laemmli 1982). In chromosomes condensed for cell division, Condensin and Topo II form an axial scaffold that the chromatin is attached to in consecutive loops of 80–120kbp (Earnshaw and Laemmli 1983; Earnshaw and Heck 1985; Gasser et al. 1986; Maeshima and Laemmli 2003).

Condensin I is spread evenly along the chromosomal axis (Coelho et al. 2003); in organisms that have Condensin II, it is found primarily at the centromere and in a bead-like pattern along the chromosomal axis (Ono et al. 2003, 2004).

Condensin I is a cytoplasmic protein for most of the cell cycle, only associating with the chromosomes at prometaphase after nuclear envelope breakdown; contrarily, Condensin II remains in the nucleoplasm throughout the cell cycle and binds to chromatin at prophase (Sutani et al. 1999; Ono et al. 2004; Hirota et al. 2004; Gerlich et al. 2006).

The major part of the Condensin I complexes seems to bind in a fluctuating fashion, exchanging with a cytoplasmic pool; in HeLa cells, only a small fraction of Condensin I, but about half of all Condensin II is bound stably to chromatin during mitosis (Gerlich et al. 2006).

In most organisms, chromatin condensation still happens in the absence of Condensin, but is slow, aberrant, or incomplete (f.e. Steffensen et al. 2001; Hagstrom et al. 2002; Kaitna et al. 2002; Coelho et al. 2003; Somma et al. 2003; Hudson et al. 2003); only under special experimental conditions where single, unreplicated chromatids are condensed in *Xenopus laevis* egg extract or in *Drosophila double parked* mutants, Condensin proves necessary for condensation (Cuvier and Hirano 2003; Dej et al. 2004).

Once mitosis has progressed, metazoan cells mutant for Condensin components show a phenotype called "chromatin bridging"; at anaphase, the chromosomal arms of diverging chromosomes seem to remain connected by threads of chromatin (Saka et al. 1994; Strunnikov et al. 1995; Bhat et al. 1996). In

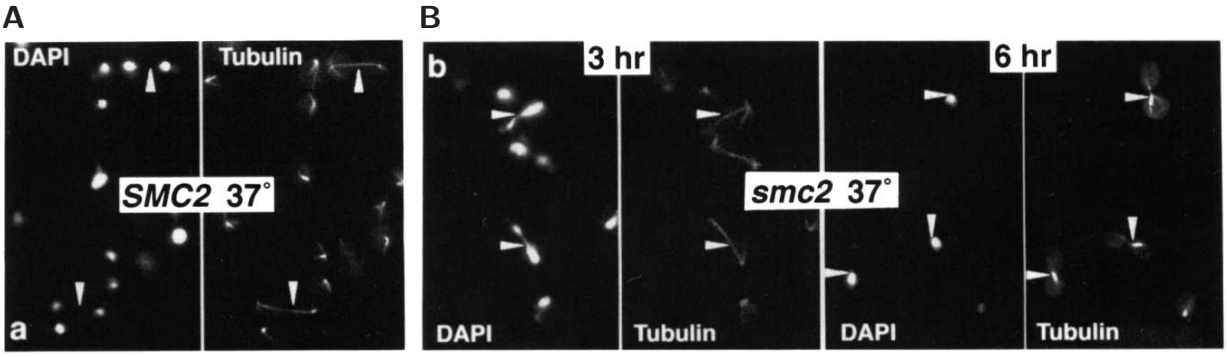

FIGURE 1.6. Budding Yeast cells (*S. cerevisiae*), wild type ("SMC2") and smc2-6 mutant ("smc2"). DNA is visualized with DAPI, mitotic spindle with anti-Tubulin antibody. **A** Wild type. Cells in telophase are recognizable by their long-stretched mitotic spindles (indicated by arrowheads). Chromatin is cleanly segregated into two new nuclei, visible in the DAPI stain. **B** smc2-6 heat-sensitive mutant yeast cells. After 3h at the nonpermissive temperature of 37°C, anaphase leads to chromatin bridging (arrowheads). After 6h, the surviving cells have arrested in the early stages of mitosis, recognizable by the short spindles (indicated by arrowheads). Images from STRUNNIKOV ET AL. 1995

some cases, only centromeres are able to seperate; this is to be expected in Condensin I mutants of organisms that use Condensin II in their centromeres. Sometimes, anaphase is not initiated at all, with cells getting stuck at metaphase (DEJ ET AL. 2004).

Chromatin bridging might be caused by lacking resolution of repetetive rDNA clusters (see below, 1.3.2; D'AMOURS ET AL. 2004; TOMSON ET AL. 2006; WANG ET AL. 2006; D'AMBROSIO ET AL. 2008A), by premature decondensation of chromosomes, or by chromatids not being disentangled by Topoisomerase II. (CUVIER AND HIRANO 2003; COELHO ET AL. 2003) The latter would be caused by failure of Condensin-mediated Topo II recruitment; HUDSON ET AL. 2003 have shown that the axial scaffold of mitotic chromosomes, uniting most Topo II molecules in the cell, is completely missing in SMC2 mutant cultured chicken cells.

Mitotic phenotypes in *Drosophila*. In *Drosophila* embryonic development, the mitotic phenotype of Condensin mutants does not become apparent at first due to a large supply of maternal mRNA; the hypomorphic alleles *Cap-G*^{K1} and *Cap-G*^{K2} only show chromatin bridging in anaphase 15 (DEJ ET AL. 2004), lethal *barren* and *gluon* alleles in anaphase 16 (BHAT ET AL. 1996; STEFFENSEN ET AL. 2001; HAGSTROM ET AL. 2002; HUDSON ET AL. 2003).

In *Drosophila Cap-G* mutants, the number of prometaphase nuclei in the dorsal ectoderm of stage 10 embryos is increased (Dej et al. 2004); cells seem to be stuck in a suspended mitosis. The number of mitotic figures visible in sections of later embryos seems to be reduced in Condensin component mutants, implying that cells can revert out of mitosis (Cobbe et al. 2006).

Drosophila embryonic epidermal cells seem to attempt cytokinesis in spite of chromatin bridging (Bhat et al. 1996). Neural cells, however, seem to be reduced in number and increased in size in *Drosophila barren* mutants (Bhat et al. 1996); it is unclear whether this is due to apoptosis of one or both daughter cells, a failure of Cytokinesis leading to a binucleate or tetraploid cell, or reversion out of mitosis and arrest of cell cycle. In the brain of third instar larvae hemizygous for the weak allele *cap-g*^{K3} , aneuploid and polyploid cells can be detected besides the usual mitotic defects (Dej et al. 2004).

Condensin mutations in tumorigenesis. About 5% of all human cancer genomes and transcriptomes feature mutations of Condensin components (reviewed in Strunnikov 2010).

The genomic instability caused by double strand breaks after chromatin bridging is thought to be among the driving forces behind cancer. The randomized distribution of chromosome fragments leads to what is called a loss of heterozygousity for groups of genes; this way, recessive tumorigenic alleles can express their phenotype in a hemizygous situation. This speeds up the cellular evolution towards more aggressive growth.

In *Drosophila*, genome instability alone does not lead to tumor growth (Castellanos et al. 2008); it has even been shown to cause cell cycle exit into G1 phase and premature differentiation in larval neuroblasts and adult intestinal stem cells (Gogendeau et al. 2015). In the wing and eye discs, chromosomal instability triggers apoptosis; if apoptosis is genetically blocked, the cells overgrow massively. Such wing disc cells loose their typical shape, delaminate out of their epithelium, become invasive and can even form metastases after transplantation into a new host's abdomen (Dekanty et al. 2012, 2015).

Condensin and the organization of interphase chromatin

Condensin also seems to play a role in the spatial arrangement of interphase chromatin.

In human (Cabello et al. 2001), *X. laevis* (Uzbekov et al. 2003) and *S. cerevisiae* cells (Freeman et al. 2000), Condensin I has been found binding to the rDNA in the nucleolus well before mitosis, during G2 phase. In *S. cerevisiae* and *Schizosaccharomyces pombe*, Condensin was shown to bind to all genes that are transcribed by RNA polymerase III (some snRNA and snoRNA genes and all rRNA and tRNA genes) as well as the RNA polymerase II -transcribed ribosomal protein genes, clustering them around the nucleolus (Haeusler et al. 2008; Iwasaki et al. 2010). The "B-Box" sequence GTTCxAxxC, part of the promoter for RNA polymerase III, seems to be a loading site for both Condensin and Cohesin by Scc2-Scc4 (D'Ambrosio et al. 2008b). There even exist isolated B-Boxes without any further promoter elements (Noma et al. 2006).

The preference of Condensin for B-Boxes is not based on direct binding; the complex rather interacts with the RNApol III transcription factors TFIIIB and TFIIIC, assembled on the DNA strand (Haeusler et al. 2008).

In *Schizosaccharomyces pombe*, Condensin binds to the TATA-binding protein (TBP) and thus localizes to active RNApol II promoters; this may be part of the regulatory mechanism of ,,gene bookmarking" (see below, section 1.3.2 p. 30). However, it also leads to the recruitment of strong RNApol II promoters to the centromere/tDNA cluster (Iwasaki et al. 2015; Nakazawa et al. 2015).

Homologous chromosome association in *Drosophila*. In dipterans, homologous chromosome pairs are closely aligned over their whole length ("paired") in most cell types throughout development (Stevens 1908; Metz 1916). This phenomenon is similar, but not identical to the chromosome pairing at meiosis; while the somatic cell lineage establishes pairing during cell cycle 14 (Hiraoka et al. 1993), the germ line only does so for the last five mitoses leading up to meiosis (reviewed in Joyce et al. 2013)

In Condensin II component knock-downs in cultured *Drosophila* Kc167 cells, pairing of heterochromatic regions is enhanced (Joyce et al. 2012).

Polytene chromosomes are a phenomenon that is considered to be related to chromosome pairing: Chromatids sticking to each other, multiplied by repeated rounds of DNA replication without a subsequent mitosis, aligned gene by gene over their full length. The ovary nurse cells of *D. melanogaster* at certain developmental stages form polytene chromosomes that remain in strict alignment of homologous chromatids for their first four rounds (of up to twelve) of DNA replication.

After the fifth round of replication, all replicated chromatids of each pair of chromosome disengage their arms from each other, remaining connected only at the centromeres. The chromosomes take on the form of discrete, spherical "chromatin territories" with interspersed chromatin-free "interchromatin compartments" (Dej and Spradling 1999). The centromeres locate to the nuclear periphery. (Bauer et al. 2012)

In *Drosophila Cap-H2* mutants, this transition from closely aligned chromatids to chromatin territories is blocked; also, the centromeres at the nuclear periphery cluster together and are joined by the pericentric heterochromatin, which in wild type cells would be dispersed throughout the nucleus (Bauer et al. 2012).

Distance measurements between pairs of simultaneous fluorescent *in situ* hybridizations on pairs of loci on the same chromosome also show that chromosomes of *Cap-H2* and *SMC4* mutants are less condensed; they grow longer with each round of replication, whereas wild type chromosomes retain a constant length (Bauer et al. 2012).

Later on in the development of *Cap-H2* (and also *Cap-D3*) mutant nurse cells, the polytene chromosomes fail to disassemble normally (Hartl et al. 2008).

Cap-H2 overexpression dissolves the normally persistent polytene chromosomes in larval salivary gland cells (Hartl et al. 2008), reforming them into chromatin territories similar to those seen in nurse cells. This is concomitant with a contraction in chromosome length (Bauer et al. 2012).

Condensin in transcriptional regulation

There is a wide variety of examples for Condensin function in transcriptional regulation. Most cases seem to be based either on the formation and dissolution of large chromatin loops, Condensin's related role in condensation/decondensation, or a chromatid disentangling activity similar to what Condensin does at anaphase.

Condensin as a mediator of regulatory long distance interactions. In *Drosophila*, Barren is necessary for the function of the Polycomb (Pc) repression complex (PRC).

In a transgenic construct, an ectopic *Fab-7* Pc binding site (a "Polycomb response element") is able to repress an adjacent reporter gene. The repressive activity of *Fab-7* sites depends on physical association with a second *Fab-7* element, natural or ectopic. This physical association is independent of linear distance on chromosomes (Bantignies et al. 2003). Both in mutants of Pc group proteins and *barren*, this repressive effect of ectopic *Fab-7* sites is lost (Lupo et al. 2001).

One copy of *barr* ^{L305} enhances the phenotype of the *Fab-7* ^{2} mutation, effecting a complete reduction of the 7th abdominal tergite. Also, Condensin I and Topoisomerase II colocalize with each other on known Pc repression complex binding sites within the BX-C locus. Moreover, Barren and Topo II coimmunoprecipitate with the 140 kDa isoform of the Pc group protein Polyhomeotic (Ph) (Lupo et al. 2001). *ph* mutants, intriguingly, show massive chromatin bridging early in embryogenesis.

A phenomenon probably related to the constant chromosome pairing in *Drosophila* (see above, section 1.3.2 p. 27) is transvection: The influencing of a gene's transcription by a mutation in an enhancer on the homologue sister locus (reviewed in Duncan 2002). Mutants of the Condensin II–Kleisin Cap-H2 show an increase of transvection, while Cap-H2 overexpression conversely reduces it (Hartl et al. 2008).

During their maturation, B lymphocytes undergo a rearrangement of their genome called V(D)J recombination. This creates the gene for the B cell receptor, the unique antibody B lymphocytes present on their surface and secrete

upon activation. For V(D)J recombination the κ Immunoglobulin (Igκ) locus among others, coding for parts of the light Ig chain, has to achieve a physical contraction by establishing long-distance chromatin interactions.

On the Igκ locus of mouse pro-B cells, the Polycomb group proteins YY1 and EZH2 interact with Condensin I and Cohesin. Deletion of the YY1 REPO domain, which is necessary for interaction with Condensin, produces the same defects in B cell development as a YY1 knock-out, namely partial failure of the physical contraction of the Igκ-locus (Pan et al. 2013).

Gene regulation by chromatin condensation and decondensation. In animal cells, transcription is halted during mitosis (reviewed in Gottesfeld and Forbes 1997). Once mitosis is completed, the cell's specific pattern of gene expression mostly resumes as it was before. This mechanism is called "gene bookmarking". It seems to be based on TATA-binding protein (TBP) remaining bound to promoters during mitosis and interacting with both Condensin I and Protein Phosphatase 2A, having the latter dephosphorylate and thus deactivate Condensin. This seems to keep promoters uncondensed during mitosis, helping TBP to resume transcription instantly (Xing et al. 2008).

Conversely, when in Cap-H mutant DT40 chicken cells a Cap-H rescue construct is shut off before mitosis, the expression level of those genes that normally are strongly expressed and would associate with Condensin I will be reduced after mitosis (Kim et al. 2013).

Other transcription factors, like HSF2, also seem to interact with Condensin and trigger the same bookmarking mechanism as TBP (Xing et al. 2005). In dividing chicken DT40 cells, 30% of SMC2 and 42% of Cap-H bind to active promoters, which comprise only 3% of the genome (Kim et al. 2013). The situation in *S. pombe* is similar (see above, 1.3.2 27, Iwasaki et al. 2015; Nakazawa et al. 2015).

In *Drosophila*, heterozygous Condensin I mutants seem to be modifiers of position effect variegation, altering the expression level of reporter genes that are located close to heterochromatic chromosome regions. Dej et al. 2004 see *barr* ^{L305}, *cap-G*^{K1} and *cap-G*^{K2} as suppressors of variegation (enhancing the expression of

a heterochromatized w^+ gene); however the quantitative study by Cobbe et al. 2006 sees only the SMC4 allele *gluon*$^{88-82}$ and to a much lesser extent *SMC2* ^{jsl2} as such, reporting *gluon*^{17C}, *gluon*$^{88-41B}$, *gluon*$^{88-37}$, *barr* ^{L305} and *cap-G* ^{64} as enhancers of variegation.

In mammals, Quiescent T Cells prior to activation by their specific antigen show a permanent condensation of most of their chromatin that depends on Condensin II (Rawlings et al. 2011). In the mouse mutant *nessy*, an amino acid substitution in Condensin II β–Kleisin causes a defect in T-cell development (Gosling et al. 2007).

Condensin in human diseases

The protein MCPH1, which in humans causes primary microcephaly when mutant, is among other things a regulator that interacts with Condensin II and probably competes for the latter's chromosomal binding sites. Cells from patients with a mutation of MCPH1 show a premature chromosome condensation during G2 phase (Trimborn et al. 2006; Yamashita et al. 2011). *Drosophila* mutants of *mcph1* show chromatin bridging.

Some human cancer cell lines carry mutations of Condensin components (Strunnikov 2010); for example, some Pyothorax-associated lymphoma (PAL) derived cell lines are mutant for the Condensin SMCs hCap-C and hCap-E (Ham et al. 2007). This is probably connected to the mitotic defects exhibited by Condensin mutants (see above, section 1.3.2, p. 26).

1.3.3 The Cohesin complex

Molecular composition and structure

Cohesin is a protein complex necessary for sister chromatid cohesion and heterochromatin formation. It is characterized by the subunits SMC1 (Hirano et al. 1997; Hirano and Mitchison 1994) and SMC3. The two SMCs dimerize with their "hinge" and "head" domains (Haering et al. 2002; Anderson et al. 2002).

In the Mitosis-specific form of Cohesin, they are joined by the α-Kleisin Scc1 (Birkenbihl and Subramani 1992, 1995; Michaelis et al. 1997; Guacci et al. 1997). In "meiotic" Cohesin, Scc1 is replaced by the α-Kleisin Rec8.

This trimer associates stably with a pair of chromatids (Kulemzina et al. 2012). However, it interacts with various regulatory subunits that mostly bind to the Kleisin:

- Scc3, a HEAT repeat protein, binds to Scc1 (Tóth et al. 1999; Losada et al. 2000).
- Pds5 (Precocious Dissociation of Sisters), a HEAT repeat protein which binds to Scc3 and the Kleisin Scc1 (Denison et al. 1993; Panizza et al. 2000; Hartman et al. 2000), but can also bind to the SMCs' hinge region (Mc Intyre et al. 2007).
- Wapl (Wings apart -like), a helical repeat protein which binds to Scc1, Scc3 and Pds5 (Verná et al. 2000; Kueng et al. 2006; Gandhi et al. 2006; Shintomi and Hirano 2009; Kulemzina et al. 2012), stimulates dissociation of the Kleisin from SMC3 and thus release from chromatin (Chan et al. 2012; Buheitel and Stemmann 2013; Eichinger et al. 2013; Hara et al. 2014).
- Sororin binds to Pds5 and seems to be a competetive inhibitor of Wapl. It associates with Cohesin from S phase on, stabilizes Cohesin's binding to chromatin and is degraded once mitosis is completed (Rankin et al. 2005; Schmitz et al. 2007; Lafont et al. 2010; Nishiyama et al. 2010).
- Shugoshin (Sgo), which binds to Scc1 and Scc3. For this binding site, it competes with Wapl. It recruits Protein phosphatase 2A (PP2A) to Cohesin, preventing it from being permanently phosphorylated. This way, it promotes and protects sister chromatid cohesion at the centromeres (Wang and Dai 2005; Kitajima et al. 2006; Hara et al. 2014).

A single Cohesin can embrace two strands of DNA, linking them topologically (Haering et al. 2008). In electron-microscopic images, the two SMCs can often be seen as a ring (see Fig. 1.7, Anderson et al. 2002; Gruber et al. 2003). This

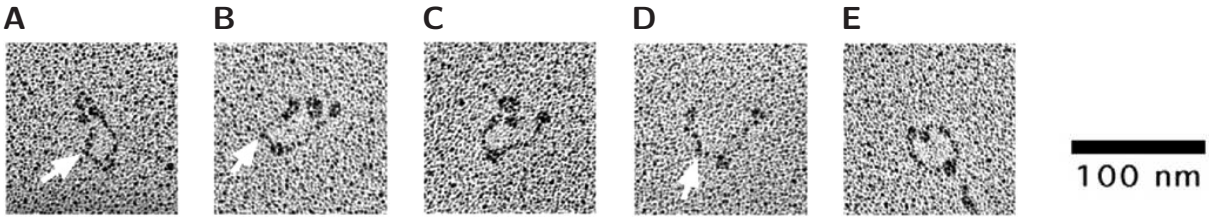

FIGURE 1.7. Electron micrographs of human Cohesin, modified from ANDERSON ET AL. 2002. The common kinks in the SMCs' coiled-coil stalks are indicated with white arrows. Shown configurations are sorted from the more abundant (left) to the less abundant (right). Some configurations might be more or less abundant *in vivo*, due to preparational artefacts. **A** 47% of all complexes are closed rings with a roughly globular association on one side that seemingly is an assembly of several substructures, probably the non-SMC subunits. **B** In 33%, the bulky aggregate appears more stretched out so that the presumable SMC head domains are discernible from the subcomplex between them. **C** 20% show one of the presumed SMC heads detached from the non-SMC subcomplex. **D** 11% of SMC dimers are not associated with a larger complex at all; about half of these have an open "V" configuration, while others **E** form a ring.

contrasts to Condensin, which looks roughly rod-shaped with no central opening (YOSHIMURA ET AL. 2002; ANDERSON ET AL. 2002). FRET studies imply that the SMC head domains interact in direct contact with each other and the Kleisin, without the latter having to bridge any gap (MC INTYRE ET AL. 2007); the open ring shape seems to be due to kinks in the SMCs' coiled-coil stalks (see Fig. 1.7, ANDERSON ET AL. 2002; GRUBER ET AL. 2003). *S. pombe* Cohesin SMCs contain 13 Proline residues in the coiled-coil domains, which might work as helix-breakers and confer flexibility to these domains (SAKAI ET AL. 2003).

In contrast to 8S Condensin, the Cohesin SMC dimer alone has almost no affinity to ssDNA and very low affinity to linear dsDNA *in vitro*. However, the hinge domain might still have a function beyond SMC dimerisation: Atomic force microscopic images sometimes show the coiled-coil region bending around, extending the hinge region towards the head (SAKAI ET AL. 2003). Artificial dimers of isolated SMC1 and SMC3 hinge domains also can coimmunoprecipitate isolated SMC1 head domains (MC INTYRE ET AL. 2007).

As a holocomplex with at least the Kleisin, Cohesin can bind to cruciform DNA and Histone-associated DNA (AKHMEDOV ET AL. 1998; SAKAI ET AL. 2003).

In vivo, Cohesin seems to be loaded onto DNA by the Scc2-Scc4 complex (MICHAELIS ET AL. 1997; FURUYA ET AL. 1998; TÓTH ET AL. 1999; WATRIN ET AL.

2006). Loading seems to happen by opening the hinge domains (Gruber et al. 2006; Buheitel and Stemmann 2013); it also depends on ATP hydrolysis by the SMC's ATPase "heads" (Arumugam et al. 2003; Weitzer et al. 2003). ATPase activity is stimulated by the Kleisin Scc1 and only occurs during loading onto DNA (Lammens et al. 2004; Arumugam et al. 2006).

Cohesin can dissociate from DNA in two ways: Upon cleavage of Scc1 by Separase, or by dissociation of Scc1 from the SMC3 head, regulated by additional protein factors.

Cohesin in mitosis

Cohesin is loaded onto chromatin in telophase. At DNA replication in S phase, the SMC3 head is acetylated (Tóth et al. 1999; Skibbens et al. 1999; Ivanov et al. 2002) and the complex is joined by Sororin, displacing Wapl and stabilizing the association with the now duplicated sister chromatids (Zhang et al. 2008; Rowland et al. 2009; Sutani et al. 2009; Lafont et al. 2010; Nishiyama et al. 2010).

On the chromosomal arms, Cohesin dissociates in prophase (Losada et al. 1998; Waizenegger et al. 2000) by opening the interface between SMC3 and the Kleisin (Buheitel and Stemmann 2013). This is triggered by phosphorylation of Scc3 and Sororin and subsequent replacement of Sororin by Wapl, and deacetylation of SMC3 (Gandhi et al. 2006; Kueng et al. 2006).

On the centromere, this pathway is inhibited by Shugoshin (Shintomi and Hirano 2009); here, Cohesin is released only at anaphase onset, when Scc1 is cleaved by Separase/Separin (Uhlmann et al. 2000). This prolonged cohesion at the centromere contributes to the typical X-shape of metaphase chromosomes.

Once telophase is reached, Cohesin is once more loaded onto the chromatids, where it seems to have vital functions during interphase.

Mutants of Cohesin components, regulators or loading factors often show premature separation of chromosomes during mitosis (Lee and Orr-Weaver 2001). This can result in genomic instability (Percival et al. 2015).

In *Drosophila*, cells without functional Cohesin fail to form a metaphase plate; instead, sister chromatids segregate asynchronously, in an erratic, unreliable fash-

ion, sometimes moving forth and back between spindle poles. After a mitotic arrest that lasts for about 20min, chromosomes decondense abruptly and cytokinesis is initiated, with the cleavage furrow cutting through all chromatids that get in the way (Pauli et al. 2008).

Cohesin in transcriptional regulation

In *S. cerevisiae*, Cohesin is enriched both on the centromere and in intergenic regions between convergent RNA-polymerase-II-transcribed genes. In contrast to Condensin, which tends to remain at its loading site, Cohesin seems to get pushed downstream by RNApol II (Glynn et al. 2004; Lengronne et al. 2004; reviewed in Ocampo-Hafalla and Uhlmann 2011).

However in Metazoa, this sliding mechanism seems to have little impact on Cohesin distribution, as Cohesin's binding half-life of about 20min is not long enough to be pushed along the full length of a human (Gerlich et al. 2006; Parelho et al. 2008) or *Drosophila* gene (Misulovin et al. 2008; Gause et al. 2010).

In *Drosophila*, Cohesin and the loading factor Nipped-B are found preferentially at the promoters of actively transcribed genes; they are, however, excluded from genes silenced by Polycomb group (PcG) repressors (Dorsett 2009; Misulovin et al. 2008; Schaaf et al. 2009).

Mutants of Cohesin components and loaders show altered expression of certain genes like *cut* that are regulated by distant enhancers, implying that Cohesin is necessary for long-range interaction (Rollins et al. 1999; Dorsett et al. 2005). Mutations of Cohesin components modify the phenotypes of many mutations in *Drosophila* (reviewed in Dorsett 2009); for example in *vtd* mutants, the phenotype of Kr^{If} is modified towards ectopic appendage-like outgrowths in the eyes. This seems to be an heritable epigenetic effect, as it lasts for at least five generations even if the genetic background is restored to vtd^{+} (Sollars et al. 2003).

In postmitotic, differentiating *Drosophila* neural cells, artificial inactivation of the Cohesin complex leads to severe defects in axon pruning (Pauli et al. 2008). Somatically generated clones of $SMC1^{-}$ neurons show axon pruning defects and

reduced expression of the Ecdysone receptor EcR-B1. Postmitotic expression of transgenic SMC1 in such neurons rescues the phenotype; overexpression of EcR-B1 partially also does. A reduced dosage of EcR-B1 aggravates the phenotype; presumably, Cohesin regulates the Ecdysone receptor (Schuldiner et al. 2008).

Inactivation of Cohesin in *Drosophila* salivary leads to altered transcription levels of many genes; 419 genes changed at least 1.5-fold, several tens of genes up to over a hundred fold. Cohesin is found enriched at the transcription start sites of about half of these genes. (Pauli et al. 2010).

In C.elegans, mutants of Scc4 show guidance defects in migrating cells and axons (Takagi et al. 1997; Bénard et al. 2004).

In Zebrafish, changes in dosage of Cohesin components that do not inhibit mitosis have been shown to alter gene expression levels (Horsfield et al. 2007). Partial knockdown of Scc1/Rad21 in zebrafish embryos produced a defect of neural crest cell targeting, producing among other things heart defects resembling those in below-mentioned (p. 37) human Cornelia deLange Syndrome and CAID (Schuster et al. 2015).

In mammals, Cohesin is enriched on its Scc2-4 mediated loading sites and, among others, on CCCTC-Binding Factor (CTCF) binding sites. At these, Cohesin binding depends on functional CTCF (Rubio et al. 2008), and CTCF function depends on intact Cohesin (Parelho et al. 2008; Wendt et al. 2008). During mitosis in human cells, CTCF remains bound to chromatin (Burke et al. 2005) and accumulates on the centromeres (Zhang et al. 2004). The vertebrate Scc3 paralogue SA1/STAG1 interacts directly with CTCF (Rubio et al. 2008).

Mechanistically, CTCF-dependent enhancer insulation as well as other regulatory functions of Cohesin seem to involve the formation of large chromatin loops (Nativio et al. 2009; Schmidt et al. 2010).

In human cell lines, Cohesin has been shown to share CTCF-free binding sites with tissue-specific regulator proteins like the Estrogen Receptor (Schmidt et al. 2010).

Cohesin in human diseases

In humans, mutations of Cohesin components, loaders and regulators give rise to a number of syndromes that are called Cohesinopathies. Many present with abnormal mitosis figures; some symptoms, however, seem more likely to be caused by defects in gene regulation. Phenotypically, the more severe of these syndromes with their phocomelia and dismelia resemble the effects of fetal exposition to Thalidomide (a purely superficial similarity, as this drug works by inhibition of angiogenesis; D'Amato et al. 1994, reviewed in Vargesson 2015).

A few examples for Cohesinopathies are Cornelia deLange Syndrome, Roberts Syndrome, and Chronic Atrial and Intestinal Dysrhythmia.

Cornelia deLange Syndrome (CdLS) is characterized by mental and physical retardation, heart defects, characteristic facial features, hirsutism and abnormalities of upper limbs and many other body parts and organs. CdLS is caused by mutations of Scc2 (Krantz et al. 2004; Tonkin et al. 2004), SMC1, or SMC3 (Musio et al. 2006; Deardorff et al. 2007). Mutations of the SMCs often lead to lighter cases showing only mental retardation. In cells from CdLS patients with Scc2 mutation, precocious sister chromatid separation can be detected (Kaur et al. 2005). CdLS is a quite common disorder, with about 1 in 10000 humans afflicted.

Roberts syndrome is characterised by varying degrees of growth deficiency of prenatal onset, reduction of limbs, craniofacial anomalies, microcephaly, and mental deficiencies. Many of the more severe cases are stillborn. Lighter forms of this syndrome, with survival into adulthood, are called **SC phocomelia syndrome** (Schüle et al. 2005).

Roberts syndrome is caused by a variety of mutations of the acetyl transferase ESCO2, which acetylates the SMC3 head region, promoting Cohesin binding to sister chromatids at S phase (Vega et al. 2005; Schüle et al. 2005). Cells from Roberts syndrome patients show abnormal mitosis figures, centromeres and nucleoli (Tomkins and Sisken 1984).

Chronic Atrial and Intestinal Dysrhythmia (CAID) patients suffer from a malfunction of the cardiac sinus node, resulting in a decreased heart rhythm, and from chronic intestinal obstruction caused by pathological changes of the intestinal musculature and nervous system.

CAID is caused by a mutation in the Cohesin component Shugoshin-like 1 (SGOL1). Cells from patients with CAID show overactive TGF-β signaling, a centromeric cohesion defect during mitosis, an accelerated cell cycle and premature cell senescence; however, no aneuploidy is observed (Chetaille et al. 2014).

Cohesin components, regulators and loaders are also often mutated in human cancer cell lines (reviewed in Strunnikov 2010; Solomon et al. 2014; Losada 2014; Orgil et al. 2016); STAG2/SA2 is one of only twelve genes that are mutated in more than three different types of cancer (Lawrence et al. 2014).

1.3.4 This study: The effect of Condensin and Cohesin mutations on *Drosophila* embryonic myogenesis

Here, we identify a *D. melanogaster* mutant with heavily disturbed embryonic musculature as carrying a *barren* point mutation. We show that other *barren* alleles as well as *Cap-G* mutants show the same or a similar phenotype. In contrast, mutations of *Cap-D2* or the Cohesin components *SMC1* and *vtd* show no such phenotype.

We use an UAS-regulated rescue construct and various tissue-specific Gal4 driver lines to narrow down the time and cell type when Condensin is necessary for myogenesis. This allows us to identify the mechanism that causes the phenotype, telling apart regulatory from mitotic effects of the Condensin mutations.

We find that the phenotype is a loss of muscle identity. It seems to be caused by a lack of Barren before the last mitosis that gives rise to the muscle founder cells, the carriers of the identities of the various muscles; thus, it is most likely an effect of aberrant mitoses.

Chapter 2

Materials and Methods

2.1 Materials, Reagents and Instruments

2.1.1 Instruments

Microscopic equipment

Stereo microscopes	M3	
	M3B	Wild, Heerbrugg, Switzerland
	Stemi DV4	
	Stemi SV6	Zeiss, Jena
CO_2 anaesthesia pads		Workshops Philipps-Universität Marburg
CO_2 supply system		Linde, Düsseldorf
Epifluorescence stereo microscope	SZX9	Olympus, Planegg

DIC microscope	Axioskop	Zeiss, Jena
Camera	Powershot G5	Canon
Camera	AxioCam ICc 1	Zeiss, Jena
Software	AxioVision	Zeiss, Jena
Epifluorescence microscope	Axiophot	Zeiss, Jena
Camera	AxioCam ICc 3	Zeiss, Jena
Software	AxioVision Release 4.8	Zeiss, Jena
Epifluorescence and CID microscope	ApoTome	Zeiss, Jena
CID grid	ApoTome	Zeiss, Jena
Camera	AxioCam	Zeiss, Jena
Software	AxioVision	Zeiss, Jena

Other instruments

DNA gel electrophoresis apparatus	Workshops Philipps-Universität Marburg

		Workshops MPI Martinsried
DNA gel electrophoresis voltage supply	PowerPac 300	BioRad, München
	Power Pack P25	Biometra, Göttingen
DNA electrophoresis gel UV transilluminator	TI1	Biometra, Göttingen
DNA electrophoresis gel documentation camera and printer	??	Biotech-Fischer
	UVsolo	Biometra, Göttingen
Microcentrifuge	Biofuge pico	Heraeus Instruments, Hanau
Cryomicrocentrifuge	Biofuge fresco	Heraeus Instruments, Hanau
Cryocentrifuge	Megafuge 1.0 R	Heraeus Instruments, Hanau
PCR cycler	Mastercycler Personal	Eppendorf, Hamburg
	Personal Cycler	Biometra, Göttingen
Photometers	Ultrospec 3000	
	Gene-Quant 1300	Pharmacia, Freiburg
pH meter	GPRT 1400A	Greisinger electronic
	pH211	Hanna Instruments

UV Crosslinker	UV StratalinkerTM 2400	Stratagene, LaJolla, USA
Water baths	C10	Haake, Karlsruhe
	C1	Haake, Karlsruhe
	GFL 1002	GFL, Burgwedel
Cryo water bath	KH-3	Biometra, Burgwedel
Heater block	HBT130-2	Haep Labor Consult, Bovenden
	Dri-Block DB 2A	Techne, Wertheim
70°C Oven		Mammert
Magnetic stirrer	Variomag Mono	H+P Labortechnik, München
Heater plate with magnetic stirrer	IKA Combimag RCT	IKA-Werke, Staufen
Vortex shaker	Reax 200	Heidolph, Schwabach
Speed Shaker	Vibrax VXR Basic	IKA-Werke, Staufen
Microfuge cup holder for speed shaker	Typ VX 2 E	IKA-Werke, Staufen
Dish Shaker	WT12	Biometra, Burgwedel
3D shaker	Rocky 3D	Föbel Labortechnik, Lindau

2.1.2 Chemicals and Reagents

Primary Antibodies

Antibody	*Typical dilution*	*Source*
Anti - βGalactosidase, Mouse monoclonal	1:2000 - 1:5000	Promega, Madison, USA
Anti - βGalactosidase, Rabbit polyclonal	1:2000	Cappel, Hamburg
Anti - β3Tubulin, Rabbit polyclonal	1:5000	Leiss et al. 1988
Anti - β3Tubulin, Guinea pig polyclonal	1:5000	Leiss et al. 1988
Anti - Mef2, Rabbit polyclonal	1:5000	Bour et al. 1995
Anti - Lmd, Rabbit polyclonal	1:2000	Duan et al. 2001
Anti - BP102, Mouse monoclonal (ab12455)	1:50	Abcam, Cambridge
Anti - GFP, Mouse monoclonal	1:1000	Covance, Princeton, USA
Anti - GFP, Rabbit polyclonal (ab6556)	1:1500	Abcam, Cambridge
Alkalic Phosphatase-coupled Sheep polyclonal Anti - DIG F_{ab} fragment	1:5000 (for spot test)	Roche Diagnostics, Mannheim
Biotinylated Anti - DIG, Goat	1:200	Roche Diagnostics, Mannheim

Anti - FasIII, Mouse monoclonal (7G10)	1:50	Patel et al. 1987 / DSHB (p. 102)

Secondary Antibodies

Biotinylated Goat polyclonal Anti - Rabbit-IgG	1:1000	Vector Laboratories, Burlingame, USA
Biotinylated Goat polyclonal Anti - Rat-IgG	1:1000	Vector Laboratories, Burlingame, USA
Biotinylated Horse polyclonal Anti - Mouse-IgG	1:1000	Vector Laboratories, Burlingame, USA
DyLight488-coupled Goat polyclonal Anti - Rabbit-IgG	1:50-1:100	Dianova, Hamburg
Alexa488-coupled Goat polyclonal Anti - Guinea pig-IgG	1:50-1:100	Dianova, Hamburg
Cy2-coupled Goat polyclonal Anti - Rabbit-IgG	1:50-1:100	Dianova, Hamburg
Cy3/Cy5-coupled Goat polyclonal Anti - Rabbit-IgG	1:200-1:300	Dianova, Hamburg
Cy2-coupled Goat polyclonal Anti - Guinea Pig-IgG	1:50-1:100	Dianova, Hamburg
Cy3/Cy5-coupled Goat polyclonal Anti - Guinea Pig-IgG	1:200-1:300	Dianova, Hamburg
Cy2-coupled Goat polyclonal Anti - Mouse-IgG	1:50-1:100	Dianova, Hamburg
DyLight488-coupled Goat polyclonal Anti - Mouse-IgG	1:50-1:100	Dianova, Hamburg

Cy3/Cy5-coupled Goat polyclonal Anti - Mouse-IgG	1:200-1:300	Dianova, Hamburg
Cy2-coupled Goat polyclonal Anti - Rat-IgG	1:50-1:100	Dianova, Hamburg

Enzymes and enzyme kits

AccuPrime Proof Reading Polymerase	Invitrogen, Karlsruhe
Restriction endonucleases	MBI Fermentas, St.Leon-Roth
	New England Biolabs, Frankfurt
	Amersham Pharmacia Biotech, Freiburg
	Roche Diagnostics, Mannheim
RNase A	Boehringer, Mannheim
T4 DNA-Ligase	Roche Diagnostics, Mannheim
Taq DNA Polymerase	Peqlab, Erlangen

Other reagent kits

DIG RNA Labeling and Detection Kit	Roche Diagnostics, Mannheim
Epon Epoxy embedding kit	Fluka, Neu-Ulm

JETsorb Kit	GENOMED, Bad Oeynhausen
JETstar Plasmid Kit 2.0	GENOMED, Bad Oeynhausen
TOPO TA Cloning Kit	Invitrogen, Karlsruhe
TSA Fluorescein System	Perkin Elmer, Rodgau
TSA Tetramethylrhodamine System	Perkin Elmer, Rodgau
Vectastain ABC Kit Elite PK-6100 Standard	Vector Laboratories, Burlingame, USA

Other chemicals

DAB	Sigma, Deisenhofen
Dan Klorix (Sodiumhypochloride solution)	Colgate Palmoliv, Hamburg
Fluoromount G	Southern Biotechnology Associates, Birmingham, USA
Hybond-N membrane	Amersham, Braunschweig
Mass Ruler DNA-Ladder, Mix	MBI Fermentas, St. Leon-Roth
NBT-X-phosphate	Roche Diagnostics, Mannheim
Non-immune Goat serum	
Non-immune Horse serum	Vector Laboratories, Burlingame, USA

Oligonucleotides / Primers	MWG Biotech, Ebersberg
Triton X-100	Roth, Karlsruhe
Tween 20	Sigma, Deisenhofen

2.1.3 Composition of solutions, buffers and media

Solutions and media for bacterial cultures

Ampicillin stock	100 mg/ml in 70% Ethanol
Chloramphenicol stock	34 mg/ml in 70% Ethanol
Kanamycin stock	50 mg/ml in 70% Ethanol
LB medium	10 g/l Baktotrypton, 5 g/l yeast extract, 5 g/l NaCl
LB agar	1,5% (w/v) Bactoagar in LB medium

Solutions for DNA extraction

Silanizing solution	Dichlordimethylsilane in 1.1.1-Trichlorethane
S1	50 mM Tris, 10 mM EDTA, 100 μg/ml RNAse A in H_2O dd, adjusted to pH 8 with HCl
S2	200 mM NaOH, 1% (w/v) SDS in H_2O dd

S3	2,6 M Potassium acetate in H_2O dd, adjusted to pH 5,2 with acetic acid
E1	10 mM EDTA, 100 μg/ml RNase A in H_2O dd
E2	200 mM NaOH, 1% (w/v) SDS in H_2O dd
E3	3,2 M Potassium acetate in H_2O dd, adjusted to pH 5,0 with acetic acid
E4	600 mM NaCl, 100 mM Sodium acetate, 0,15 % (v/v) Triton X-100 in H_2O dd, adjusted to pH 5,0 with acetic acid
E5	800 mM NaCl, 100 mM Sodium acetate in H_2O dd, adjusted to pH 5,0 with acetic acid
E6	1,25 M NaCl, 100 mM Tris in H_2O dd, adjusted to pH 8,5 with HCl
Extraction Buffer for Genomic Fly DNA	0,1 M Tris, 0,1 M EDTA, 1%(w/v) SDS in H_2O dd, adjusted to pH 9 with HCl
SquiB	1 mM EDTA, 25 mM NaCl, 10 mM Tris in H_2O dd, adjusted to pH 8,2 with HCl

Solutions for DNA gel electrophoresis

10x TBE	0,89 M Tris, 0,89 M Boric acid, 2 mM EDTA
DNA electrophoresis gel	0,5%-2% Agarose solved in boiling TBE, 0,6 mg/l% Ethidium bromide added at 60°C
10x loading buffer	40% Glycerine, 0,9% (w/v) Boric acid, 0,1% (w/v) Bromophenol blue (optionally 0,1% (w/v) Xylene cyanol) in TBE

Media for *Drosophila* culture

Drosophila culture medium	60% (w/v) Maize flour (organic), 60% (w/v) Malt extract, 7,15% (w/v) Fructose, 1,2% Yeast, 0,7% (w/v) Agar, 0,6% Propionic acid, 0,2% Nipargine
Grape juice bottle agar	5% (w/v) Sucrose, 0,8% (w/v) Nipargine in Grape juice, diluted 1:4 at 70°C in water with 2% Agar
Apple juice plate agar	5% (w/v) Sucrose, 0,8% (w/v) Nipargine in Apple juice, diluted 1:4 at 60°C in water with 5,2% Agar

Solutions for embryonal microinjection

10x Injection buffer	1mM $NaHPO_4$, 50mM KCl
Vector solution for microinjection	2,5μl 10x injection buffer, 2,5μl pπ25.7wc helper plasmid, 5μg vector plasmid; fill to 20μl with sterile H_2Odd
Heptane glue	Brown adhesive packet tape is incubated shaking in heptane for a few hours to solve the adhesive glue in the heptane

Solutions for *Drosophila* embryo handling

TNX	0,7% NaCl, 0,1% Triton X-100 in H_2O
TNX/Klorix	50% Dan Klorix in TNX
10x PBS	1,3 M NaCl, 70 mM Na_2HPO_4, 30 mM NaH_2PO_4 in H_2O demin.
PBT	0,1% Tween 20 in PBS
FPBS	40 g/l Paraformaldehyde in PBS, solved at 60°C
PBTB	1% (w/v) milk powder in PBT

Solutions for *in situ* hybridization

20x SSC	3 M NaCl, 0,3 M Sodium citrate in H_2O dd; adjust to pH 7,0 with HCl
HS	50% Formamide, 25% 20x SSC, 0,1% Heparin (50 mg/ml), 0,1% Tween 20 in H_2O dd
10x DIG1	1 M Tris, 1,5 M NaCl in H_2O dd; adjust to pH 7,5 with HCl
DIG2	0,5% blocking reagent in DIG1, solved at 60°C
DIG3	0,1 M Tris, 0,1 M NaCl, 0,05 M $MgCl_2$ in H_2O dd; adjust to pH 9,5 with HCl

2.1.4 Online Resources

Bloomington Drosophila Stock Center (BDSC)	`flystocks.bio.indiana.edu`
Vienna Drosophila RNAi Center (VDRC)	`www.vdrc.at`
Developmental Studies Hybridoma Bank (DSHB)	`dshb.biology.uiowa.edu`
FlyBase (Gramates et al. 2017)	`flybase.org`
FlyMove (Weigmann et al. 2003)	`flymove.uni-muenster.de`
OligoCalc oligonucleotide properties calculator (Kibbe 2007)	`biotools.nubic.northwestern.edu/OligoCalc.html`
PubMed Literature Database	`www.ncbi.nlm.nih.gov/pubmed`
NCBI basic local alignment search tool (BLAST)	`blast.ncbi.nlm.nih.gov/Blast.cgi`

2.2 *Drosophila* stocks

"BL" stands for stock numbers of the Bloomington Drosophila Stock Center (BDSC), "v" stands for stock numbers of the Vienna Drosophila RNAi Center (VDRC)

Name	**Chromosomal region**	**Source**	**Comment**
Acer ^{k07704}	29D4	BL10679	
ap^{md544}*-Gal4*	41F8	BL3041	
barr ^{k14014}	38B1-B2	BL11117	
barr ^{L305}	38B1-B2	BL4402	
bHLH54F-lacZ		Ismat et al. 2010	βGal-Expression in the longitudinal visceral founder myoblasts
Cap-D2 ^{f03381}	99B7	BL18648	
Cap-G ^{64}	49E7-F3	BL9456	
Cap-G ^{6}	49E7-F3	BL5562	
da-Gal4			ubiquitous driver
Df(2L)BSC341	37B11–D3	BL24365	covers *CG17572*
Df(2R)BSC135	56C11–D5	BL9423	covers *CG9416*
Df(2R)BSC429	51C2–D1	BL24933	covers *SMC2*
Df(3L)BSC395	68F1–F2	BL24419	covers *rols*
Df(3R)01215	99A6–C1	BL5424	covers *Kul*, *Cap-D2*
Df(3R)BSC491	95A7–A10	BL24995	covers *CG18754*, *SPE*
Df(3R)BSC547	99B5–C2	BL25075	covers *Kul*, *Cap-D2*

Name	*Chromosomal region*	*Source*	*Comment*
Df(3R)BSC620	99C5–D3	BL25695	covers *TACE*
Df(3R)BSC714	13E14–14A8	BL26566	covers *mmd*
Df(3R)BSC846	99A1–B10	BL27919	covers *Kul, Cap-D2*
Df(3R)Exel6197	95D8–E1	BL7676	covers *SMC1*
Dr / TM3, Sb, Dfd-lacZ (="TDLZ")	Chromosome III	Gift by A. Holz, Giessen	*Drop (Dr)* eye marker over a TM3 balancer with *Stubble (Sb)* bristle marker and *Deformed (Dfd)-lacZ* embryonic marker
Dr / TM3, Sb, ftz-lacZ (="TFLZ")	Chromosome III		*Drop (Dr)* eye marker over a TM3 balancer with *Stubble (Sb)* bristle marker and *fushi tarazu (ftz)-lacZ* embryonic marker
E831	22E1, 36E1–E3, 28B1-B2, 47A1–A7	Gift by C. Klämbt, Münster; Hummel et al. 1999a,b	EMS-induced allele with at least four mutations, one of them *barren*
E832		Gift by C. Klämbt, Münster; Hummel et al. 1999a,b	Sister line from the same mutagenesis screen as E831, but with a different set of mutations
glu ^{k08819} (SMC4)	36A12-A13	BL10831	
If / CyO, hg-lacZ	Chromosome II	Gift by M. Affolter, Basels	*Krüppel $^{Irregular\ facets\text{-}1}$ (If)* eye marker over *Curly of Oster (CyO)* balancer with *Doux ^{Curly}* wing marker and *hindgut (hg)-lacZ* embryonic marker
Kul-dsRNA	Chromosome II	v28347	RNAi construct

Name	*Chromosomal region*	*Source*	*Comment*
kuz ^{3}	34C4-C6	BL3653	
kuz $^{e29\text{-}4}$	34C4-C6	BL5804	
Mef2-Gal4	Chromosome III	Ranganayakulu et al. 1998	*Mef2* driver, active from early on in all myoblasts
Neu3 ^{c01955}	88C10-D1	BL10769	
Neu3 ^{MB01428}	88C10-D1	BL23312	
rols-Gal4		Gift by C. Stute, Marburg	*rols* driver, active in founder cells and muscles
rP298-Gal4	X Chromosome	Menon and Chia 2001	*duf* driver, active from early on in founder cells and muscles
rP298-lacZ	X Chromosome	Nose et al. 1998	*duf* marker, in founder cell and muscle nuclei
Rya-R44F ^{16}	44F1-F2	BL6812	
SMC1 ^{exc46}	95D11	BL25718	
SMC2 ^{jsl2}	36A12-A13	BL9455	
sns pro3-Gal4	Chromosome II	Gift by S. Abmayr, Kansas City; Kocherlakota et al. 2008	*sns* driver, active in FCMs
Sp / CyO, hg-lacZ; Dr / TM3, Sb, Dfd-lacZ	Chromosome II, III		Double balancer: *wingless* $^{Sternopleural\text{-}1}$ *(Sp)* bristle and *Dr* eye marker over *CyO, hg-lacZ* and *TDLZ*
Sp / CyO, hg-lacZ; Dr / TM3, Sb, ftz-lacZ	Chromosome II, III		Double balancer: *wingless* $^{Sternopleural\text{-}1}$ *(Sp)* bristle and *Dr* eye marker over *CyO, hg-lacZ* and *TFLZ*

Name	*Chromosomal region*	*Source*	*Comment*
Sp / CyO; TM2, Ubx / MKRS, Sb (="CSTM")	Chromosome II, III		Triple balancer: *wingless* $^{Sternopleural\text{-}1}$ *(Sp)* bristle marker over *CyO* balancer / wing marker; *TM2* balancer with *Ultrabithorax (Ubx)* haltere marker over MKRS balancer with *Sb* bristle marker
TGX	X Chromosome	Gift by A. Michelson, Boston	*twist* driver, active from early on in the whole mesoderm; Baylies and Bate 1996
UASP-barr-eGFP III.1	Chromosome III	Gift by S. Heidmann, Bayreuth; Oliveira et al. 2007	*barren* rescue construct with GFP marker
UASP-barr-eGFP III.2	Chromosome III	Gift by S. Heidmann, Bayreuth; Oliveira et al. 2007	*barren* rescue construct with GFP marker
vtd $^{80Fh\text{-}1}$	80F	BL26164	
24B-Gal4 (How-Gal4)	Chromosome III	Reim and Frasch 2005	ubiquitous driver

2.3 Molecular and bacterial methods

2.3.1 DNA extraction from adult flies

A number of flies comprising a volume of about 0,5ml are anaesthetized at 4°C or killed in ether. The flies are then crushed with a pestle in an 1,5ml microcentrifuge

cup with 500μl Extraction Buffer for Genomic Fly DNA. The resulting suspension is incubated at 65°C for 20min.

70μl 8M potassium acetate are added, and the mixture is placed on ice for 30min.

Then the suspension is centrifuged for 15min at maximum speed at 4°C. The pellet is discarded, the clear supernatant is centrifuged again for 15min at maximum speed at 4°C. The pellet again is discarded, the supernatant in a new cup mixed with 0,5 volumes of isopropanol, cooled to -20°C. This mixture is centrifuged for 20min at maximum speed at 4°C.

The supernatant is discarded, the pellet washed twice by centrifugation for 10min each at maximum speed and 4°C first in 500μl 70% ethanol, then 300μl 70% non-denatured ethanol.

The pellet is dried by placing the open cup in a water bath at 37°C for 10min. Then it is solved in 100μl H_2O dd.

2.3.2 DNA extraction from *Drosophila* embryos

Up to ten fresh or recently fixed embryos are mashed in 20μl SquiB. Another 30μl SquiB and 1μl Proteinase K (20g/μl) are added; then the mixture is incubated for 30 min at 37°C and for 2 min at 82°C. From the supernatant, the DNA is precipitated with ethanol in a fresh cup as described below (section 2.3.5, p. 57) and solved in 5μl H_2O dd.

2.3.3 Photometric measurement of DNA concentration

The concentration of a DNA solution can be measured by its ultraviolet light absorption at a wavelength of 260nm.

For this, a quartz glass cuvette is filled with H_2O dd and placed in a photometer. The photometer is adjusted to a wavelength of 260nm and calibrated to a reference optical density (OD) of zero.

Next, the DNA solution is diluted 1:250 in 500μl H_2O dd, filled into the emptied quartz glass cuvette and the OD_{260} is measured. The DNA concentration

in $\mu g/\mu l$ can be calculated as follows:
$Concentration = OD_{260} \times Dilution factor/21$

2.3.4 Estimation of DNA concentration after DNA gel electrophoresis

DNA concentrations can be estimated by comparing the signal of a DNA solution on an agarose gel with a standard.

The DNA sulution is diluted 1:10, 1:100 and 1:1000, mixed with loading buffer and loaded onto a DNA electrophoresis gel along with a standard of known DNA concentration.

Electrophoresis is performed as described below. The gel, stained with ethidium bromide, is analyzed on an UV transilluminator.

2.3.5 DNA precipitation with ethanol

Various alcohols can precipitate DNA from a solution. This allows to remove impurities and to produce a DNA solution with higher concentration.

To precipitate a DNA solution with ethanol, 0,1 volumes of 3M sodium acetate and 2,5 volumes of 96% non-denatured ethanol, cooled to -20°C are added. This mixture is incubated at -20°C for 15min, then centrifuged at maximum speed for 30min at 4°C.

The supernatant is discarded and the pellet washed by centrifugation for 10min at 4°C in 200μl 70% non-denatured alcohol.

The pellet is dried by placing the open cup in a water bath at 37°C for 10min. Then it is dissolved in the desired amount of H_2O dd.

2.3.6 Amplification of DNA fragments by polymerase chain reaction

(Mullis et al. 1986; Saiki et al. 1988)

Polymerase chain reaction (PCR) as used here allows the in vitro amplification of an arbitrary stretch of DNA of at least 2kbp of length. This target sequence must be flanked by short known sequences. The technique can also be used to

attach short sequences to the amplified stretch, namely target sites for restriction endonucleases.

The DNA molecule that contains the sequence to be amplified is called the template. Short DNA molecules of 20bp–60bp length, called the primers, are designed to be complementary to sequences at the ends of the target sequence, facing inwards with their 3' end. These two should have a similar melting temperature.

Short sequences that are to be added at the ends of the PCR product can be inserted at the 5' ends of the primers. Restriction endonuclease target sequences that are to be digested while the PCR product is still linear need an overhang of at least 4bp for the restriction endonucleases to be able to bind.

Besides the template and the primers, a heat resistant DNA polymerase and the four desoxynucleotide triphosphates (dNTPs) are necessary.

In a volume of about 20μl -50μl , the mixture will contain:

- 10ng–100ng template DNA
- 25pmol of each primer
- 1/10 volume 2mM dNTPs
- 1/10 volume 10x reaction buffer (supplied with the enzyme)
- 1U DNA polymerase
- H_2O dd

The amplification happens in three steps:

First, the strands of the DNA are melted, i.e. separated by warming to 95°C for between 10s and 1min.

Next, the mixture is cooled down to the annealing temperature of the primers, usually between 50°C and 70°C, for about 30s. The primers can now bind to their complementary sequences at the ends of the target sequence.

Third, the mixture is heated to the working temperature of the polymerase, usually 68°C or 72°C. The longer the target sequence is, the longer this temperature must be held; the common Taq polymerase (from *Thermus aquaticus*) polymerizes about 1000 nucleotides per minute.

These steps are programmed in a thermocycler and repeated about 30-40 times. They are usually preceded by a prolonged melting step to denature the template completely, and followed by indefinite cooling to 4°C until the mixture is removed from the thermocycler.

The exact thermocycling sequences used in this study, along with various primer sequences, are given in section B, p. 134.

2.3.7 Topoisomerase mediated ligation

Vaccinia virus topoisomerase I has the ability to bind a certain target sequence on a DNA molecule, nick one strand, let the DNA unwind and religate the nick. This is used in TOPO vectors. These are linearized vectors with topoisomerase molecules bound to their ends. Upon contact with a free linear DNA molecule, the enzyme ligates it to the DNA molecule it is bound to and dissociates.

In this study, two TOPO vectors are used: pCR II TOPO TA and pCR II TOPO blunt. The former has a 5' one nucleotide "T" overhang to make use of the fact that Taq polymerase always attaches one non-specific nucleotide to the 3' end of the DNA strand it synthesizes, usually an Adenine. The T–A base pairing enhances the effectivity and specificity of the TOPO ligation. For polymerase formulations that do not attach the unspecific "A" overhang to their product, pCR II TOPO blunt without an overhang is used. The insert will be ligated with equal likelihood in either orientation.

The reaction is prepared as follows:

- 0,25μl -1μl TOPO vector
- 2μl PCR product
- *ad* 6μl H_2O dd

2.3.8 Sequencing

For sequencing, DNA samples are sent to AGOWA / LGC Genomics, Berlin, in a volume of 10 μl , diluted in H_2O dd. DNA content should be either 100 ng of plasmid DNA, 100 ng of a PCR fragment shorter than 500 bp, 200 ng of a PCR fragment between 500 bp and 2 kbp, or 400 ng of Fragments over 2 kbp.

Standard sequencing primers targeted at widespread plasmid sequences can be added by the company on request; alternatively, 20 pmol of a sequencing primer are added.

2.3.9 Restriction endonuclease digest

Restriction endonucleases (often called restriction enzymes) cut DNA strands at specific palindromic target sequences of 4–8 nucleotides. Often, they leave an overhang on one of the DNA strands. This overhang can be used as a "sticky end" to increase the efficiency of a ligation; the sequence recognition of the enzymes allows for a quick method to verify the identity of DNA molecules.

An analytical digest is typically composed like this:

- H_2O dd *ad* 10μl
- 1μl 10x reaction buffer (supplied with the enzyme)
- 0,25μl Restriction enzyme
- 0,25μg – 0,5μg DNA

The mixture is incubated for at least 45min at the temperature optimum of the enzyme, typically 37°C.

Preparative digests with more DNA are incubated with more enzyme in a larger volume for a longer duration. If the DNA to be digested is already linear, the restriction site must be at least four base pairs away from the DNA's end, and a tenfold concentration of enzyme must be used.

2.3.10 DNA gel electrophoresis

Because of their phosphate groups, DNA molecules are negatively charged. In an electric field, they wander towards the positive electrode. By letting them wander through a gel matrix, they can be separated by size.

Here, mostly 1% (w/v) agarose gels are used. Gels with lower concentrations of agarose allow for a finer separation of larger DNA molecules; for the separation of very small DNA, gels of higher concentration can be used.

Agarose in the necessary concentration is solved by boiling in TBE; after cooling to about 60°C, ethidium bromide solution is added to a final concentration of 0,6 mg/l. A gel is then cast in a frame with a comb placed at one end to create loading wells for the DNA samples.

Most proteins do not interfere with DNA gel electrophoresis, so the reacted mixtures of restriction endonuclease digests or PCRs can be used directly as samples. To let the DNA solutions sink down in the gel's loading wells, they must be made more dense by mixing with 20% 10x loading buffer. Besides glycerine, the loading buffer also contains negatively charged dyes that wander through the electric field roughly at the speed of 300bp DNA (bromophenol blue) or 1000bp DNA (xylene cyanol). This is to make the loading of the sample and the subsequent progress of the electrophoresis visible.

The electrophoresis chamber with the gel is filled with TBE, and the samples are loaded into the gel wells. In one well, a marker consisting of DNA fragments of known size and concentration is loaded. A voltage of about 7V/cm distance between the electrodes is applied for 30min-60min, depending on the running distance allowed by the size of the gel.

The ethidium bromide from the gel, a red fluorescent substance, intercalates in the DNA molecules; this way, the DNA bands can be easily observed on an UV transilluminator.

2.3.11 DNA extraction from an electrophoresis gel

After DNA fragments of different lengths have been separated by agarose gel electrophoresis, they can be extracted from the gel for further use.

For this, the relevant DNA band is cut out of the gel. To avoid destruction of the DNA by UV light , the gel is split in parallel to the running direction, cutting the sample lane into a smaller part that remains attached to the marker lane, and a bigger part that is used for DNA extraction. On an UV transilluminator, the part with the marker is notched at the level of the DNA band of interest. This gel part is then used as a pattern to cut out the relevant slice from the bigger part of the gel.

Mechanical elution

DNA can be extracted mechanically from a gel slice with the help of a centrifuge. For this, glass wool and fine glass beads are soaked in silanizing solution and dried. A hole is drilled into the bottom of a 0,5ml PCR cup with a heated needle. A few glass beads are layered over the hole. Over these, a bit of silanized glass wool is stuffed down in the cup.

The gel slice is placed in the prepared cup, which in turn is placed in a 1,5ml microcentrifuge cup. This contraption is then centrifuged at top speed for 5min. The DNA is precipitated from the eluate with ethanol as described above (section 2.3.5, p. 57).

DNA extraction with chaotropic agents and silica

Substances that are able to disorganize the tertiary structure of macromolecules by blocking and disrupting hydrogen bonds are called chaotropic agents. Many such chaotropic substances, like NaI or guanidium chloride ($C(NH_2)_3Cl$), are able to dissolve agarose gels.

In the presence of chaotropic agents, DNA binds to silica; so after dissolving a gel slice in a chaotropic buffer, the DNA can be captured with a silica column or silica beads.

In this study, two different commercial kits were employed for gel dissolving DNA extraction from: The JETSorb gel extraction kit (Genomed), which uses a silica suspension, and the GFX kit, which uses a silica matrix in a spin column. These kits were used according to their manuals.

2.3.12 Ligation using ligase

To ligate an arbitrary DNA sequence, called the insert, into an arbitrary vector, both must be linearized with restriction enzymes as described above.

It is preferable to use restriction enzymes that leave overhangs, as these can associate, enhancing the efficiency of ligation. Religation of the vector with itself is prevented by using two restriction enzymes that produce different overhangs; the insert must conversely be prepared with two compatible restriction enzymes.

This also makes sure that the insert can be ligated into the vector in only one orientation.

Vector and insert are prepared freshly, as the ligase relies on the DNA strands having phosphorylated ends, which tend to get dephosphorylated during storage. The unused fragments and all remaining enzymes and buffers from the digests are removed by gel electrophoresis and subsequent extraction as described above.

In an end volume of 20μl – 30μl with 10% 10x ligation buffer and optionally 5% PEG-4000, 1U T4 ligase is mixed with 50ng-400ng vector and about a threefold molarity of the insert.

The mixture is incubated over night at 16°C – 18°C; the next day, it can be used for transformation.

2.3.13 Transformation of chemically competent *E. coli* cells

A portion of chemically competent *E. coli* DH5α or TOP10 (Invitrogen) cells is thawed on ice. 3μg DNA are added (when transforming ligation mixtures, 20μl are used, as these often suffer from low efficiency) and left on ice for 30min.

Next, the mixture is heat shocked for 30s-90s at 42°C and then cooled on ice for 1min. 200μl LB medium, warmed to 37°C, are added, and the mixture is incubated shaking at 37°C for 1h.

The suspension with the bacteria are plated onto an agar plate with the antibiotic that the vector plasmid confers resistance against, to select for successful transformants. The plate is incubated over night at 37°C or over the weekend at room temperature, until bacterial colonies become visible; sometimes, somewhat longer incubation periods are necessary.

2.3.14 Analytical plasmid preparation by alkalic lysis

(Birnboim and Doly 1979)

Bacterial colonies are picked from an agar plate and inoculated in 3ml LB medium with 50-100μg/ml of the antibiotic the plasmid conveys resistance against. These cultures are incubated over night at 37°C.

The next day, about 2ml of each culture are filled into a 2ml microcentrifuge cup and centrifuged for 1min at top speed (13000rpm). The supernatant is discarded, the pellet is resuspended in 250μl S1 solution. 250μl S2 are added, and the mixture is incubated at room temperature for 5min.

Next, 250μl S3 are added, and the mixture is centrifuged for 10min at top speed. The supernatant is transferred into a new 1,5ml microcentrifuge cup, mixed with 600μl isopropanol and centrifuged at 4°C for 20min at top speed.

700μl 70% ethanol are added to the drained pellet and centrifuged at top speed for 10min at 4°C.

The pellet is again drained, and the open cup is placed in a water bath at 37°C to let residual ethanol evaporate. 50μl H_2O dd are added, and the pellet is solved by shaking at room temperature for at least 30min.

2.3.15 Large scale high purity plasmid preparation

For long term storage as well as for applications that need larger amounts or higher purity of DNA than what "mini" plasmid preparation affords, the JETstar II kit (Genomed) is used for "midi" scale plasmid preparation.

A picked bacterial colony or 5μl -20μl of bacterial suspension from a mini preparation are inoculated into 50ml LB medium with 100μg/μl of the antibiotic that the plasmid in question confers resistance against. This culture is incubated at 37°C over night.

The next day, a JETstar column is flushed with 10ml E4 solution for equilibration.

The bacterial suspension is centrifuged in a 50ml centrifuge tube for 10min at top speed (4500rpm). The drained pellet is resuspended in 4ml E1 solution. 4ml E2 solution are added and the mixture is incubated for 5min at room temperature. 4ml E3 are added, and the mixture is centrifuged for 10min at top speed.

The supernatant is filled onto the column, without all solid precipitates. After the supernatant has run through, the column is washed with 20ml E5.

The column is eluted with 5ml E6. The eluate is split into 5 2ml microcentrifuge cups. Each portion is mixed with 800μl isopropanol and centrifuged at top speed for 30min at 4°C.

The drained pellets are centrifuged with 1ml non-denatured 70% ethanol at top speed for 10min at 4°C.

The supernatant is discarded, and the open cups are placed in a water bath at 37°C for 10min to let residual ethanol evaporate. Then, each pellet is solved in 40μl H_2O dd by shaking for 30min.

Typically, this protocol yields DNA concentrations from 0,5μg/μl to 2μg/μl.

2.4 *Drosophila* methods

2.4.1 *Drosophila* stock keeping and crossing

Drosophila stocks and crossings are kept in transparent plastic tubes, typically 7cm high and 2cm wide, filled 2cm high with *Drosophila* culture medium. A little bit of dry yeast is added on top of the medium immediately before use. The tubes are closed with a plug of polymeric foam; fine pored foam has the advantage of not letting mites pass.

For stock keeping, ideally about 20 adult flies are placed in a fly tube. After four to six weeks at 18°C, the medium is used up and the adult flies are knocked into a fresh tube.

For crossing, *Drosophila* culture medium must be as fresh as possible. Virgin females must be used, as *Drosophila* females store sperm and are capable of laying fertile eggs for several days after just one mating; they are also reluctant to mate again during this time (Feng et al. 2014). Ideally, three or more females and more males than females should be placed in a fly tube. Offspring start to hatch after about 10 days at 25°C and after about 20 days at 18°C.

For easier handling and examination, flies can be anaesthesised with CO_2 or Ether.

2.4.2 Balancer chromosomes

(reviewed in Lindsley and Zimm 1992)

Balancer chromosomes contain large inversions that prevent crossing over with their non-balancer sister chromosomes, one or more dominant visible markers

that allow for easy detection of the balancer chromosome in the adult fly, and one or more recessive lethal alleles that kill flies in a homozygous setting with two copies of the balancer chromosome.

A recessive lethal allele that would normally slowly disappear from a population can be kept over a balancer chromosome as a stable stock. However, if the sister chromosome to the balancer chromosome does not carry a lethal mutation, the balancer chromosome itself will be selected out of the stock.

To tell homozygous and heterozygous embryos apart, so called "blue balancers" are used. These chromosomes carry a lacZ transgene, fused to a promoter that gives a characteristic expression pattern during embryonic development, like for example *hindgut-lacZ (hg-lacZ)* or *fushi tarazu-lacZ (ftz-lacZ)*. An α-β Gal antibody stain on a number of embryos will reveal all those that carry the balancer chromosome.

Instead of *lacZ*, *GFP* can be used as a reporter gene; such balancer chromosomes are sometimes called "green balancers".

In this study, the *CyO, hg-lacZ* blue balancer ist used for the second chromosome. It expresses βGal in the hindgut, starting at stage 9,accumulating its signal throughout the whole embryonic development.

As blue balancers for the third chromosome, *TM3, Sb, Dfd-lacZ* (="TDLZ") is used when later stages of embryonic development are analyzed; it expresses βGal in parts of the head. For earlier embryos, *TM3, Sb, ftz-lacZ* (="TFLZ") is used. It gives βGal expression in a striped, segmental pattern that gets very weak towards the end of embryonic development.

To keep a balancer chromosome as a stock, it is combined with a sister chromosome that carries a recessive lethal allele and a dominant visible marker, like *Krüppel* $^{Irregular\ facets\text{-}1}$ *(If)* or *wingless* $^{Sternopleural\text{-}1}$ *(Sp)* for the second chromosome or *Drop (Dr)* for the third.

To create a stock that holds a certain mutation over a certain balancer, the mutant flies are crossed against flies from the balancer stock. All offsprings that show the balancer's dominant marker but not the marker from the balancer stock's sister chromosome are collected for the new stock.

To introduce a homozygous viable mutation or transgene on the X chromosome into a stock with a balancer for the second or third chromosome, males from the stock are crossed against females from a balancer stock that carries the desired X-chromosomal gene. This step is repeated with F1 males. The new stock is then established from the progeny.

2.4.3 Generation of transgenic flies with P-element vectors

(Rubin and Spradling 1982; Spradling and Rubin 1982)

The P element is a DNA transposon that is ubiquitous in modern wild *Drosophila* but is absent in lab strains that were sampled from the wild before about 1920. It consists of a transposase gene flanked by two inverted 31bp repeats, the Transposase's target sequences. Only in germ line cells the transposase mRNA is spliced correctly to produce active Transposase protein; in somatic cells, an inactive Transposase working as a competetive inhibitor is produced instead.

To use the P element as a vector for the transformation of flies, the transposase gene is replaced with whatever sequence is to be inserted into the fly genome, and one or more marker genes for a dominant visible phenotype (usually a mini-*white* gene). This construct is assembled in a bacterial plasmid vector for easy amplification in *Escherichia coli*.

The P element vector is then injected into the posterior area of blastoderm stage *Drosophila* embryos together with a helper plasmid that contains a complete transposase gene, but not the flanking inverted repeats. When the pole cells (the germ line cells) separate from the soma, the Transposase translated from the helper plasmid pastes the area between the inverted repeats into the germ line cell's genome in a more or less random location.

Microinjection

Before use, the vector solution is centrifuged at maximum speed at 4°C to remove all traces of solids, as they would clog the needle.

Embryos are collected hourly from *white*$^-$ (*w*$^-$) egglays, dechorionated and rinsed as described above. They are glued to a cover slip with heptane glue and

overlayered with Voltalef oil (low molecular weight poly-chlorotrifluoroethylene, PCTFE) to prevent dehydration. Each embryo is injected in its posterior end with a needle drawn from a glass micropipette. The coverslip with the embryos is then transferred to an apple juice agar plate, again overlayered with Voltalef oil and incubated at 25°C.

Collecting the transgenic flies

After about 24h, larvae will hatch; these are collected into a fly tube with *Drosophila* culture medium.

After eclosion, the adult flies, which partly have transformed germ line cells, are crossed against w^- flies; in the next generation, transformed flies can be recognized by their pale orange to yellow eye color, which is caused by the *white*$^+$ marker transgene.

Separating multiple insertions by meiotic recombination

In *D. melanogaster*, only the germ line cells of female flies go through crossing over at meiosis; so to separate two insertions on the same chromosome into different offsprings, the chromosome must be kept over a non-balancer chromosome in a female fly. To isolate multiple insertions of the transgene, the transgenic flies are crossed against w^- flies for several generations, using always female offspring.

Identification of the chromosome carrying the P-element and establishment of stocks

These flies are then crossed against a double balancer like CSTM or *Sp/CyO,hg-lacZ; Dr/TM3,ftz-lacZ*; this crossing is repeated with the male w^+ offspring. Some second generation offspring will now have a dominant marker over a balancer for one chromosome and the w^+-marked transgene of interest over a balancer on the other chromosome. Both these flies and their siblings with a wild type situation on the non-transgenic chromosome pair can be collected to establish stocks; if the P-element insertion does not create a lethal allele, homozygous transgenic flies will appear in the next generation.

2.4.4 Ectopic expression with the Gal4–UAS system

(Brand and Perrimon 1993)

Gal4 is a transcriptional activator protein from *Saccharomyces cerevisiae* that binds to the Upstream Activating Sequence (UAS) and activates the expression of a downstream gene. This is a mechanism that remains functional when expressed transgenically in *Drosophila*.

Typically, the Gal4 and UAS components will come from two different fly strains crossed together.

The Gal4 strain or "driver" is often created by enhancer trap mutagenesis: An insertional vector carrying the Gal4 ORF with a core promoter, but without enhancer is inserted randomly into the genome. This way, it sometimes will be expressed under the control of an enhancer in the vicinity of its site of insertion.

It is also possible to create a driver by inserting a preassembled construct consisting of a known, specific enhancer sequence and the *Gal4* gene into the fly genome.

Many well characterized driver strains can be ordered from *Drosophila* stock centers.

The UAS sequence can be included in constructs together with a core promoter sequence, often in multiple repeats. This can be used to express a tagged version of a protein of interest, perhaps as a rescue construct in a mutant; to ectopically misexpress a gene or simply to have a reporter gene like *lacZ* or *eGFP* expressed in the pattern of Gal4 driver activity.

2.4.5 Egglays

To receive *Drosophila* eggs, stock flies or a crossing are kept on grape or apple juice agar.

For smaller numbers of flies, small fly tubes filled about 1cm high with grape juice agar are used; a little bit of dry yeast is added on top of the medium, and the tube is closed with a polymeric foam plug.

For larger numbers of flies, a tube of about 5cm diameter is set on an apple juice agar plate; the other end of the tube is closed with wire mesh or gauze. On the apple juice agar, a little bit of rehydrated, creamed dry yeast is added.

The flies start to lay eggs quite instantly; if they are left on the egglay medium for example for 12h, the eggs harvested will be mostly 12h old.

2.4.6 Formaldehyde fixation of *Drosophila* embryos

(Frasch et al. 1987; Dequin et al. 1984)

Embryos are collected by wiping them off the egglay agar medium with a brush and TNX/Tween. They are dechorionated with TNX/Klorix under microscopic control until the chorion is dissolved (typically a few minutes). The TNX/Klorix solution is then drained completely, and the embryos rinsed once in PBT. Then they are overlayered with heptane and transferred into microfuge cups with equal amounts of heptane and FPBS, typically 300μl – 500μl each, depending on the amount of embryos. The cups are then vigorously shaken on a Vibrax shaker for 15min; embryos for use in *in situ* hybridizations are shaken for 20min. Heptane and FPBS are then drained and the embryos rinsed once in fresh heptane. Then 300μl – 500μl each of methanol and heptane are added to the embryos and vigorously shaken on a Vortex shaker. The liquid is removed together with all embryos that have not sunken to the bottom. The embryos are rinsed twice in methanol and then left in another 500μl of methanol. Before further use, the embryos should be incubated in methanol over night; they can be stored in the methanol for years.

2.4.7 Antibody stains

Antibodies against a specific protein can be generated by immunizing an animal against it. With some luck, the antibody will bind to its antigen even when it is in a fixed whole-mount *Drosophila* embryo.

In this context, all antisera, purified antibody solutions and all partly purified products in between, monoclonal or polyclonal, are here referred to (somewhat imprecisely) as "antibodies".

Detecting the bound antibody usually involves having a "secondary antibody" bind to it; this is an antiserum from an animal immunized against antibodies from the species the primary antibody was raised in. It contains polyclonal antibodies

targeting several epitopes on the surface of the primary antibody, thus amplifying the potential signal.

It is possible to perform a double stain with two different primary antibodies on the same embryo. If the antibodies have been generated in different species, they can be labeled differentially with two different secondary antibodies.

Primary antibody solutions can typically be used two or three times before the antibody is used up; some can be used more often, increasing in signal clarity as unspecifically binding components get absorbed by the embryos.

Primary antibody incubation

A number of embryos that makes a volume of roughly 20μl are transferred into an 1,5ml microcentrifuge cup with a cut up 1ml pipette tip. They are rehydrated by washing 3x 10min in PBT.

The primary antibody is diluted in PBT as listed (2.1.2) to a volume of 250μl –500μl and incubated on the embryos either for 45min – 2h at room temperature under gentle shaking or overnight at 4°C.

In a double stain, the two antibodies can be applied in parallel as one solution, or sequentially one by one.

Blocking

After incubation with the primary antibody, the embryos are washed 3x for 10min in PBT.

To saturate unspecific binding potential, the embryos are incubated for 20min – 30min in PBT with 2% non-immune ("normal") serum, preferentially from the species the secondary antibody was generated in. This step is called "blocking".

2.4.8 Immunofluorescent stain

Secondary antibodies that are coupled to fluorophores are a quick method of detection that also allows for advanced microscopic techniques like computed image deconvolution (CID).

Incubation

The secondary antibodies are diluted as listed (2.1.2) in PBT with 2% non-immune goat serum. In a double (or multiple) stain, the detection of the different primary antibodies can happen in parallel in the same solution.

Incubation is for 1h – 2h gently rocking at room temperature. The embryos are then washed 3x 10min in PBT.

Mounting

The embryos are drained and mixed with 40μl Fluoromount. They are transferred to a microscopic slide and spread around with a needle tip. A coverslip is put on carefully, so as not to entrap any air bubbles. Residual air is pushed out by gently pressing the coverslip down.

2.4.9 Immunohistochemical stain

A very sensitive way to detect the primary antibody is immunohistochemical staining with a biotinylated secondary antibody and peroxidase in an Avidin-Biotin complex (ABC).

Avidin binds Biotin with high affinity in four independent binding sites. When Avidin is incubated with polybiotinylated horseradish peroxidase, complexes with several molecules of peroxidase and Avidin are formed. These complexes can permeate into the fixed embryo, where the Avidin binds to the Biotin groups on the secondary antibody, which in turn is still bound to the primary antibody.

The peroxidase can then be detected by its ability to oxidate a soluble chromogen into an insoluble pigment.

Preincubation of secondary antibody

To remove components with unspecific binding activity, the secondary antibody is incubated at room temperature for at least 30min on a fresh batch of fixed embryos (wild type or any other) that have been rehydrated as described above. For this, the secondary antibody is diluted 1:200 in PBT with 2% serum of the species in which the secondary antibody has been generated (typically goat or horse).

This preincubated antibody can be stored or used instantly.

Secondary antibody incubation

The preincubated antibody solution is diluted 1:5 in PBT with 2% serum, yielding a final antibody dilution of 1:1000. 500μl of this solution are added to the drained embryos and incubated gently shaking at room temperature for 45min – 2h.

After this, the embryos are washed 3x for 10min in PBT.

Detection

While the embryos wash, for every batch of embryos 4μl Vectastain ABC Solution A and 4μl solution B are added to 500μl PBT and incubated gently shaking at room temperature for 30min.

The solution is then added to the drained embryos and incubated gently shaking at room temperature for another 30min.

The embryos are washed 3x for 10min in PBT and transferred with 500μl PBT into small glass dishes. 10μl -20μl DAB (10mg/ml), 5μl H_2O_2 (1%) and 10μl NiCl (1% w/v) are added; if this is the second round of a double stain, the NiCl is left out.

The staining process is observed under a stereo microscope. When the stain is strong enough, the staining solution is drained and replaced with PBT. The embryos are transferred back into microcentrifuge cups and washed 3x for 10min in PBT.

The used staining solution and anything that has come into contact with it is decontaminated with Klorix to destroy the mutagenic DAB.

Mounting in EPON

The embryos are washed in 96% ethanol once briefly, then another time for 10min under gentle shaking, then over night at 4°C.

For mounting, they are transferred onto a microscopic slide together with as little ethanol as possible. Excess ethanol is allowed to evaporate, but the embryos must not dry out completely.

A drop of EPON is dripped on and the embryos are spread around with a needle tip. A coverslip is laid on them carefully to avoid air bubbles to be trapped.

If the space under the coverslip is not filled completely with EPON, little drops are added at the edges so they can be sucked under by capillary forces.

The slide is then baked overnight at 70°C to harden the EPON.

2.4.10 Fluorescent *in situ* hybridisation (FISH)

(Lécuyer et al. 2008, simplified)

RNA probe synthesis by *in vitro* transcription

RNA *in situ* hybridization allows to visualize the distribution of mRNAs in a formaldehyde-fixed embryo. The technique is based on the formation of nucleic acid double strands from an RNA that occurs in the embryo and a labeled probe RNA or DNA.

Here, RNA probes labeled with the digoxigenin (DIG) hapten are used. These probes are produced by *in vitro* transcription from a DNA template using a bacteriophage T3, T7 or SP6 RNA polymerase. The template DNA is kept in a vector that can be amplified in bacteria and has promoter sites for the phage RNA polymerases, facing into the insert from both sides.

The sequence of the probe must be in the "antisense" direction, so the probe can form a duplex with the target RNA. As a negative control, a probe in "sense" direction is often also synthesized.

With a short probe sequence, *in vitro* transcription is likely to run into the vector sequence. To prevent this, the vector is linearized by digestion with a restriction enzyme cutting downstream of the desired sequence. When using a long insert for probe generation (>1kbp), this step is not necessary, as the processivity of the phage RNA polymerases is rather limited.

The RNA probe is sythesized using the DIG RNA Labeling and Detection Kit (Roche Diagnostics, Mannheim). The reaction is mixed as follows:

- H_2Odd ad 20μl
- 2μl 10x Transcription buffer
- 2μl DIG RNA labeling mix
- 1μl RNA polymerase

- 1μg template DNA

The reaction is incubated for 2h at 37°C. After that, the DNA is precipitated with ethanol and solved in 50μl H_2Odd.

Testing the probes

The efficiency of the probe synthesis is variable. To assay the signal strength a probe yields and to gain a clue on the concentration it must be applied in for *in situ* hybridization, it is diluted 1:10, 1:100 and 1:1000 and spotted on a Hybond N membrane in spots of 1μl .

After drying, the membrane is fixed with ultraviolet light using the autocrosslink setting of the UV Stratalinker. The membrane is rinsed shortly with DIG1, then blocked in DIG2 for 10min.

Then, the membrane is incubated gently rocking for 15min in 5ml DIG1 with 1μl phosphatase-coupled anti-DIG antibody. The membrane is then washed twice for 5min in DIG1.

For detection of the signal, the membrane is equilibrated in DIG3, then developed for 10min in 2ml DIG3 with 10μl NBT and 10μl X-phosphate. Then, the membrane is washed thoroughly in tap water and dried.

Hybridization

A volume of up to 50μl of formaldehyde-fixed embryos (preferentially fixed for 20min to reduce bloating during hybridization) is washed 3x for 10min in 500μl PBT, then equilibrated in 500μl PBT/50% HS and 100% HS for 10min each.

Then the embryos are prehybridized in 200μl HS at 56°C for at least 2h. The hybridization probe is meanwhile diluted in 50μl –100μl HS in a concentration depending on the signal strength of the probe (typically around 1:50). This probe solution is boiled at 98°C for 15min and then pipetted on the drained embryos while keeping them at 56°C. The embryos are incubated with the probe solution over night at this temperature.

The next day, the embryos are drained and washed 3x 10min in HS, preheated to 56°C. Then they are equilibrated with HS/25% PBT, HS/50% PBT and PBT/25% HS for 10min each at 56°C. After that, they are washed 3x 5min in PBT at 56°C.

The embryos are cooled to room temperature and washed for another 5min in PBT,then blocked for 10min in PBTB.

Detection

1μl biotinylated anti-DIG-antibody (0,5μg/μl) is diluted in 200μl PBTB. The embryos are incubated in this antibody solution for 2h at room temperature, or, preferentially, at 4°C over night.

After incubation, the embryos are washed 6x 10min in PBTB, then once with PBT and twice with PBS for 5min each.

1μl tyramide conjugate is diluted 1:100 in tyramide reaction buffer, added to the rinsed embryos and incubated for 2h. For this step and all the following, the embryos should be protected from light, to prevent fluorophore bleaching.

The embryos are washed 6x 10min at room temperature or over night in PBS. Then they are mounted in Fluoromount as described under "Immunofluorescent stain" (section 2.4.8, p. 71).

Double labeling with anti–βGal antibody

Most Antibodies do not seem to work on embryos on which an *in situ* hybridization has worked; the only known exception is polyclonal rabbit anti–βGalactosidase (Cappel, Hamburg).

This primary antibody can be applied together with anti-DIG or right afterwards with a short wash in between. The fluorophore-conjugated anti-rabbit secondary antibody can be applied before the tyramide reaction or afterwards.

Alternatively, the whole anti–βGalactosidase stain can be executed after the tyramide reaction.

Chapter 3

Results

3.1 The *rols7* mRNA requires its 3'-trailer for localization in somatic founder cells, and is also localized in visceral founder cells

3.1.1 In visceral founder cells, the *rols7* mRNA is intracellularly localized

In Kesper 2005, it was shown that the *rols7* transcript in the somatic founder cells is localized in spots close to the cell membrane. In this study, an improved fluorescent *in situ* hybridization (FISH) protocol (Lécuyer et al. 2008) is used with an antisense RNA probe generated from *rols* LD1 cDNA, on embryos carrying the rP298-lacZ marker (Nose et al. 1998). The embryos are stained with polyclonal rabbit anti-βGalactosidase antibody (Cappel, Hamburg) to visualize the lacZ-expressing founder cell nuclei (other anti-βGalactosidase and anti-β3Tubulin antibodies do not work effectively on *in situ* hybridized embryos).

These experiments show that the founder cells of the circular visceral muscles also have *rols7* transcript localization; the localization towards the inner side of the band of founder cells can give the impression of a narrow stripe of *rols* transcript running along each side of the forming gut (Fig. 3.1 E, F).

The same *in situ* hybridization technique and immunofluorescent anti-βGal stain applied on embryos carrying bHLH54F-lacZ, which marks longitudinal visceral founder cells (Georgias et al. 1997; Kusch and Reuter 1999; Ismat et al. 2010), shows the *rols* transcript localized in spots close to the tips of these spindle-shaped cells (Fig. 3.2 C, D).

3.1.2 The 3'-trailer of the *rols* mRNA is necessary for transcript localization in somatic founder cells

While a 2 kbp region upstream of the *rols7* transcription start is a sufficient promoter to drive a reporter gene strongly in all somatic founder cells (Kesper 2005), such a reporter construct does not reproduce the intracellular localization of the *rols7* transcript (Kesper, personal communication).

As mRNA localization is often achieved by the transcript's 3'-trailer, a reporter construct named pRODO was created, featuring the 2 kbp *rols7* regulatory region, a complete eGFP reading frame, and 1.8 kbp of the *rols* downstream sequence. This was achieved by excision of the *lacZ* reporter gene and SV40 trailer from the ROPOZ construct (Kesper 2005) and subsequent insertion of an eGFP and *rols* genomic downstream sequence, preassembled in another plasmid (Jacobs 2006).

The long *rols* genomic downstream region was included to isolate the reporter gene from the rest of the P-element vector and the genomic surrounding; also, the seven polyadenylation signals in this sequence, roughly the 5-fold of what is to be statistically expected (Jacobs 2006), might have a biological significance.

In the fly, pRODO is supposed to be transcribed in the somatic founder cells into an mRNA coding for eGFP, with the 300 bp *rols* mRNA trailer. Antibody staining against GFP shows that the reporter gene is expressed as expected (Fig. 3.3).

Fluorescent *in situ* hybridization (FISH) with an RNA probe against eGFP on pRODO embryos with an rP298-lacZ founder cell nuclear marker shows that the reporter mRNA gets intracellularly localized, much like wild type *rols* mRNA (Fig. 3.4).

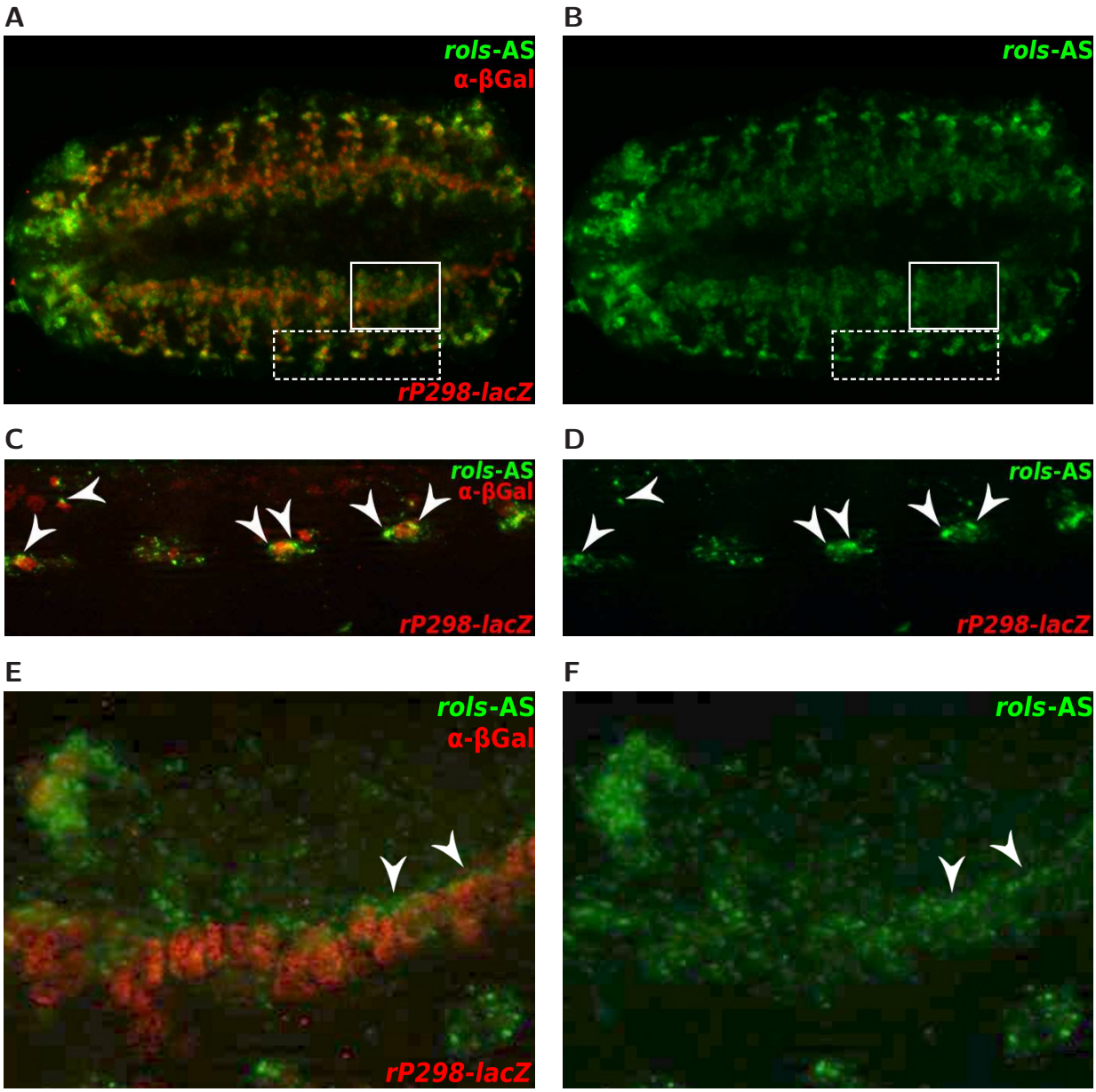

FIGURE 3.1. **In the circular visceral muscle founder cells, the *rols* mRNA is intracellularly localized.** Fluorescent *in situ* hybridization with a *rols* antisense RNA probe in green. rP298-lacZ (stained red with anti-βGal antibody) marks the founder cells of all embryonic muscles. **A** , **B** Overview: Stage 12 embryo, ventral view. Area in dashed frame is shown enlarged in figures C and D, area in thick frame in E and F. **C**, **D** Image composed from three consecutive CID sections, focussing on the somatic founder cells. The *rols* transcript is localized to patches in the periphery of the cells (arrowheads), as shown in KESPER 2005. **E** , **F** CID image, focussed on the circular visceral myoblasts. The *rols* transcript appears localized to the periphery of the founder cells (arrowheads), forming a band of transcript along one side of the founder cell band.

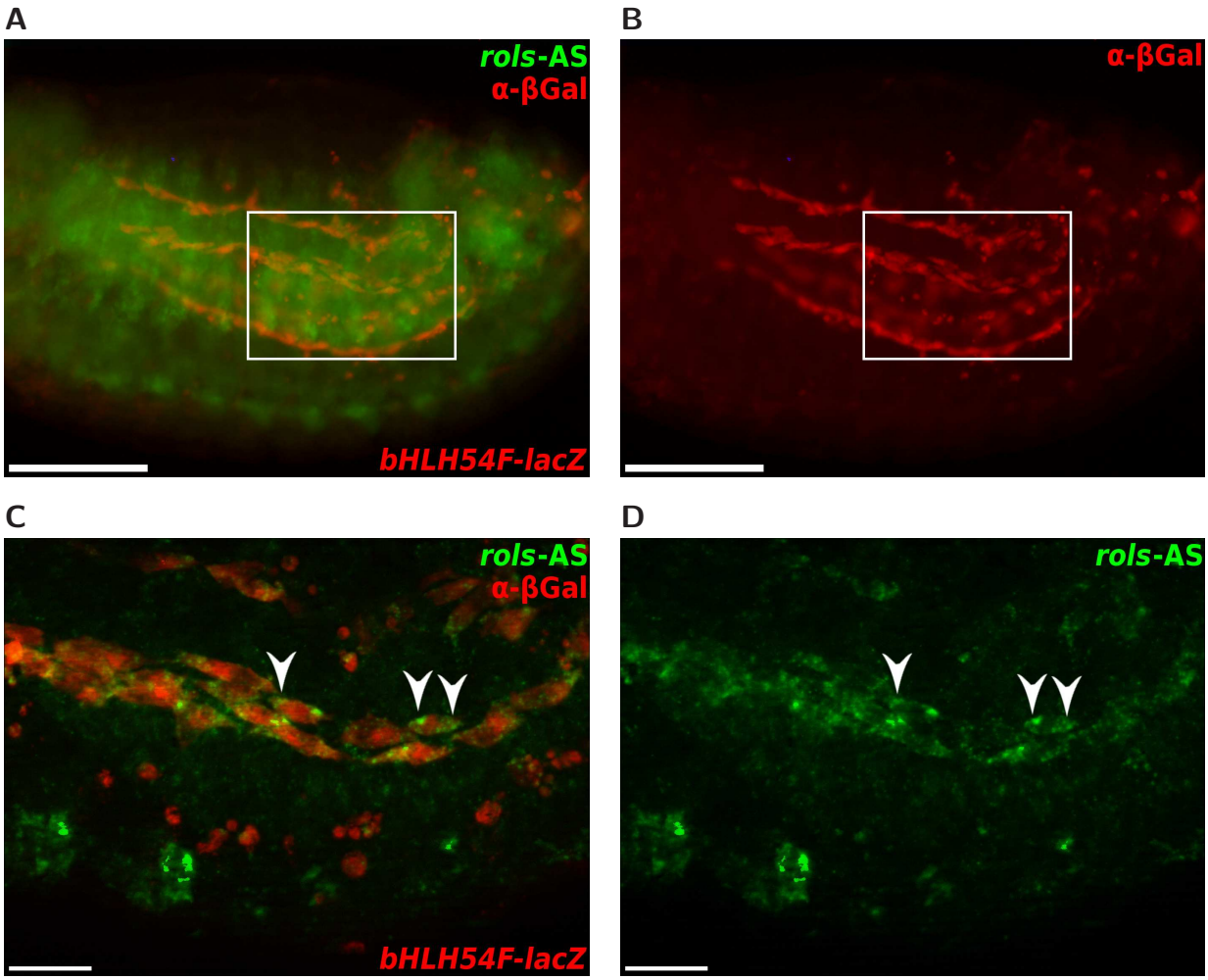

FIGURE 3.2. **In the longitudinal visceral muscle founder cells, the *rols* mRNA is intracellularly localized.** Fluorescent *in situ* hybridizations with a *rols* antisense RNA probe on a *bHLH54F-lacZ* embryo that expresses β-Galactosidase in its longitudinal visceral founder cells. FISH in green, anti-βGal stain in red. **A** , **B** Overview: Stage 13 embryo. Scale bar: 100μm. Framed area enlarged in the following images. **C** , **D** Images composed from several consecutive CID sections. The *rols* mRNA is localized at the poles of the spindle-shaped founder cells (arrowheads). Scale bar: 20μm

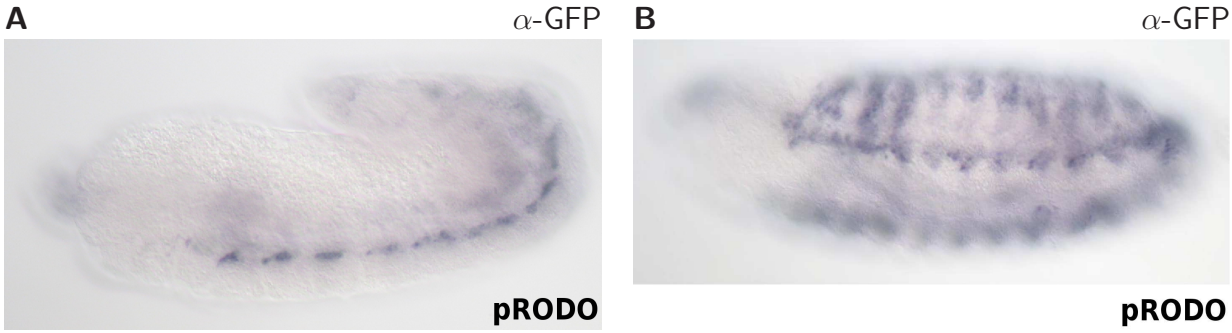

FIGURE 3.3. **An immunohistochemical anti-GFP stain on pRODO6.1 embryos shows the expression of pRODO in the somatic expression domain of *rols*.** **A** Stage 10. The eGFP reporter protein is detected in the earliest groups of founder cells. **B** Stage 12. eGFP protein is detected in the forming musculature.

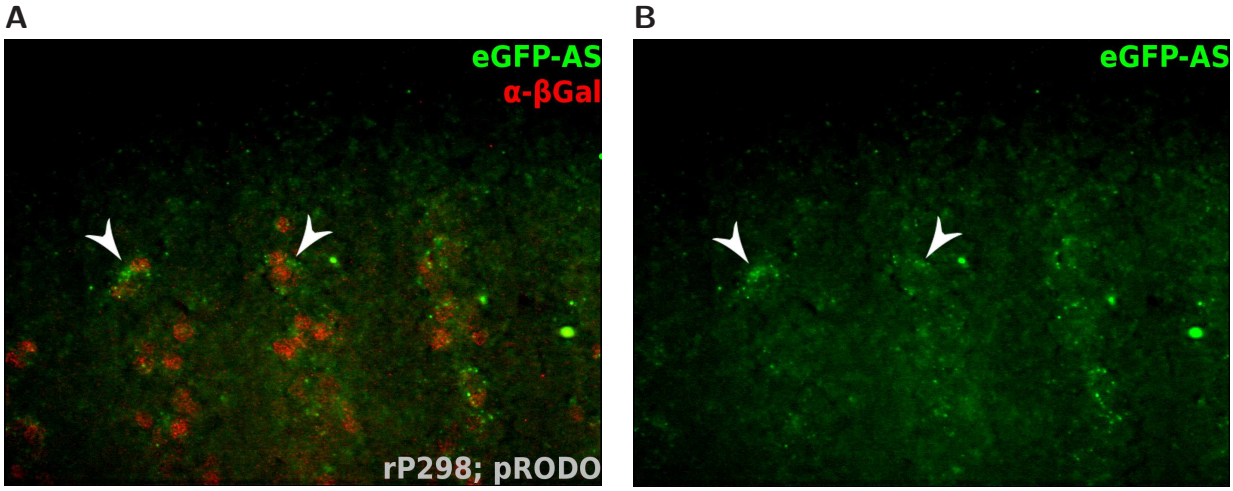

FIGURE 3.4. **The pRODO reporter mRNA is intracellularly localized like *rols* mRNA.** Fluorescent *in situ* hybridization with an eGFP antisense RNA probe (green) on an embryo from a crossing of rP298-lacZ with pRODO6.1 flies; image composed from a CID stack. The eGFP reporter mRNA is localized into spots (arrowheads) outside of the nuclei. **A** shows the rP298-positive founder cell nuclei in red.

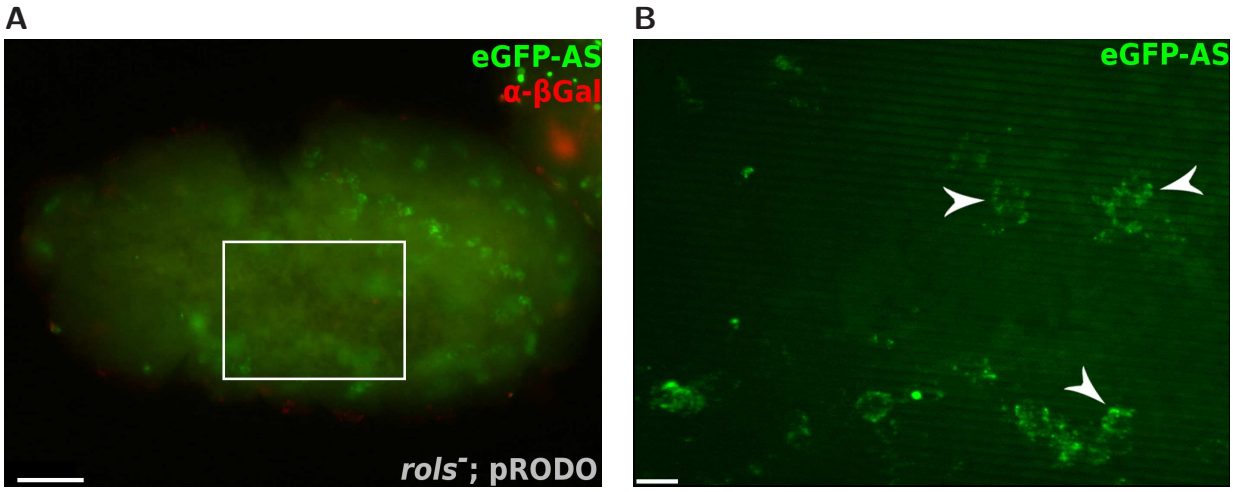

FIGURE 3.5. **Even in the absence of any native *rols* mRNA, pRODO mRNA is intracellularly localized.** Early stage 12 embryo with pRODO reporter in a *rols* deficient *Df(3L)BK9* background. *In situ* hybridization with an antisense RNA probe against eGFP in green. **A** α-βGal antibody stain in red. No balancer stain is visible, so the embryo is homozygous *rols*$^{-}$. Scale bar 50μm **B** Enlargement of framed region in A. Image composed from a CID stack. The reporter transcript is localized in patches (arrowheads). Scale bar 10μm.

Often, mRNA localization involves di- or multimerization of transcripts facilitated by special RNA:RNA interaction domains, which are distinct from the sequence domains recognized by the localization machinery (FERRANDON ET AL. 1997; HACHET AND EPHRUSSI 2004; BULLOCK ET AL. 2003; JAMBOR ET AL. 2011; HARTSWOOD ET AL. 2012). This allows transcripts to be localized by "piggy backing" based on mere partial homology, even when they do not contain the localization signal itself.

To exclude this possibility, the FISH experiment is repeated on embryos carrying pRODO and rP298 in a *rols*$^{-}$ background, showing that the pRODO reporter transcript gets localized independently from wild type *rols* mRNA (Fig. 3.5).

3.2 For normal myogenesis, Barren is required before the progenitor division

3.2.1 The E831 myogenic mutation in 38A7-B2 is not complemented by *barren* mutants

E831 is an EMS-induced lethal mutant of the second chromosome (Hummel et al. 1999a,b). It was found to show a muscle phenotype by Anne Holz, in her screen that led to the identification of *wasp* and *Arp3* as relevant for myogenesis (Schäfer et al. 2007; Berger et al. 2008). An initial complementation analysis identified three lethal mutations on the chromosome (Reichert 2004). In Jacobs 2006, a refined complementation analysis brought the number of lethal mutations up to four, narrowing down the site causing the E831 muscle phenotype to chromosomal region 38A7-B2. For this study, several known lethal mutations from that region were tested for lethality in a transheterozygous situation with the E831 chromosome; thus, *barren* was identified as allelic to the E831 38A7-B2 mutation.

Both transheterozygous *barr* ^{L305} /E831 (Fig. 3.6 C) and homozygous *barr* ^{L305} embryos (Fig. 3.6 D) show a muscle phenotype much like that of a homozygous E831 embryo (Fig. 3.6 B). The same goes for the P-element insertion *barr*^{k14014}, both in homozygous embryos and in all transheterozygous permutations (not shown).

If E831 contains a *barren* mutation, you would expect E831 embryos to also show the aberrant phenotype of the central nervous system (cns) that is typical for *barren* mutants (Bhat et al. 1996). A stain with the BP102 antibody, which decorates the cns, shows that this is the case (Fig. 3.7).

3.2.2 The E831 chromosome contains a nonsense mutation of *barren*

For molecular identification of the *barr* mutation in E831, the mutant *barren* gene from that line needed to be amplified and sequenced.

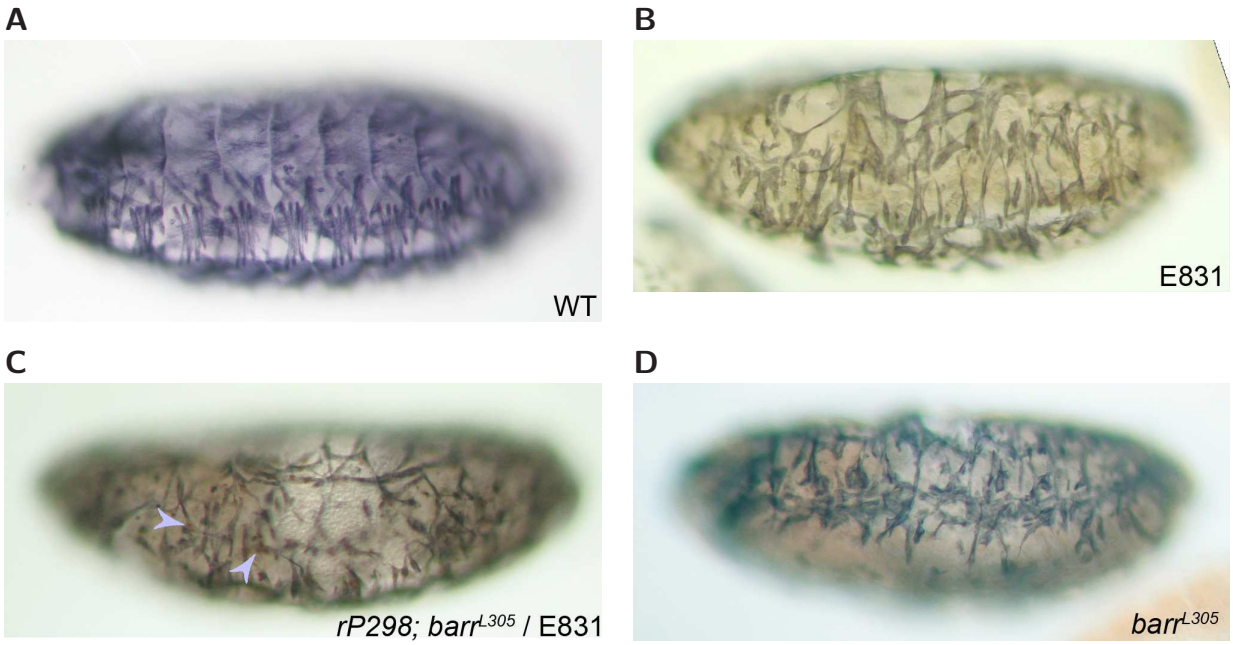

FIGURE 3.6. **The mutation causing the muscle phenotype in the mutant line E831 is allelic to *barren*.** Embryos are histochemically stained with antibodies against β3Tubulin to show the musculature. **A** Wildtype embryo, stage 17. **B** E831 embryo, stage 16-17. Note the disoriented muscles and the large dorsal gaps in the muscle pattern. **C** Transheterozygous *rP298; barr* ^{L305} */E831* embryo, stage 16. An additional antibody stain against βGal on this rP298-lacZ embryo shows the nuclei of Duf/Kirre positive cells, demonstrating that at least some of the muscle fibres are multinucleated (arrowheads). **D** *barr* ^{L305} embryo, stage 16. The muscle phenotype resembles that of E831.

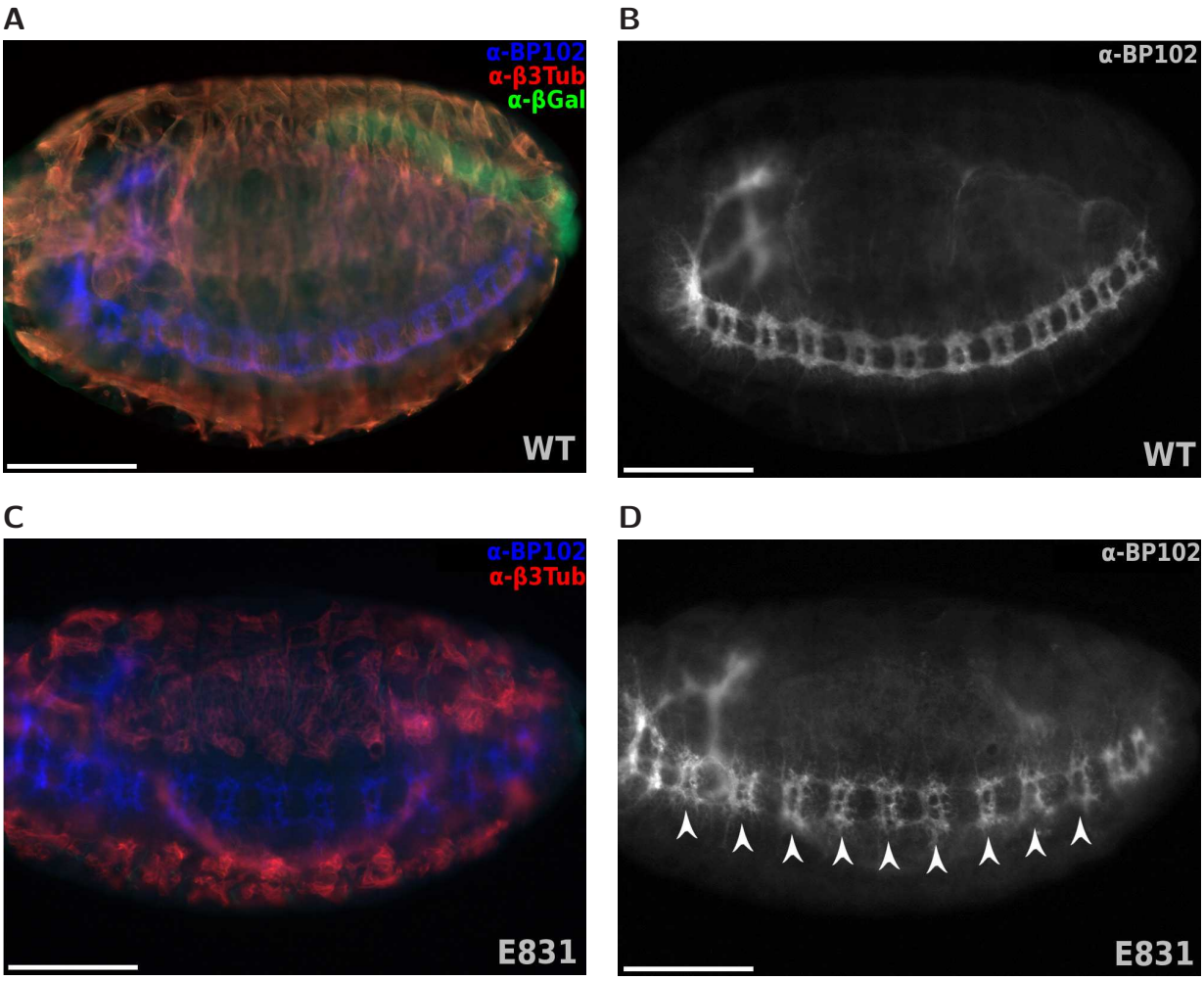

FIGURE 3.7. **As can be expected from a *barren* allel, E831 shows a disturbed central nervous system.** The cns is visualized with an α-BP102 antibody stain. **A** , **B** Wild type embryo, stage 16 **C** , **D** E831 embryo, stage 15. The ganglia appear malformed (arrowheads). Scale bars 100μm.

For this, embryos from the fly lines *rP298-lacZ; E831/ CyO, hg-lacZ* and *E832/ CyO, hg-lacZ* were immunohistochemically stained with an anti-βGal antibody, which stains the LacZ gene product. From each fly line, a few embryos that do not show the hg-lacZ marker stain were selected; these are homozygous mutant embryos that do not carry a balancer chromosome. The rP298-lacZ marker serves as an internal control to assure the effectivity of the immunohistochemical stain.

From these homozygous mutant embryos, genomic DNA was extracted. The DNA from E832 serves as a wild type control; this mutant line was created in the same mutagenesis screen as E831, using the same progenitor line, and complements all mutations in its sister.

The amplification of the gene was done in two segments of roughly 2 kbp each (for details, see Appendix B, p. 134) The PCR products were ligated into the pCRII vector. After further propagation in *E. coli* cells, the resulting plasmids were sequenced.

As expected, the sequences derived from E832 translate into a wild type Barr protein; however, the sequences from E831 indicated a two base deletion in the upstream segment (Fig. 3.8). To corroburate this finding, two additional sequencing primers, AAA TGC GCA TGG CGT CCA AG and CTG GTT CCT CTT TAG AAG CC, were used to get bidirectional sequence readout of the mutated region.

This way, the E831 *barr* mutation could be identified as a deletion of base pairs 145 and 146 of the first coding exon, with the frame shift resulting in a stop signal twelve codons downstream. The resulting mutant protein is 59 amino acids long, in comparison to the wild type 735.

3.2.3 *Cap-G* also shows a muscle phenotype

As Barren is a Condensin subunit, we tested mutants of other components of Condensin and the related Cohesin complex for their embryonic musculature phenotype. We found that *Cap-G*^{6}, a nonsense mutation and probably null allele of the non-SMC Condensin component gene *Cap-G*, has a phenotype similar to but less variable than that of *barren*: Randomly disturbed somatic muscle pattern, malformed pharynx musculature, missing or duplicated heart cells, incomplete

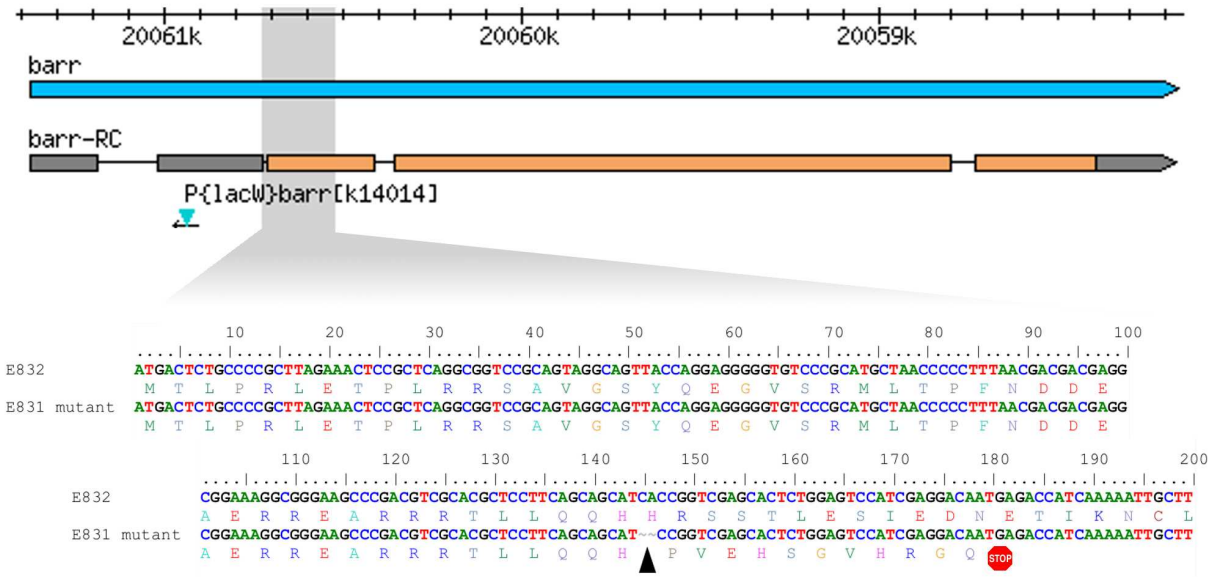

FIGURE 3.8. **The mutant line E831 contains a two bp deletion in the first coding exon of *barren*.** E831's sister line E832 gives a wild type sequence for the *barr* gene. In the E831 mutant chromosome, basepairs 145 and 146 of the first coding exon are deleted (black arrowhead). The resulting frame shift causes a stop codon (red octagon) twelve codons downstream of the deletion. The full gene span of *barren* is shown above in blue. The longest transcript variant, *barr-RC*, is shown in orange (coding region) and dark grey (non-coding region). The sequence shown in detail is indicated in the gene span in light grey. The cyan arrowhead on the small black arrow marks the P element insertion generating the allele $barr^{k14014}$.

dorsal closure. Unlike most *barren* embryos, *Cap-G*^{6} mutant embryos often show an altered overall shape. (Fig. 3.9C).

Cap-G^{64}, a D254Y missense mutation (Philp 1998; Cobbe et al. 2006), shows a severe but very variable phenotype, ranging from embryos with reduced, misarranged musculature and missing or duplicated heart cells (Fig. 3.9 A) to embryos of aberrant shape without recognizable musculature (Fig. 3.9 B). Transheterozygous *Cap-G*^{6} / *Cap-G*^{64} embryos show the variable yet often strong phenotype of *Cap-G*^{64} (Fig. 3.9 D).

The *Cap-D2*^{f03381} mutant does not show any obvious muscle phenotype (Fig. 3.10 A). Transheterozygous crossings of deletions that cover Cap-D2 show no muscle phenotype either (Fig. A.16, p. 130).

Where the Condensin complex has a SMC2-SMC4 dimer at its core, Cohesin is based upon a SMC1-SMC3 dimer. It plays a somewhat different cytophysiological role than Condensin. Defects in the Cohesin complex lead to premature sister chromatid separation during mitosis (Lee and Orr-Weaver 2001), as well as gene regulation defects during interphase (Pauli et al. 2008, 2010; Schaaf et al. 2009, reviewed in Dorsett 2009).

The *SMC1*^{exc46} deletion eliminates most of the *SMC1* gene; *SMC1*^{exc46} is lethal in a heterozygous situation with the larger covering deletion *Df(3R)Exel6197* (95D8–95E1). However, *SMC1*^{exc46} embryos show no muscle phenotype (Fig. 3.10 B).

vtd$^{80Fh\text{-}1}$ is an EMS-induced point mutation in the first protein-coding exon of the Kleisin gene *vtd* that turns the 18th residue into a stop codon (Hallson et al. 2008). It shows no embryonic muscle phenotype (Fig. 3.10 C).

3.2.4 The expression patterns of some muscle identity genes are irregular in *barr* mutants

Two subunits of Condensin, Cap-G and Barren/Cap-H, cause severe muscle phenotypes when lacking or dysfunctional. As Condensin plays roles both in cell division and in gene regulation, it is however unclear what exactly causes the

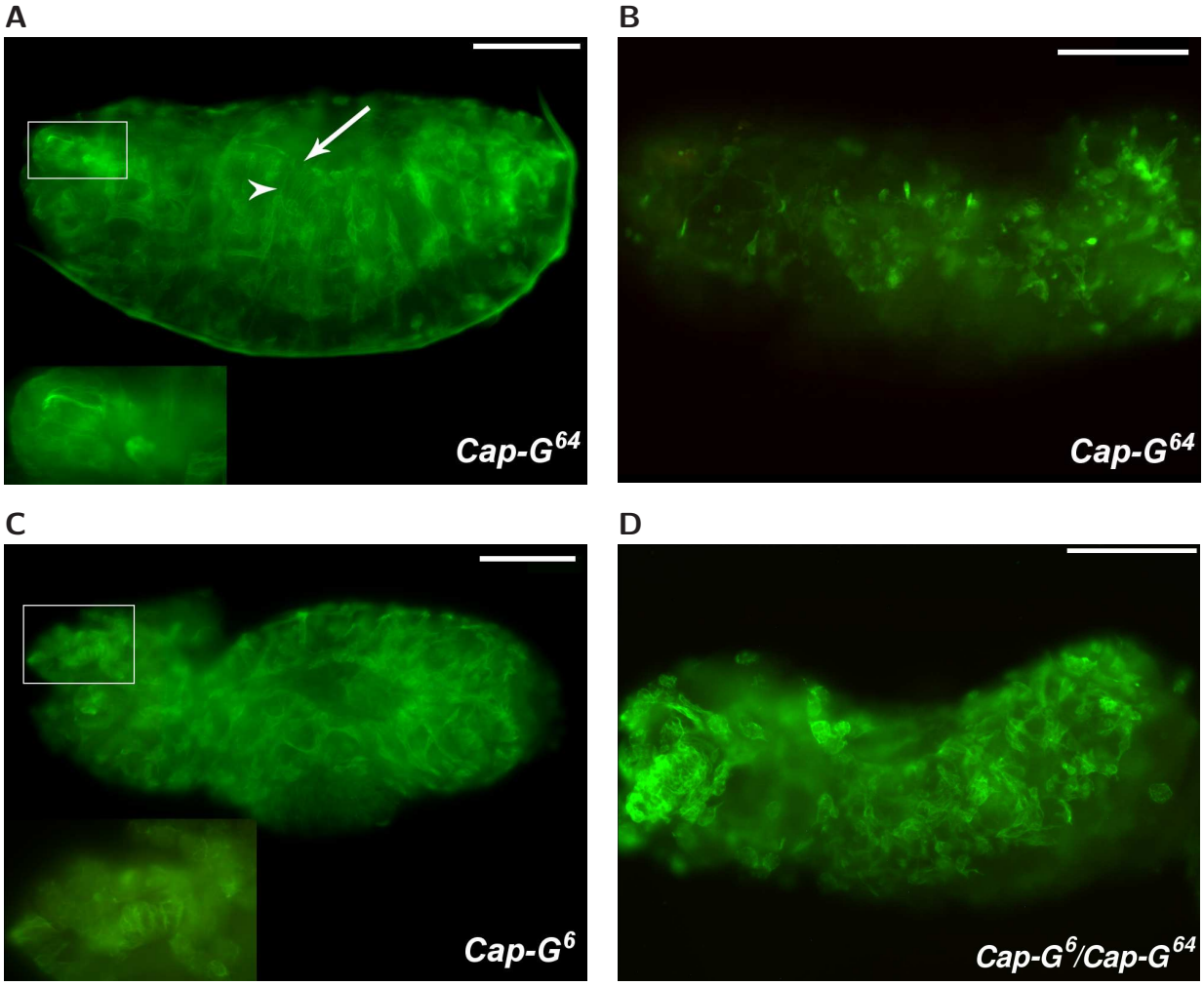

FIGURE 3.9. **Mutants of Condensin component *Cap-G* show a muscle phenotype.** Immunofluorescent stain against β3Tubulin on embryos mutant for the non-SMC Condensin component Cap-G. **A** *Cap-G*^{64} embryo, stage 16, light phenotype. Some heart cells are missing (arrow); the somatic muscle pattern is disturbed. The pharynx musculature is barely recognizable (white box, enlarged in inset). The circular visceral musculature is present (arrowhead). **B** *Cap-G*^{64} embryo, severe phenotype. No muscles are recognizable. **C** *Cap-G*^{6} embryo. The whole embryo appears twisted; dorsal closure is incomplete. The somatic muscle pattern is disturbed; the pharynx musculature is present, but appears reduced and distorted (white box, enlarged in inset). **D** Transheterozygous *Cap-G*^{6} / *Cap-G*^{64} embryo. β3Tubulin-positive cells are present, but no recognizable muscles are formed. All scalebars: 100μm.

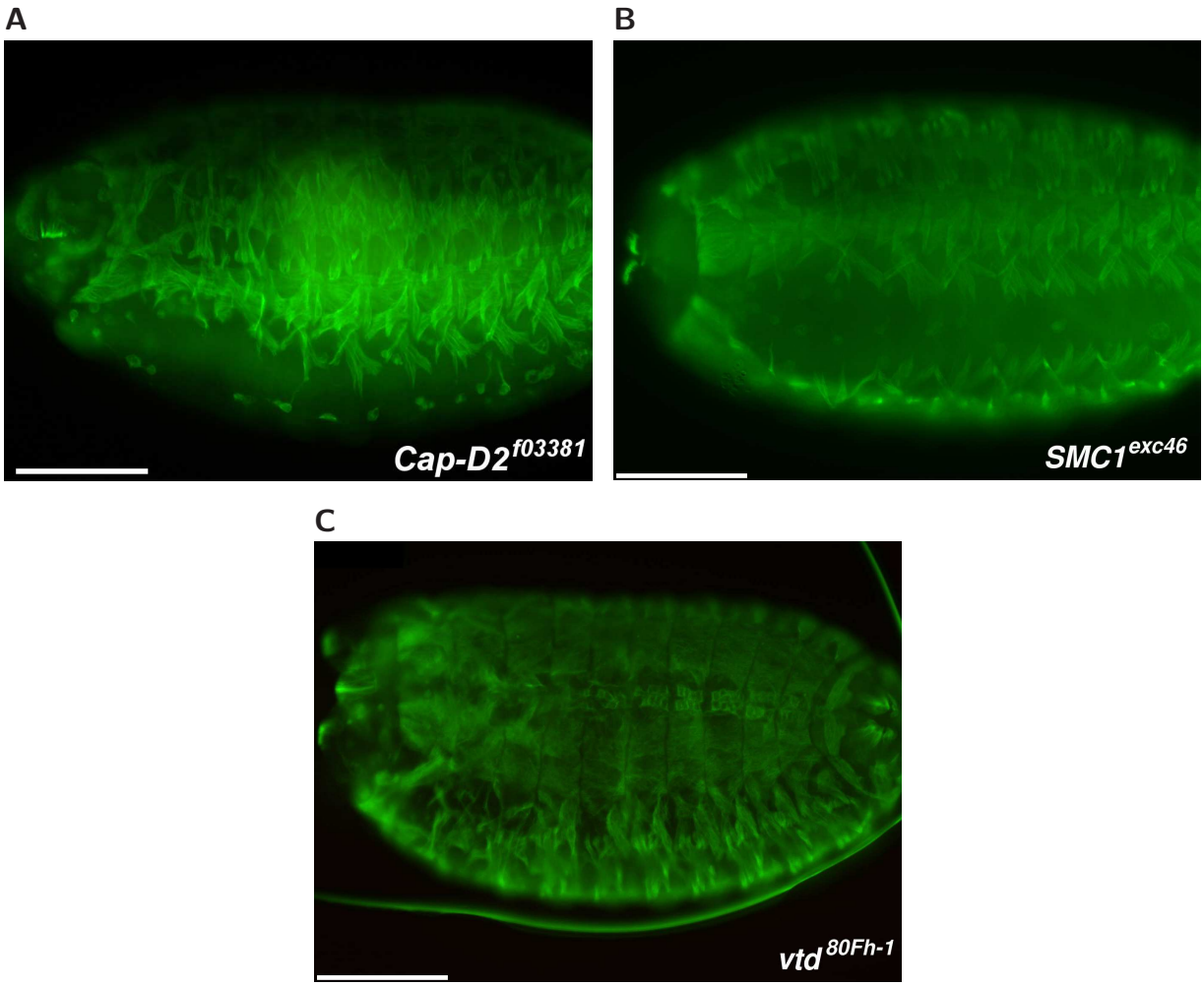

FIGURE 3.10. **Mutants of *Cap-D2* and the Cohesin subunits *SMC1* and *vtd* do not show an embryonic muscle phenotype** β3Tubulin stain showing the somatic muscle phenotype of a mutant of the Condensin non-SMC subunit Cap-D2 and of Cohesin components. **A** $Cap\text{-}D2^{f03381}$ embryo, stage 16. The muscle pattern looks normal. **B** $SMC1^{exc46}$ embryo, stage 17, ventrolateral view. The somatic musculature seems normally developed. **C** $vtd^{Fh80\text{-}1}$ mutant embryo, late stage 16, dorsolateral view. The somatic musculature seems normally developed. Scale bars: 100μm

phenotype. To analyze the role that Condensin plays in myogenesis, we try to characterize the *barren* phenotype in greater detail.

ladybird (lb) as a muscle identity gene is expressed in the Segmental Border Muscle (SBM) (Jagla et al. 1998). The *lb-PS-lacZ* fly line expresses βGalactosidase in the SBM, and particularly in the nucleus of its founder cell. An anti-βGal stain on *lb-PS-lacZ; barr* ^{L305} embryos shows that most SBMs express βGal and are comparatively intact in a *barren* mutant embryo (Fig. 3.11).

Krüppel is expressed as a muscle identity gene in the dorsal acute muscle 1 (DA1), the dorsal oblique muscle 1 (DO1), the lateral longitudinal muscle 1 (LL1), the lateral transverse muscles 2 and 4 (LT2 and LT4), the ventral longitudinal muscle 3 (VL3), the ventral acute muscle 2 (VA2) and the ventral oblique muscles 2 and 5 (VO2 and VO5) (Ruiz-Gómez et al. 1997). In an anti-Krüppel stain on a wild type embryo, not every nucleus that should express Krüppel is equally well visible, but the pattern looks regular (Fig. 3.12 A). In a *barren* mutant, this regular pattern is disturbed (Fig. 3.12 B).

3.2.5 Both founder cells and FCMs seem to get specified in *barr* mutants

All myoblasts and muscle cells express the transcription factor Mef2 from early on. An antibody stain against Mef2 shows no clear differences between a *barren* embryo and the wild type at an early stage of myogenesis (Fig. 3.13), so basic determination of the myoblast lineage obviously is unaltered in a *barren* mutant.

From the Mef2-expressing clusters of myoblasts, muscle precursor cells are singled out by a process of lateral inhibition; all other cells become FCMs. The muscle precursor cells undergo one mitosis; the nuclei of the resulting founder cells can easily be identified with the rP298 marker, a *lacZ* enhancer trap in the *Duf/Kirre* gene.

In young *barren* embryos prior to myoblast fusion, the number and position of rP298-positive nuclei seems to be normal; however, minor aberrations cannot be ruled out (Fig. 3.14). In older *barren* embryos, the number of rP298-positive nuclei varies from normal to a reduction of an estimated 50% (Fig. 3.15).

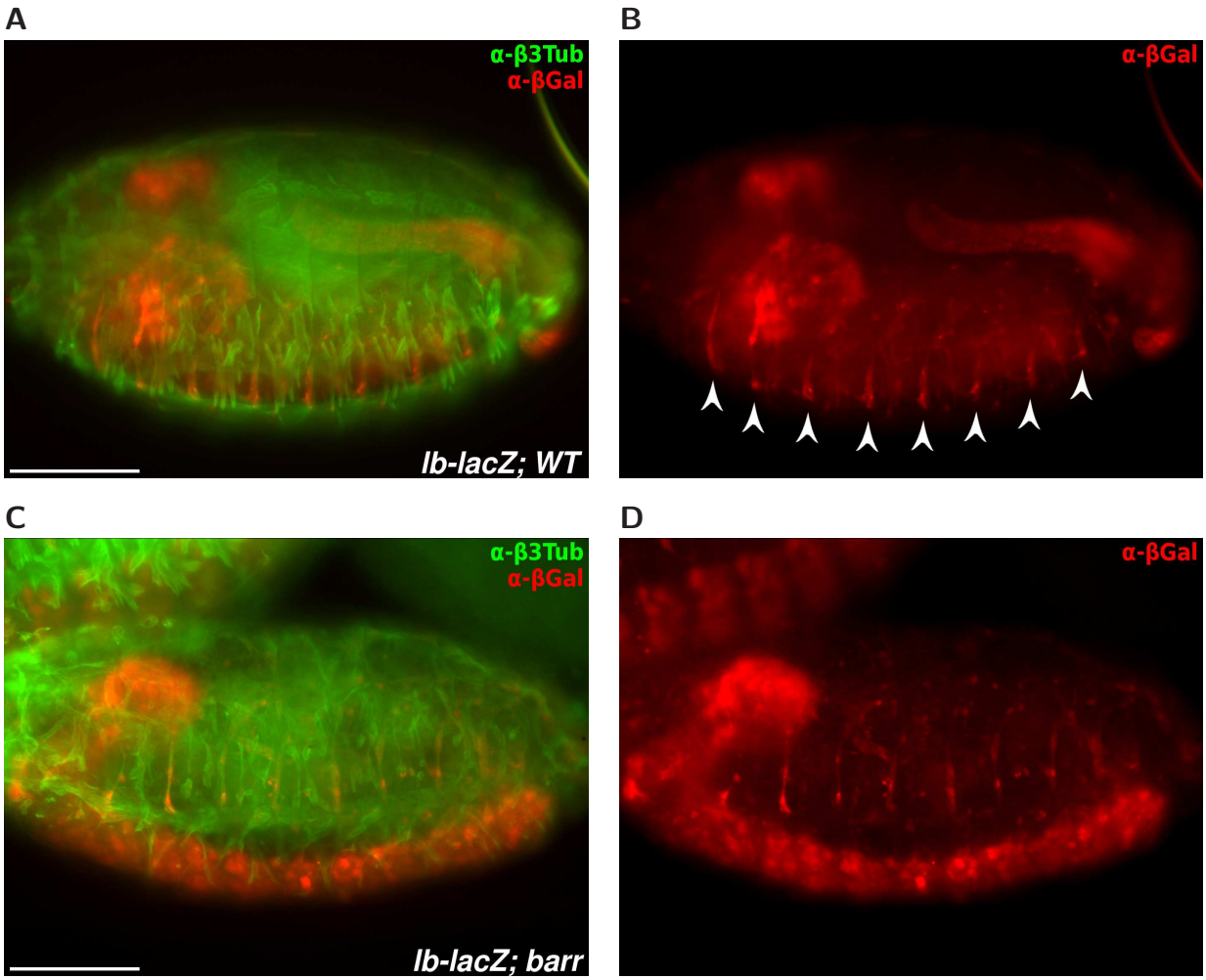

FIGURE 3.11. **In *barr* embryos, the muscle identity gene *lb* shows its normal expression pattern in the SBMs, which correspondingly appear relatively normal.** Embryos with *lb-PS-lacZ* marker. **A** Stage 15 balancer embryo showing wild type musculature. **B** The βGal signal reporting Ladybird expression is visible in the central nervous system and in the segmental border muscles (arrowheads). **C**, **D** Stage 16 *barr* ^{L305} mutant. While most of the musculature is in disarray, the segmental border muscles are in their normal positions.

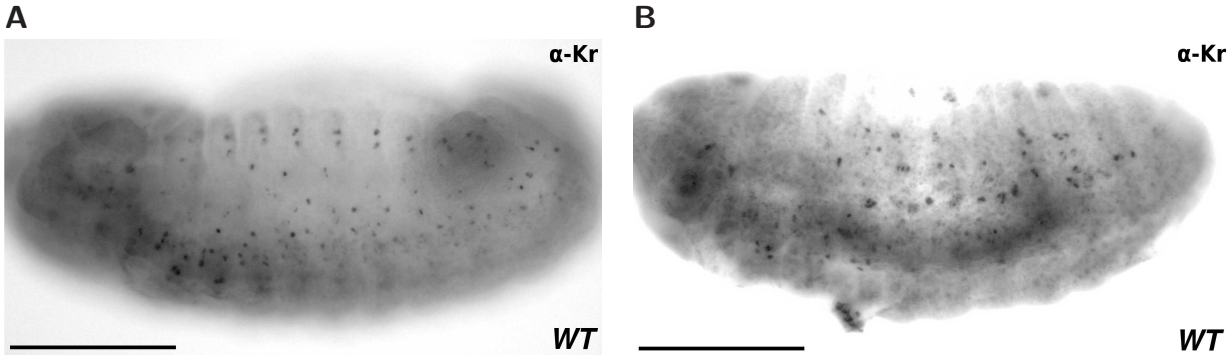

FIGURE 3.12. **In *barr* embryos, the pattern of Kr-positive cells appears disturbed.** Embryos stained with α-Krüppel (Kr) antibody; for each image, two optical sections were combined. **A** Wild type balancer embryo, stage 13. **B** Stage 14 *barr* ^{L305} embryo. The pattern of Kr-positive cells is disturbed. Scale bars: 100μm

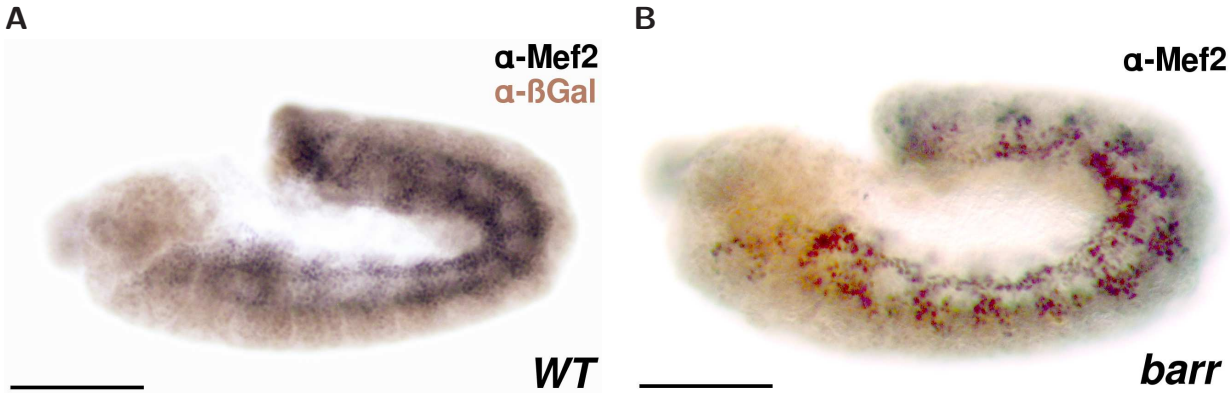

FIGURE 3.13. **The number and distribution of Mef2-positive myoblast nuclei appears normal in early *barren* embryos.** α-Mef2 stain. **A** Wild type embryo, stage 11. **B** *barr* ^{L305} embryo, stage 11. The Mef2 expression pattern does not seem to differ from the wild type. Scale bars: 100μm.

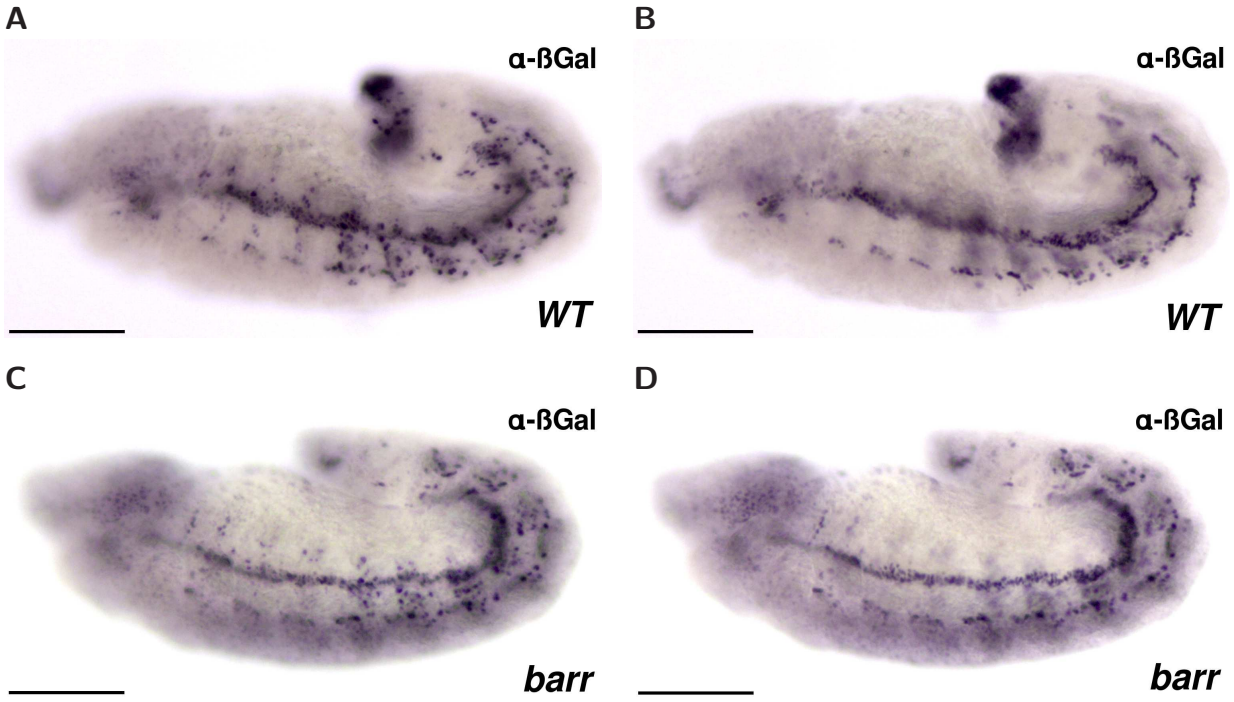

FIGURE 3.14. **In early *barren* embryos, the pattern of rP298-positive muscle founder cells appears normal.** The rP298-lacZ marker expresses β-Galactosidase in all muscle founder cells. **A** Wild type balancer embryo, early stage 12. Image combined from two optical sections. **B** The same wild type embryo; optical section through a deeper layer. **C** *barr* ^{L305} embryo, late stage 11. Image combined from two optical sections. **D** The same *barr* ^{L305} embryo; optical section through a deeper layer. No obvious difference to the wild type is visible. Scale bars: 100μm.

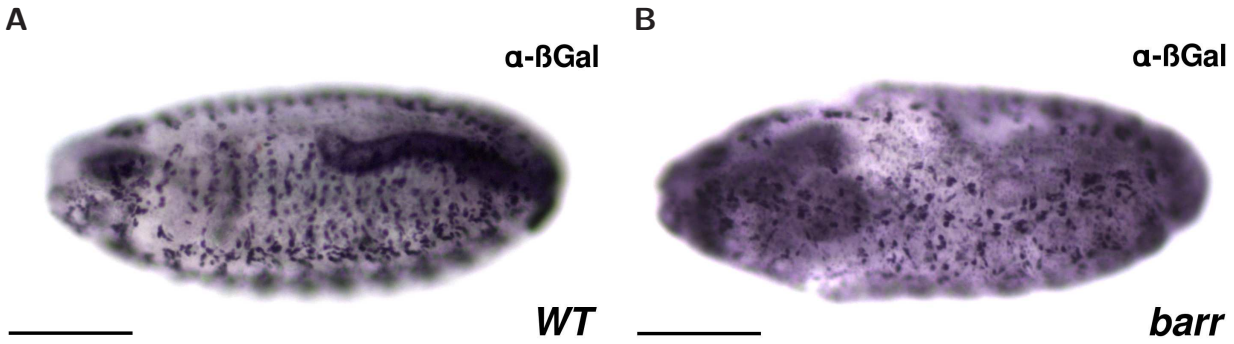

FIGURE 3.15. **In late stage *barren* embryos, the number of rP298-positive muscle nuclei can be reduced.** α-βGal stain on rP298 embryos in stage 15-16. **A** Wild type embryo. Image combined from two optical sections. **B** *barr* ^{L305} embryo. In this strong phenotype, the rP298-positive nuclei seem somewhat reduced in number, and their regular pattern is disturbed. Scale bars: 100μm.

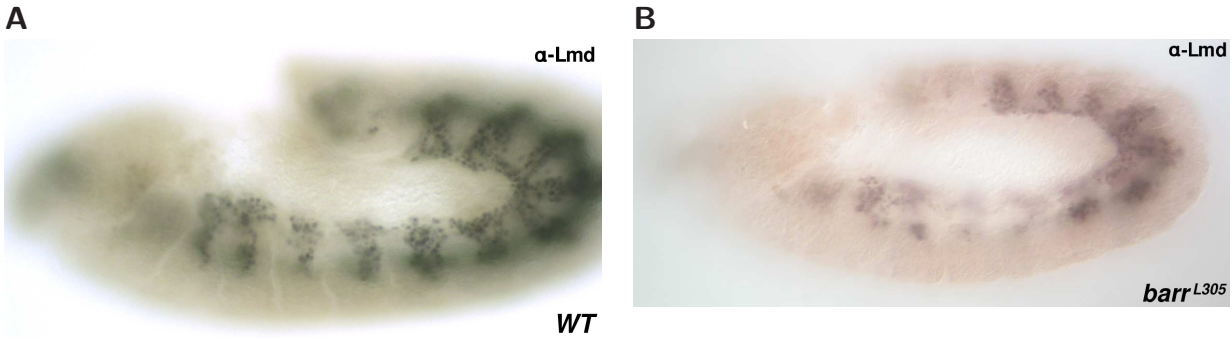

FIGURE 3.16. **FCMs seem to be correctly specified in *barren* embryos.** α-Lmd stain. **A** Wild type balancer embryo, late stage 11. The Lmd-positive FCMs form a segmental pattern. **B** The Lmd-positive cells appear in the normal FCM pattern in this stage 11 *barr* ^{L305} embryo.

An anti-Lameduck (Lmd) antibody decorates the FCMs. In an anti-Lmd stain of *barren* embryos, the mass and distribution of FCMs at an early stage of myogenesis looks normal (Fig. 3.16).

3.2.6 Double mutants of *barren* and *rols* seem to show an additive phenotype, implying that the barren defect affects the founder cell lineage

Even if the FCMs get correctly specified in *barren* mutants, the reduction of muscle nuclei at later stages of embryonic development in some embryos could still be explained with a reduction of FCMs after their determination, or a fusion defect. To test whether Barren is essential for FCM survival, a double mutant of *barren* and a myoblast fusion mutant is generated. If the FCMs cannot fuse with the nascent muscle fibres, their condition is rendered irrelevant as they will be cleared away by macrophages; so if *barren* is needed only in the FCMs, a double mutant of *barren* and a myoblast fusion mutant would show only the mini-muscle phenotype of the fusion mutant.

However, double mutants of *barr*^{L305} and the deficiency *Df(2L)BSC395* (which eliminates *rols*) show the mini muscles of the fusion mutant phenotype in a disarray that is typical for a *barren* mutant. There also is a more drastic reduction in muscle mass than in any single mutant (Fig. 3.17 B). Both phenotypes seem to add to each other, implying that *barren* is not (or not only) necessary for the FCMs, but for the development of the precursor/founder cells.

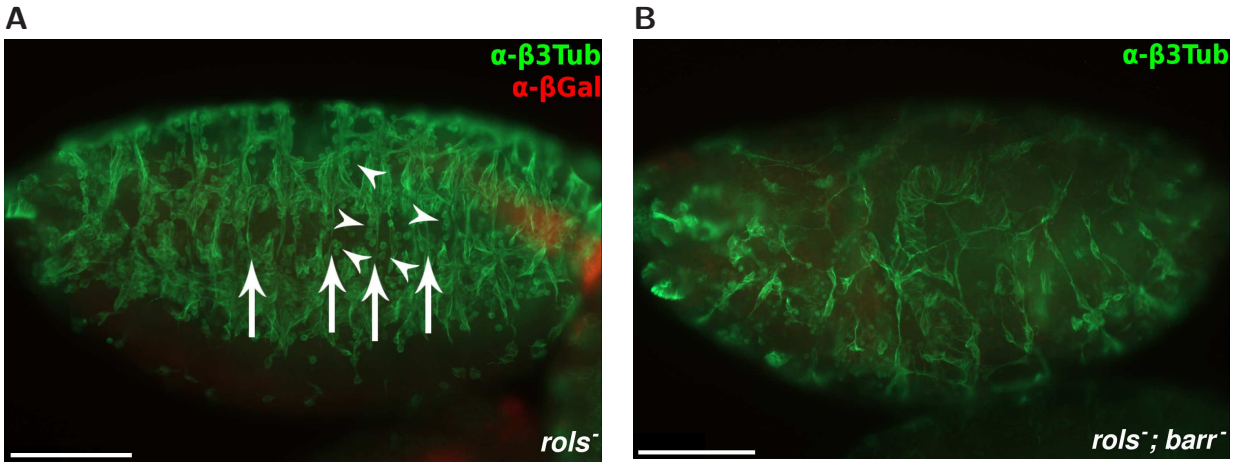

FIGURE 3.17. **A *rols; barr* double mutant shows an additive phenotype characterized by both disorientation of muscles and an aggravated reduction of muscle mass.** Antibody stain on a *rols; barr* double mutant egglay; anti-β3Tubulin in green; anti-βGal stain in red showing balancer chromosome markers. **A** *Df(3L)BSC395 (rols)* deficient embryo. SBMs are reduced to mini muscles (arrows); unfused myoblasts are visible (arrowheads). The muscle pattern is regular. Non-mutant Barren is conferred by the balancer chromosome, whose hg>>lacZ marker is visible in red. **B** *Df(3L)BSC395; barr* ^{L305} double mutant embryo. Somatic muscles are disorganized and drastically reduced in mass and number. Scale bars: 100μm

3.2.7 A *barren* rescue construct is only effective if expressed before the precursor cell division

The Gal4-UAS system allows to precisely control the expression of a transgene that carries an UAS sequence: Transcription is triggered by binding of the Gal4 transcriptional activator protein, which does not naturally occur in *Drosophila*. The gene for Gal4 in turn can be inserted into the genome as an enhancer trap or ligated in a transgenic construct downstream of a suitable transcriptional control region.

Oliveira et al. made a *barren* rescue construct with an UAS promoter that can be expressed in a tissue specific manner with the help of a Gal4 driver. Its expression can be easily detected by its eGFP tag (OLIVEIRA ET AL. 2007).

Two fly lines carrying this rescue construct on the third chromosome were obtained: *UASP-barr-eGFP III.1* and *UASP-barr-eGFP III.2*.

In a genetic background without a Gal4 driver, *UASP-barr-eGFP III.1* shows a base line expression in the embryonic heart and in some lateral structures (Fig. 3.18); *UASP-barr-eGFP III.2* shows no such expression (Fig. 3.20).

The *daughterless (da)*-Gal4 driver drives expression ubiquitously from early on in embryonic development. In an *E831/ Df(2L)Exel7077; da-Gal4/ UASP-barr-eGFP III.1* embryo (F1 from *Df(2L)Exel7077/ CyO, hg-lacZ; UASP-barr-eGFP III.1* × *E831/ CyO, hg-lacZ; da-Gal4/TM3, ftz-lacZ* crossing) that shows ubiquitous Barr-eGFP expression, the somatic muscle phenotype of homozygous *barren* mutants is reverted to the wild type (Fig. 3.19).

However, all adult offsprings of a *barr* ^{L305} */ CyO, hg-lacZ; da-Gal4* × *Df(2L)-Exel7077/ CyO, hg-lacZ; UASP-barr-eGFP III.1* crossing (which all share the genotype da-Gal4/UASP-barr-eGFP III.1) show poor locomotion, fail to inflate their wings and die within a few days post eclosion. Seemingly UASP-barr-eGFP III.1 has a lethal effect on adult flies when expressed ubiquitously, either by some effect of the transgene's insertion site, or by being mutant and either a *barren* antimorph or just generally toxic. Driving this construct with TGX (twist-Gal4) or Mef2-Gal4 (strongly active from early on in the whole mesoderm or all somatic muscles, respectively) does not have any obviously lethal effects in the adult fly.

In the adult F1 progeny of a *barr* ^{L305} */ CyO, hg-lacZ; da-Gal4* × *Df(2L)Exel-7077/ CyO, hg-lacZ; UASP-barr-eGFP III.2* crossing both Curly-winged balancer flies and straight-winged *barr* ^{L305} */ Df(2L)Exel7077* flies are present and fully viable; thus UASP-barr-eGFP III.2 seems to allow a complete rescue of the *barren* mutant with a suitable Gal4 driver. This, together with the fact that the UASP-barr-eGFP III.2 line by itself has no detectable expression and no rescue capability without a Gal4 driver (Fig. 3.21 and 3.20), recommends this fly line for cell type- and time point-specific rescue experiments.

Different Gal4 driver constructs often yield different expression levels. To allow a semi-quantitative estimation of the expression level, a standardized exposure time of 2 seconds is used for the channel showing the anti-GFP stain in all further experiments.

Driving UASP-barr-eGFP III.2 with TGX (twist-Gal4 on X chromosome) or Mef2-Gal4, which drive expression in the whole mesoderm from stage 8 or in all cells of the muscle lineage from stage 9 on, respectively, we see a complete recovery of the *barren* somatic muscle phenotype (Fig. 3.22).

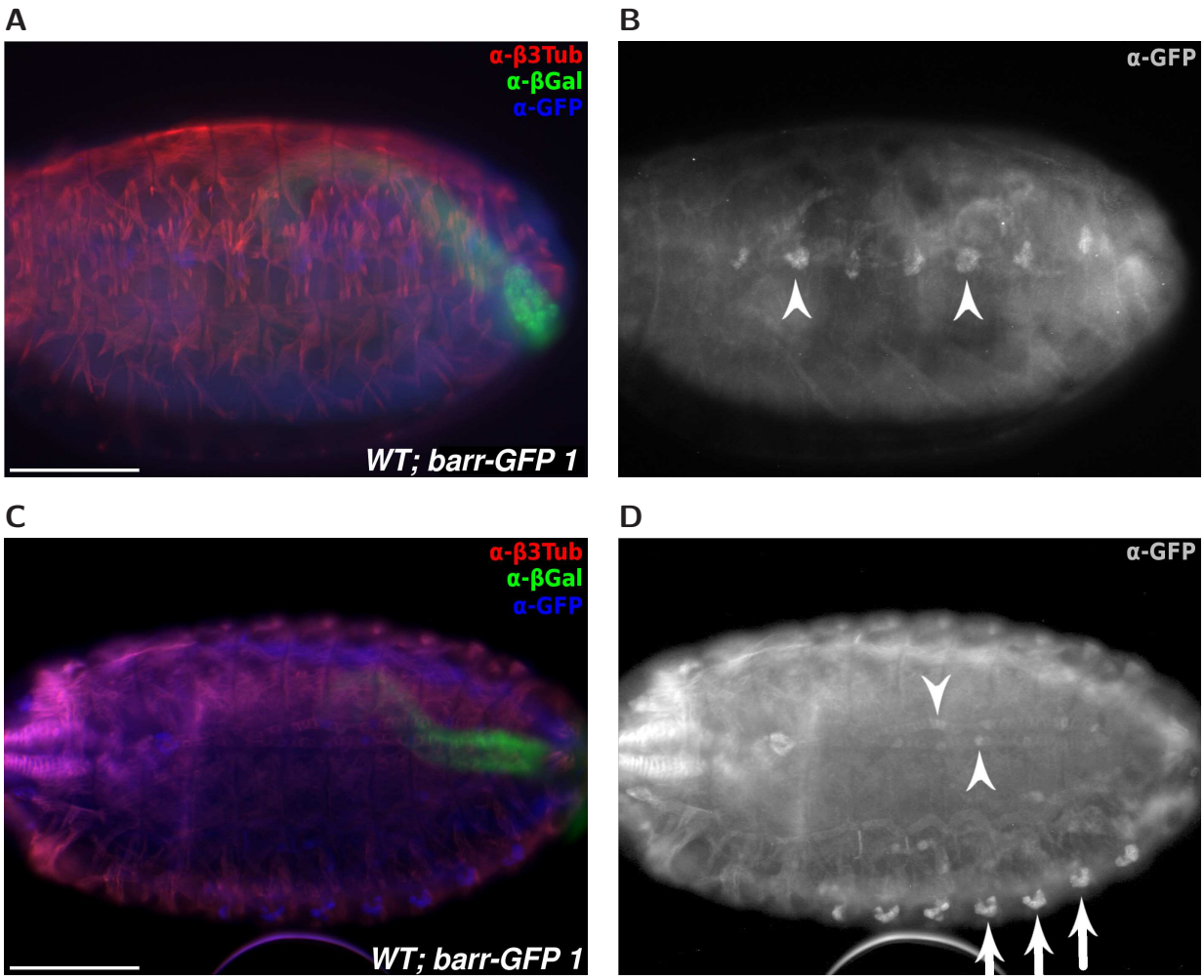

FIGURE 3.18. **UASP-barr-eGFP III.1 shows a distinctive expression pattern even without a Gal4 driver.** Embryos with UASP-barr-eGFP III.1 rescue construct without any Gal4 driver. Exposure time of the α-GFP channel (blue in left column, shown as single channel in the right column) was extended beyond the standard two seconds to give a visible signal. **A** Heterozygous *Df(2L)Exel7077/ CyO, hg-lacZ; UASP-barr-GFP III.1* stage 17 embryo, lateral view. **B** The UASP-barr-GFP III.1 construct produces eGFP expression in the vicinity of the lateral muscle bundles in segmental structures that might be tracheal pits (arrowheads). **C** Same genotype, stage 15 embryo, dorsal view. **D** barr-eGFP expression can be detected in the pharynx and in some cells of the heart (arrowheads). The lateral stain on the presumable tracheal pits is also visible (arrows). Scale bars: 100μm.

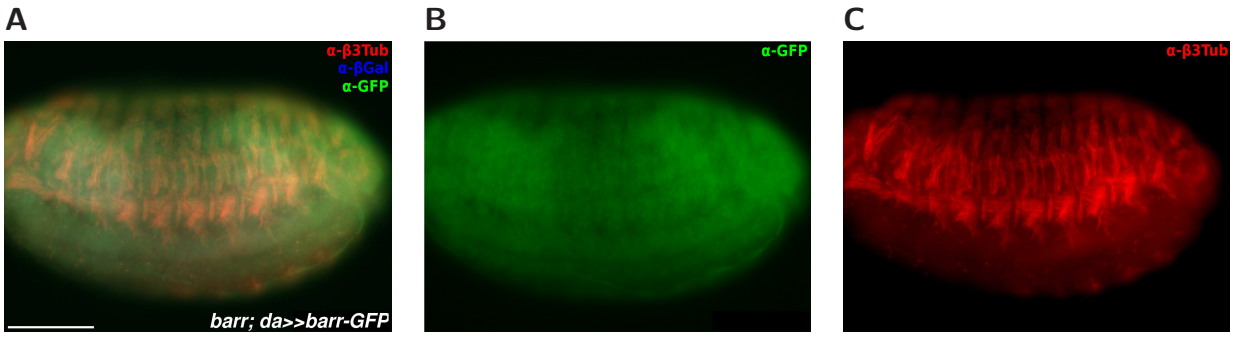

FIGURE 3.19. **Early ubiquitous expression of a barr-eGFP construct rescues the phenotype of E831.** Stage 16 *E831/ Df(2L)Exel7077; da-Gal4/ UASP-barr-eGFP III.1* embryo (from a crossing *Df(2L)Exel7077/ CyO, hg-lacZ; UASP-barr-eGFP III.1* × *E831/ CyO, hg-lacZ; da-Gal4/TM3, ftz-lacZ*). **A** α-β3Tubulin in red, α-βGal in blue, and α-GFP in green. The absence of a blue α-βGal signal in odd-numbered parasegments shows that this embryo inherited the da-Gal4 driver, not the TM3, ftz-lacZ balancer. **B** The α-GFP stain is found throughout the whole embryo, demonstrating the ubiquitous expression of Barr-eGFP. **C** The muscle pattern in β3Tubulin stain looks like the wild type. Scale bar: 100μm.

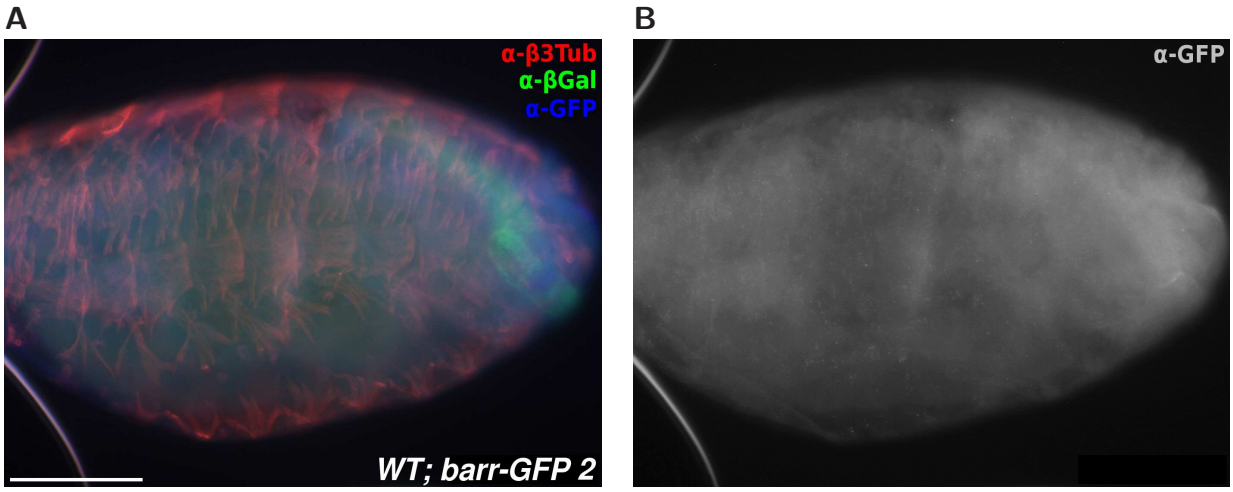

FIGURE 3.20. **Without a Gal4 driver, UASP-barr-eGFP III.2 is not expressed in a discernible pattern.** Embryos with UASP-barr-eGFP III.2 rescue construct without any Gal4 driver. Exposure time of the α-GFP channel (shown in the right image and in blue in the left) was extended beyond the standard two seconds in an attempt to give a visible signal. **A** Heterozygous *Df(2L)Exel7077/ CyO, hg-lacZ; UASP-barr-GFP III.2* stage 17 embryo, lateral view. **B** No autonomous expression pattern of Barren-GFP is visible. Scale bars: 100μm.

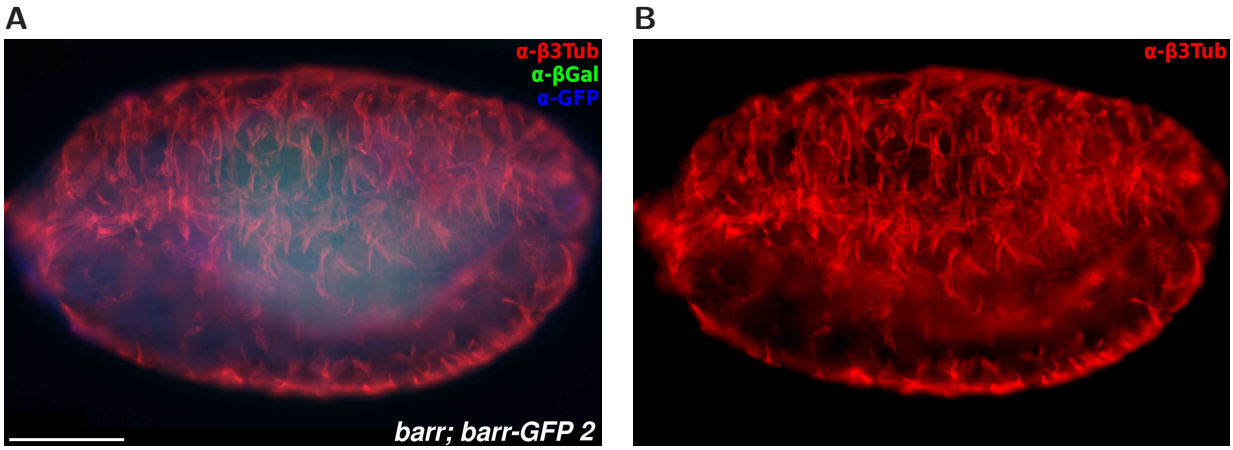

FIGURE 3.21. **Without a Gal4 driver, UASP-barr-eGFP III.2 does not rescue the *barr* phenotype.** Homozygous *Df(2L)Exel7077; UASP-barr-eGFP III.2* embryo, stage 15. The Df(2L)Exel7077 deficiency deletes *barren*; no Gal4 driver is included. **A** The α-GFP stain gives only a faint background signal in the gut, showing that barr-GFP is not expressed. **B** The α-β3Tubulin stain shows the disturbed muscle pattern of a *barren* mutant: Without a Gal4 driver, no rescue is achieved. Scale bar: 100μm

Upon myoblast fusion, the FCM nuclei loose their FCM identity and start to express the genetic program of the nascent muscle they fused into, namely muscle identity genes and founder cell specific myoblast fusion genes. One possible explanation for the chaotic muscle phenotype is *barren* causing a defect of gene regulation in FCMs, leading to a failure of FCM nuclei to undergo reprogramming.

The sns pro3-Gal4 driver becomes active at early stage 12 in FCMs. *UASP-barr-eGFP* under the control of this driver would not only supply Barren to the FCMs at the time of their fusion, but via myoblast fusion also to the nascent myotubes.

However, while Barr-eGFP in such an experiment can be seen strongly expressed in all somatic muscles after myoblast fusion, we see no rescue of the *barren* muscle phenotype (Fig. 3.23). Thus it seems likely that Barren is required prior to myoblast fusion in the progenitor/muscle founder myoblasts and not in the FCMs.

The rP298-Gal4 driver becomes active in progenitor cells around the time of their final division; it is strong enough to rescue *duf* and *rols* mutants with corresponding UAS rescue constructs (MENON AND CHIA 2001). *barr* embryos driving *UAS-barr-eGFP* with rP298-Gal4 still show the *barr* phenotype (Fig. 3.24).

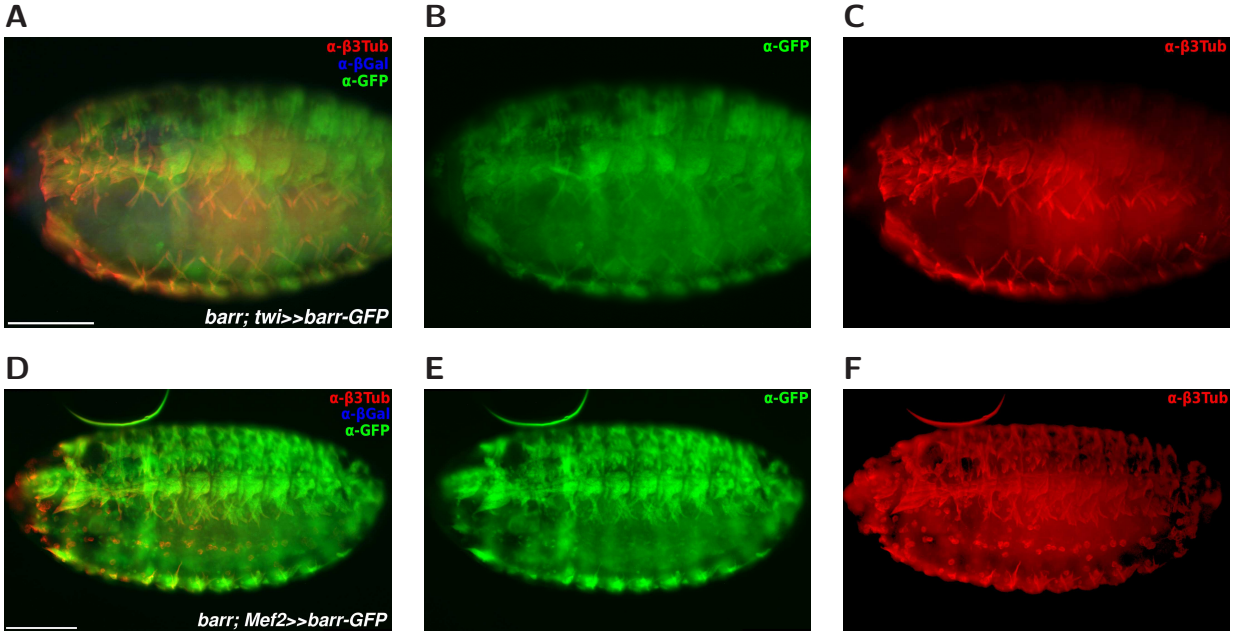

FIGURE 3.22. **Early Barr-eGFP expression in the whole mesoderm rescues the *barr* somatic muscle phenotype.** **A** *TGX; barr* ^{L305} */ CyO, hg-lacZ; UASP-barr-eGFP III.2* embryo, stage 16. **B** The α-GFP stain shows the Barr-eGFP rescue construct expressed in the whole mesoderm. The expression appears weaker than in other rescue experiments; this might be due to the twist-Gal4 driver already being inactive for a long time at the shown stage. **C** Same embryo, α-β3Tubulin stain. The somatic musculature looks like the wild type. **D** Stage 15 *barr* ^{L305} */ Df(2L)Exel7077; Mef2-Gal4/ UASP-barr-eGFP III.2* embryo (from a *barr* ^{L305} */ CyO, hg-lacZ; Mef2-Gal4* × *Df(2L)Exel7077/ CyO, hg-lacZ; UASP-barr-eGFP III.2* crossing). **E** Barr-eGFP is expressed in all somatic muscle cells. **F** Same embryo, α-β3Tubulin stain. The somatic muscle pattern looks like the wild type. Scale bars: 100μm.

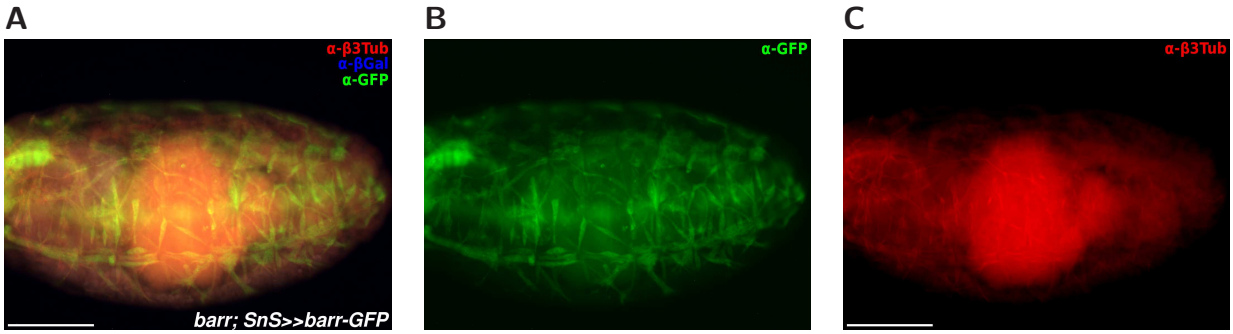

FIGURE 3.23. **sns-Gal4 driving barr-GFP does not rescue the *barr* phenotype.** Stage 16 *barr*^{L305}*, sns pro3-Gal4/ Df(2L)Exel7077; UASP-barr-eGFP III.2 /+* embryo (from a *barr*^{L305}*, sns pro3-Gal4/ CyO, hg-lacZ* × *Df(2L)Exel7077/ CyO, hg-lacZ; UASP-barr-eGFP III.2* crossing). **A**, **B**: With myoblast fusion completed, Barr-eGFP is expressed in all somatic muscle cells. **C** The α-β3Tubulin stain shows the *barr* mutant muscle phenotype. Scale bar: 100μm.

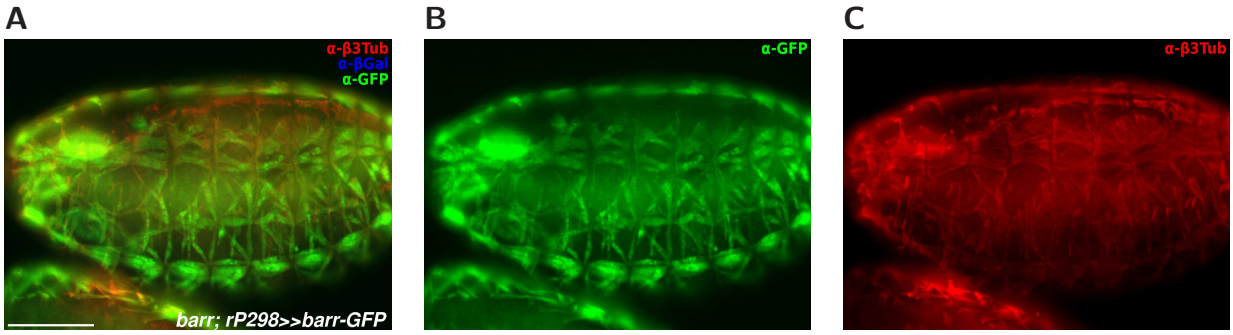

FIGURE 3.24. **rP298-Gal4 driving barr-GFP does not rescue the *barr* phenotype.** Stage 16 *rP298-Gal4; barr* ^{L305} */ Df(2L)Exel7077; UASP-barr-GFP III.2 / +* embryo (from a *rP298-Gal4; barr* ^{L305} */ CyO, hg-lacZ* × *Df(2L)Exel7077/ CyO, hg-lacZ; UASP-barr-GFP III.2* crossing). **A**, **B**: Barr-eGFP is expressed in the whole somatic musculature. **C** The α-β3Tubulin stain shows a light *barr* phenotype in the lateral muscle bundles. Scale bar: 100μm.

Chapter 4

Discussion and Perspectives

4.1 *rols* mRNA localization probably serves localized protein synthesis close to the site of fusion

4.1.1 The 3' trailer is necessary for *rols* mRNA localization in somatic founder cells

We have shown that a reporter mRNA with both the *rols7* 5' leader and *rols* 3' trailer gets localized in the somatic founder cells in a pattern similar to the localization of wild type *rols7* transcript, while a reporter mRNA that combines the *rols7* leader with an SV40 trailer (a sequence from the Simian Vacuolating virus 40) does not (D. Kesper, personal communication).

Further experimentation will be needed to test weather the *rols* trailer is sufficient for mRNA localization, or weather the *rols7* leader sequence is also necessary.

4.1.2 The *rols* mRNA is also localized in other myoblasts

The combination of fluorescent *in situ* hybridization with immunofluorescent stains on markers for specific subsets of myoblasts reveal a subcellular local-

ization of *rols* not only in the somatic founder cells, but also in the circular and longitudinal visceral founder cells.

The circular visceral founder cells show the *rols* transcript localized on their interior, gut-ward side. The longitudinal visceral founder cells often have the *rols* mRNA localized at the tips of their spindle shaped bodies, the sites of Duf accumulation (Rudolf et al. 2014).

In analogy, we can speculate that the peripheral spots to which the *rols* transcript is localized in somatic founder cells correspond to prospective filopodia or fusion sites; however, the site of Duf and Rols accumulation in the nascent myotube and, ultimately, the site of fusion may be dictated entirely by the FCM's first contact, with the speckles of *rols* mRNA just a functionless homology to the situation in the other types of muscle founder cell.

Experimental clarification of this point is difficult to achieve, as the somatic founder cells lack the stereotypic orientation and shape of their visceral counterparts, and the rP298-lacZ marker shows only nuclei, not cell shapes. Here, a new marker strategy would become necessary in future experiments, for example a combination of rP298-Gal4 and UAS-lacZ.

4.1.3 *rols* mRNA localization may facilitate efficient protein localization

The first mRNA *in situ* hybridizations in *Drosophila* were performed on oocytes or embryos at the syncytial blastoderm stage. These cells are about 0.5mm large (where myoblasts have a diameter of approximately 5μm). In these early developmental stages, mRNA localization often creates a morphogen gradient (for example *bicoid*, Driever and Nüsslein-Volhard 1988) and gives an obvious phenotype when failing.

Mutant phenotypes also have allowed to analyse mRNA localization in smaller cells, for example in cases where asymmetric mRNA distribution and the subsequent protein gradient convey an altered cell fate to one daughter cell after mitosis (like for example *prospero*, Li et al. 1997; Broadus et al. 1998).

In contrast, *rols* mRNA localization does not seem to be connected to an obvious phenotype; *rols* mutants can be rescued with constructs that do not have the native trailer (Menon and Chia 2001; Menon et al. 2005).

Today, improved *in situ* hybridization techniques give a detailed subcellular resolution; this way, Lécuyer et al. 2007 have found that 71% of all transcripts expressed during *Drosophila* embryogenesis are intracellularly localized.

Often, the localization of the mRNA prefigures the distribution of the translated protein. Even if some additional mechanism is in place for localization on protein level (like it is for example for Prospero), mRNA localization can still provide an improvement in efficiency: Moving one mRNA molecule around takes less energy than having the many protein molecules it can give rise to cross the same distance; transporting an mRNA to its target area and then derepressing its translation at the right moment can allow for a more exact temporal control of protein expression than having the protein translated at random places in the cytoplasm and relying on "just in time" delivery to its destination.

We can speculate that in *rols* rescue experiments with the non-localizing SV40 trailer, enough of the generated Rols protein reaches its destination in time to recreate the wild type phenotype, at least under lab conditions. The *rols* mRNA localization possibly has a beneficial effect on the organism's fitness under the less-than-optimal conditions the fly lives under in the wild.

4.2 The *barren* muscle phenotype is probably caused by aneuploidia

The embryonic musculature of *D. melanogaster* is highly organized and segmentally repeated; each muscle in every segment can be identified by its shape and position, which are defined by the expression of a set of muscle identity genes. In the E831 mutant line, however, this order is more or less disturbed; muscles stray seemingly at random, even crossing over segmental borders. Stains for muscle identity genes correspond with the appearance of muscles: Muscles that look more or less like the wild type, like the segmental border muscle often does, are likely to stain for their normal muscle identity genes; for the more affected muscles, not even marker stains for single muscles allow the identification of a clear pattern. More severe grades of this mutant's phenotype can also show a reduction of muscle mass and a reduced number of rP298-positive (*duf/kirre* expressing) nuclei by the end of embryonic myogenesis.

It is, however, not a defect of myoblast fusion; such a defect would typically leave a lot of unfused myoblasts crowding around the rudimentary myotubes, which conversely would still be in a relatively ordered pattern.

In this study, we have shown that this phenotype is caused by mutations of Condensin I components. E831 contains a *barren* nonsense mutation that presumingly eliminates the protein; a P element insertion ($barr^{k14014}$) and a deletion of the first exons of *barren* ($barr^{L305}$) give exactly the same phenotype. The $Cap\text{-}G^{6}$ null allele gives a similar, strong, less variable phenotype; $Cap\text{-}G^{64}$ yields embryos with no identifiable musculature whatsoever. The latter, a D254Y missense mutation affecting a protein-protein interaction domain (Cobbe et al. 2006), is seemingly a gain-of-function allel, as $Cap\text{-}G^{64}/Cap\text{-}G^{6}$ transheterozygous also mostly show the more drastic $Cap\text{-}G^{64}$ phenotype.

While it is trivial that crucial housekeeping genes like the Condensin components should severely affect the embryonic development when defective, the genesis of such a specific phenotype as the seemingly general loss of muscle identity is much less obvious.

The mRNAs for Condensin components are deposited in the oocyte before fertilization; these maternal mRNAs can cover for about the first half of embryonic develompment. This is the reason why we see structured embryos with working germ band retraction and muscular tissue of some kind, and not just undeveloped oocytes that failed in their first mitosis.

Generally, Condensin has two kinds of functions whose defect could trigger the phenotype: Regulatory and mitotic. Concretely, we can name several scenarios:

- Loss of Condensin implicates **loss of Polycomb group repression** (Lupo et al. 2001; Bantignies et al. 2003). The general derepression of genes, especially inactive muscle identity genes, might produce a muscle phenotype. However, such a scenario happening in founder cells would likely produce a more ordered phenotype than what we see, as it would end up activating the same set of genes in all muscles.

  A failure of repressional mechanisms in FCM nuclei might make syncytial myotubes behave like FCMs, possibly explaining the phenotype. However,

neither an additional myoblast fusion mutant in background nor a rescue construct expressed specifically in the FCMs can reestablish the muscle pattern, letting this hypothesis seem unlikely.

- **Indiscriminate gene bookmarking**. Gene bookmarking over mitotic cycles requires the local deactivation of Condensin near core promoters (Xing et al. 2008); general loss of Condensin might therefore, to a degree, activate all promoters. This might explain the loss of muscle identity and the seeming relevance of the progenitor division.
  In such a scenario, however, we should see a generalization of the expression of muscle identity genes; this is not what immunohistochemical stains show.

- Condensin is a modifier of position effect variegation (Dej et al. 2004; Cobbe et al. 2006); **random heterochromatinization or deheterochromatinization of muscle identity genes** might produce the chaotic muscle pattern we observe.

- A **failure of chromatid segregation during mitosis** can have various effects: Cells can initiate apoptosis; cells can revert out of mitosis (Cobbe et al. 2006; this would leave the equivalent of a cell in G2 phase); cytokinesis can fail due to chromatin bridging (leaving a binucleate or tetraploid cell, like probably the peripheral neurons in *Drosophila barren*, see Bhat et al. 1996); or cytokinesis can succeed (leading to two aneuploid cells, like seemingly in *Drosophila barren* epidermis cells; see Bhat et al. 1996).

Especially the latter scenario, comprising a randomization of the daughter cells' genetic make up, might produce the observed phenotype. This would imply, however, that the faulty gene expression program arising from the compromised founder cell nucleus cannot be corrected on access to the intact genomes of the FCM nuclei.

A strong argument for assuming a mitotic defect as the cause of the phenotype comes from rescue studies: A rescue construct that restitutes Barren protein only is effective if expressed well before the final mitosis of the muscle progenitor cells. Barren expression after that mitosis has no effect on the muscle phenotype (Fig. 4.1).

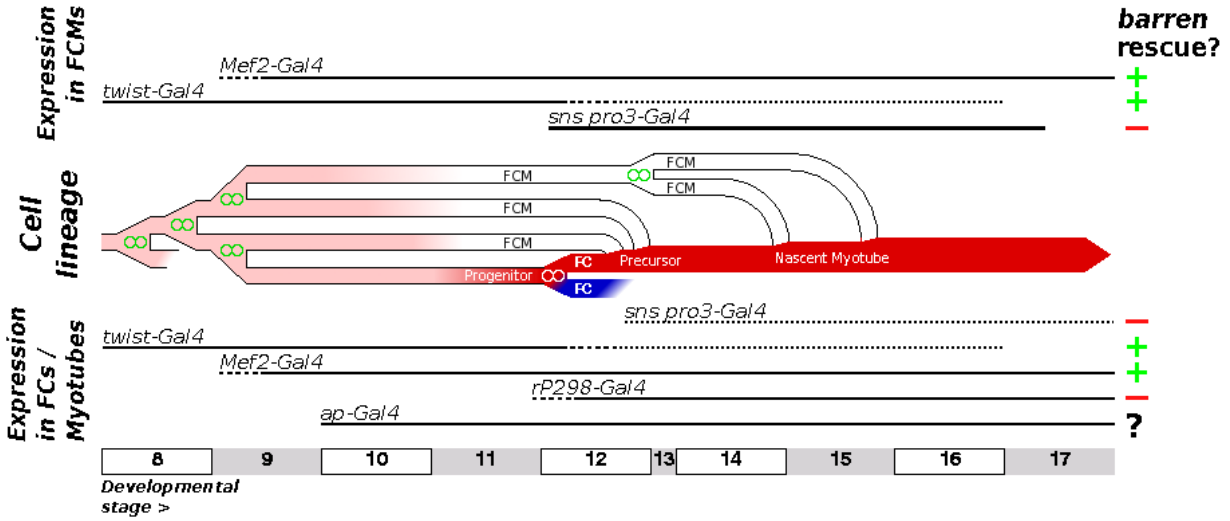

FIGURE 4.1. **Only Gal4 drivers that are active in the progenitor cell can rescue the *barren* phenotype.** The transcriptional activity of various Gal4 drivers over time in different myogenic cell types. Ability to rescue the *barr* muscle phenotype with an *UAS-barr-GFP* construct indicated to the right.
Thick black lines (——): Gal4 driver certain to be active; dashed lines (- - -): Activity of Gal4 driver driver is uncertain at this time point; dotted lines (·····): Gal4 driver is known to be transcriptionally inactive, but gene products of UAS constructs should be abundant; ∞: Mitosis. Stages and events according to HARTENSTEIN 1993 and FlyMove (WEIGMANN ET AL. 2003).

This hypothesis can also explain the variability of the *barren* phenotype: After 13 mitoses until blastoderm cellularization and three more divisions after mesoderm invagination (HARTENSTEIN 1993), the progenitor division is the 17th and final mitosis in this cell lineage. Due to a stash of maternally supplied mRNA, *barren* mutants do not become apparent during the first few mitoses; BHAT ET AL. 1996 see anaphase bridging in epidermal cells not before mitosis 16. Depending on minimal differences in the maternal *barren* mRNA supply, the progenitor division might sometimes come to pass with relatively little chromatin bridging, resulting in mostly intact daughter cells; in other cases the progenitor cell might be affected so badly that it has to revert out of mitosis, or one or both daughter cells die, resulting in reduced muscle mass.

Cap-G mutants already show anaphase bridging in mitosis 15 (DEJ ET AL. 2004), explaining their constant, strong phenotype. Condensin components whose mutants do not show a muscle phenotype might simply have a large enough supply of maternal mRNA for the embryonic/larval muscle lineage to make it through its final mitosis.

Genome instability is a feature of many cancer cell lines: The genetic make up of the cells is randomized in every mitosis, the loss of heterozygousity producing a hemizygous situation for recessive mutant alleles that can subsequently drive tumorigenesis further.

The embryonic musculature of *Drosophila* could be an intriguing model system for this. While *Drosophila* cells always require a second mutation preventing terminal differentiation or apoptosis to actually form tumors, the embryonic musculature, being already terminally differentiated, demonstrates a loss of tissue architecture in an easily observable way after seemingly only one faulty mitosis. The musculature of a Condensin mutant *Drosophila* embryo essentially presents genomic instability in a nutshell.

Perspectives on further experiments

The rP298-Gal4 driver, which becomes active around the time of the final progenitor division and is strong enough to rescue *duf* and *rols* mutants with the respective UAS constructs (Menon and Chia 2001), fails to rescue the muscle phenotype when driving a *barren* rescue construct. The latest-expressing Gal4 driver that manages to do the rescue is *Mef2-Gal4*; it is expressed in all cells of the muscle lineage, starting before progenitor cells are singled out from the crowd determined to become Fusion-competent myoblasts, and stays active during the whole myogenesis (see p. 108 Fig. 4.1).

To corroborate the finding that *barren* is necessary for the progenitor division, it would be useful to drive a rescue construct only in the progenitor cells, distinctly before their final mitosis. A driver capable of that might be *apterous*^{md544}-Gal4, an enhancer trap in the regulatory region of *apterous*, a muscle identity gene expressed in a small subset of progenitor and founder cells (see Fig. 4.1, 4.2; Bourgouin et al. 1992).

The practical problem with this experimental strategy is that *apterous* lies rather close to *barren* on the second chromosome, and is thus difficult to introduce into a *barr*$^{-}$ background.

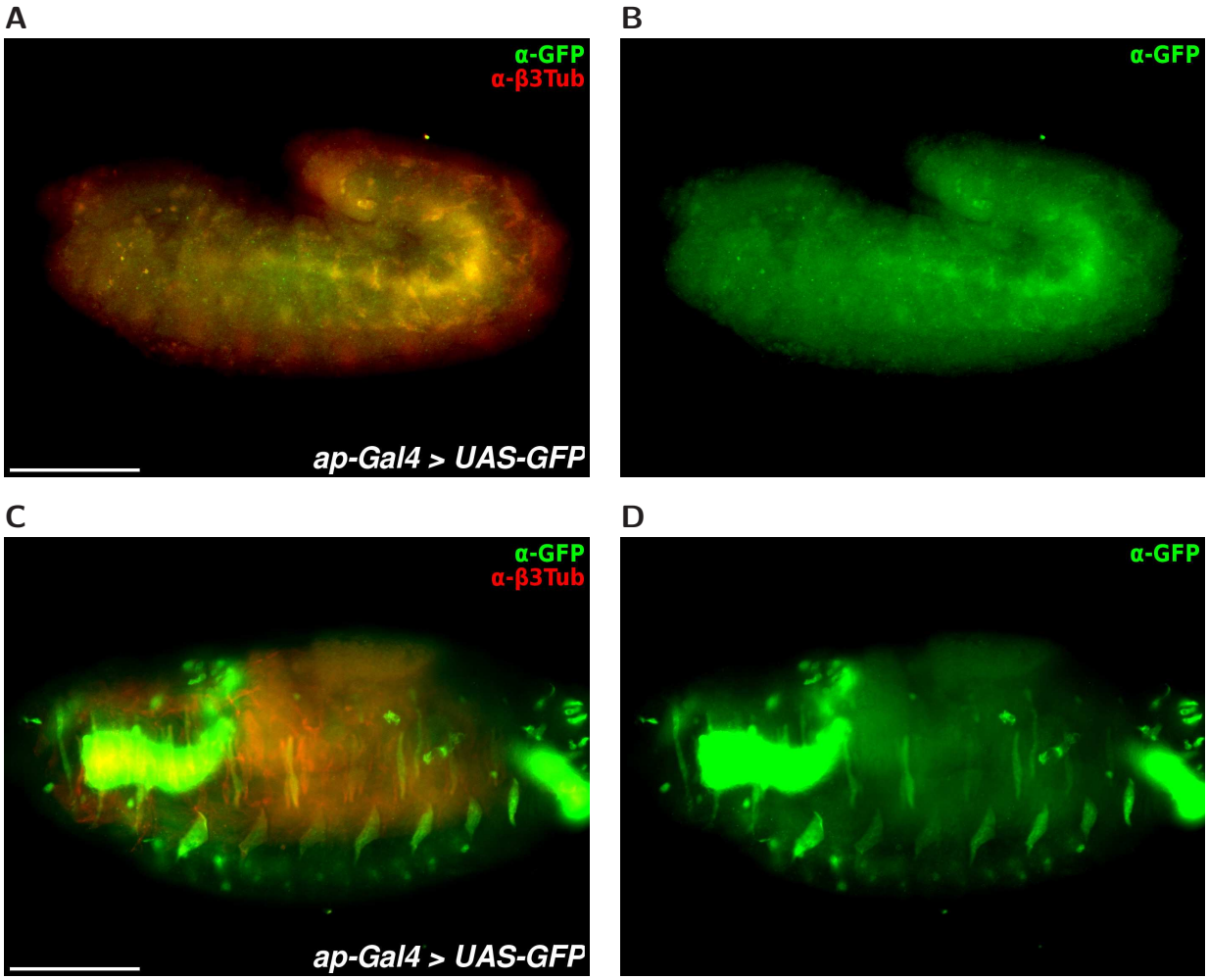

FIGURE 4.2. Antibody stains against β3Tubulin (red) and GFP (green) on *ap^{md544}-Gal4; UAS-GFP* embryos. **A**, **B** Early stage 12. *ap^{md544}* drives GFP expression in parts of the myotome. **C**, **D** Stage 17. GFP expression is detected in varying intensities in the muscles of the lateral bundles and in the VA2 muscle. It can also be seen in a ventral, segmental, cellular pattern probably part of the ventral nerve chord, and very strongly in anterior and posterior structures of unclear identity.

To further exclude the possibility that Condensin is necessary for gene regulation during myogenesis, the TEV cleavage strategy that Pauli et al. (2008) use to destroy Verthandi (the Kleisin of Cohesin) in specific cell types and time points could be adapted to Barren, or to the SMCs; this way, Condensin could be deactivated specifically after the final mitosis.

A TUNEL assay labels DNA breaks. It is usually used to visualize apoptotic cells; however, it also might be able to detect cells that sustained DNA breaks due to a defect of chromosomal segregation.

Assuming the phenotype is actually caused by a faulty progenitor division leading to aneuploid founder cells, we can suppose that other mutations that cause genomic instability have a similar effect on musculature. A variety of potential candidate genes can be taken for example from Dekanty et al. (2012) and Castellanos et al. (2008), see Table 4.1.

Relevant biological function	**Gene**	**Chromosomal region**
DNA damage check point	*atm = tefu*	88E3-E4
Condensation	*orc2*	88A3
Spindle assembly	*rod*	100C6-C7
	asp	96A19-A20
Chromosomal segregation	*fbl*	77B9-C1
Cytokinesis, Chromatin organization	*sti*	69C4
Cytokinesis	*tsr*	60B5
	dia	38E7-E8
Cell differentiation	*Medea*	100C7-D1

TABLE 4.1. Mutants that induce genomic instability, mostly from Dekanty et al. (2012) and Castellanos et al. (2008).

Appendix A

Analysis of various candidate genes

A.1 *In situ*-hybridizations of candidate genes

Gene	Chromosomal region	Protein class	mRNA expression pattern	p.	Muscle phenotype	p.
daw	23B1-B2	Activin-like ligand of TGF-β	mesoderm or cns; segmental	*115*	n.d.	
nolo	39F1-F3	Ig-ADAM-TS	mesoderm, segmental; midgut	*116*	n.d.	
CG4096	5B1	ADAM-TS	segmental; epidermal (tracheal pits ?), midgut (?), cells in head	*117*	n.d.	
CG6512	74A1-A2	Metalloprotease	mesoderm/cns (?), segmental; midgut, hindgut	*118*	n.d.	

Gene	**Chromosomal region**	**Protein class**	**mRNA expression pattern**	**p.**	**Muscle phenotype**	**p.**
Nep2	82D2	Metalloprotease	epidermis, segmentally patterned	*119*	n.d.	
Neu3	88C10-D1	ADAM	segmental in mesoderm (musculature ?) and cns; anterior and posterior	*120f*	–	*123*
mmd	14A1-A4	ADAM	n.d.		–	*124*
Acer	29D4	Metalloprotease	n.d.		–	*125*
CG18754, SPE	95A7	Secretase	n.d.		–	*125*
CG17572	37B13	Inactive serine protease	n.d.		–	*126*
Kul	99B9	ADAM	n.d.		– (RNAi:+)	*127ff*
kuz	34C4-C6	ADAM	n.d.		–	*131f*
Tace	99D1	Metalloprotease	n.d.		–	*132*
CG9416	56D2	Peptidase	n.d.		–	*133*
Rya-R44F	44F1-F2	Calcium channel	n.d.		–	*133*

A *daw* in situ hybridization

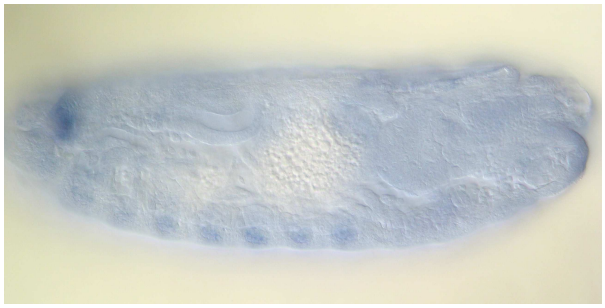

B *daw* in situ hybridization

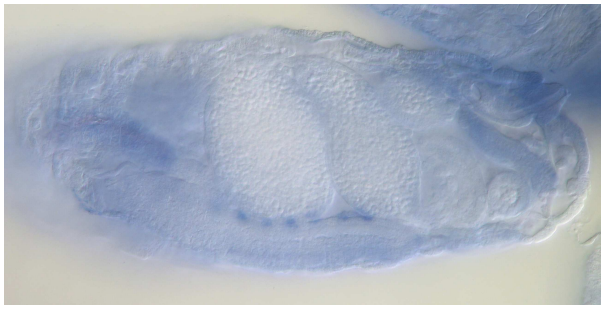

FIGURE A.1. Antisense-RNA-*in situ* hybridisations against *dawdle (daw)*, using the cDNA GH14433. *daw*, also known as *Alp23B*, was selected for analysis by Detlev Buttgereit (personal communication) because of its potentially mesodermal expression pattern. **A** Stage 12, lateral view. A segmental expression pattern is visible ventrally. **B** Stage 16, lateral view. *daw* is expressed in the pharynx, in the hindgut and in other posterior structures. Along the ventral nerve chord a regular pattern of probably two small patches of expression per hemisegment is visible.

A *nolo* in situ hybridization

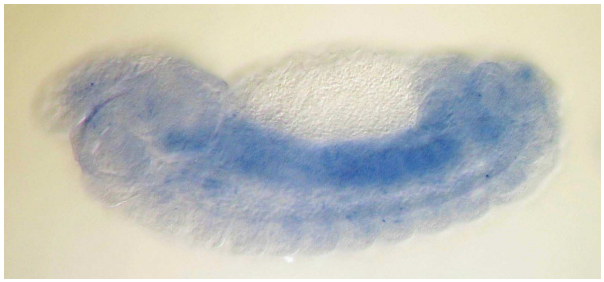

C *nolo* in situ hybridization

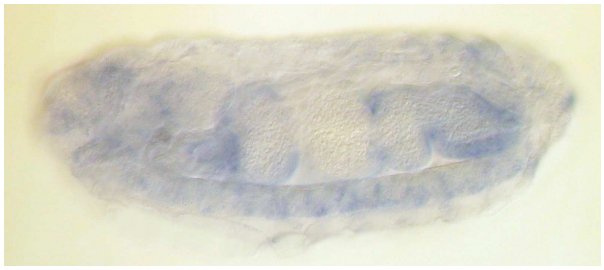

D *nolo* in situ hybridization

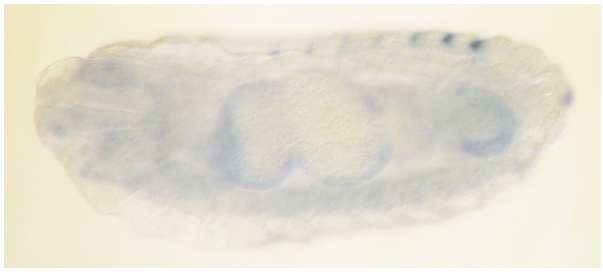

E *nolo* in situ hybridization

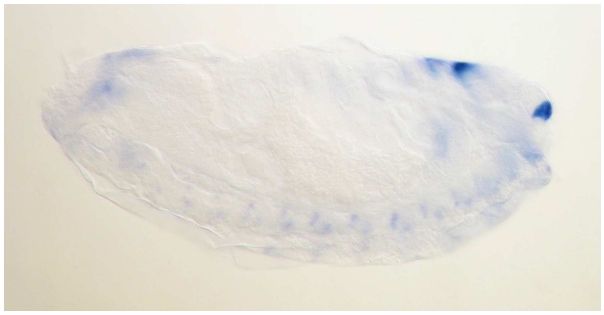

F *nolo* in situ hybridization

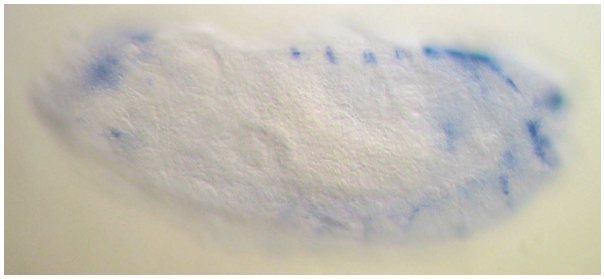

FIGURE A.2. Antisense-RNA-*in situ* hybridisations against *no long nerve chord (nolo)*, using the cDNA GH19218. *nolo* was selected for analysis by David Breier (BREIER 2009) because of its Immunoglobulin-like and ADAM-TS (a disintegrin and metalloprotease - thrombospondin) domains, which potentially play a role in myogenesis. **A** Stage 13, lateral view. The *nolo* mRNA is distributed homogenously in a broad area in the dorsal part of the abdomen, possibly part of the mesoderm. A segmental expression pattern in a deep layer of the embryo, possibly mesodermal, is visible in the ventral abdominal region. **C** Stage 16, lateral view. *nolo* is expressed in many small patches along the ventral nerve chord, in parts of the midgut walls and in several anterior structures. **D** A different optical section of the same embryo. A segmental expression pattern is visible dorsally, possibly in cells that are part of the heart. **E** Stage 17, lateral view. *nolo* is expressed in small cell clusters in the ventral nerve chord and in several anterior and posterior structures. **F** A different optical section of the same embryo. A segmental pattern of small cell clusters is visible dorsally, possibly part of the heart.

A *CG4096* in situ hybridization

B *CG4096* in situ hybridization

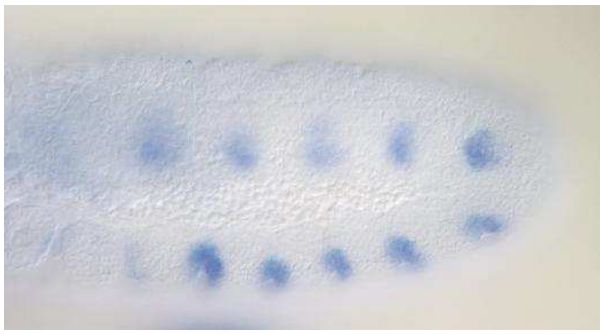

C *CG4096* in situ hybridization

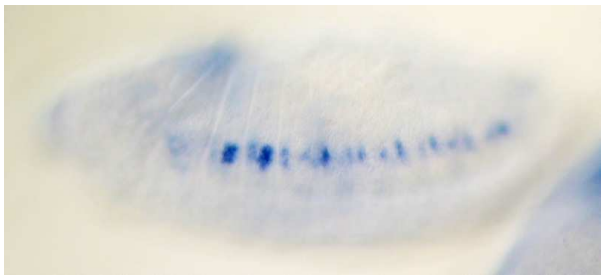

D *CG4096* in situ hybridization

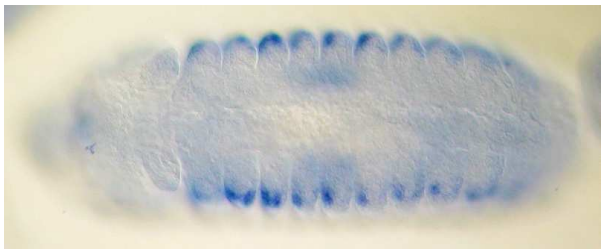

E *CG4096* in situ hybridization

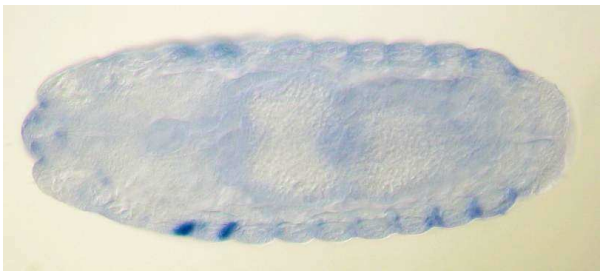

FIGURE A.3. Antisense-RNA-*in situ* hybridisations against *CG4096*, using the cDNA GH22104. *CG4096* was selected for analysis by David Breier (BREIER 2009) because of its potential role in myogenesis as an ADAM-TS. **A** , **B** Stage 11, lateral view. A segmental expression pattern is visible. **C** Stage 14, lateral view. The segmental expression domains probably correspond to the tracheal pits. **D** Stage 14, dorsal view. **E** Stage 16, dorsal view. The segmental expression pattern seems more differentiated, with the anteriormost two domains showing the strongest expression. Additional CG4096-expressing cells are visible in the head.

A *CG6512* in situ hybridization

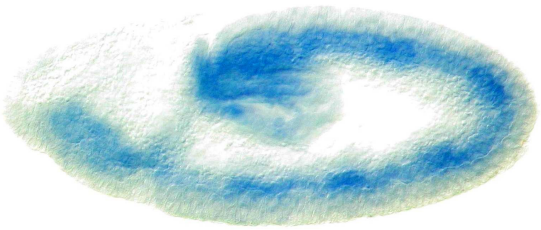

B *CG6512* in situ hybridization

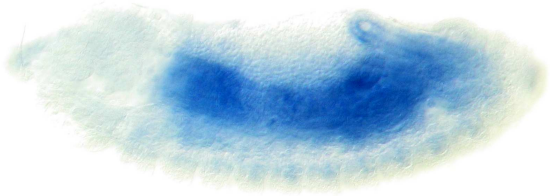

C *CG6512* in situ hybridization

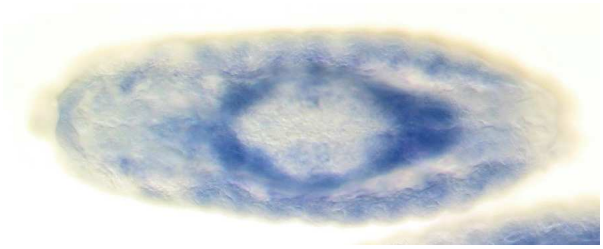

FIGURE A.4. Antisense-RNA-*in situ* hybridisations against *CG6512*, using the cDNA SD01613. The gene was selected for analysis by David Breier (BREIER 2009) because of its potential role in myogenesis as a metalloprotease.

The expression in the early ventral nerve chord and in the midgut is of doubtful relevance, as a sense-RNA *in situ* hybridization probe produces the same pattern (not shown). **A** Stage 10. *CG6512* is expressed in a stripe that might be the ventral nerve chord or the mesoderm. **B** Stage 14. Expression is visible in the midgut and ventrally in a segmental pattern, possibly corresponding to cells in the mesoderm or the ventral nerve chord. **C** Stage 15, dorsal view. *CG6512* is expressed in the midgut; the lateral segmental expression pattern probably corresponds to the mesoderm.

A *Nep2* in situ hybridization

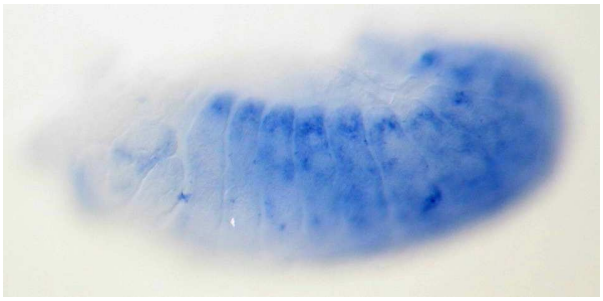

B *Nep2* in situ hybridization

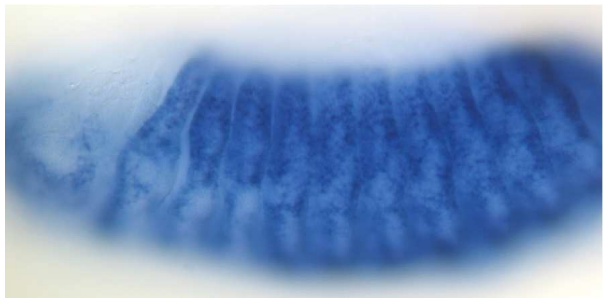

C *Nep2* in situ hybridization

FIGURE A.5. Antisense-RNA-*in situ* hybridisations against *Neprilysin 2 (Nep2)*, using the cDNA GH07643. The gene was selected for analysis by David Breier (BREIER 2009) because of its potential role in myogenesis as a metalloprotease. **A** Stage 12. *Nep2* is expressed in the abdominal part of what seems to be the epidermis. The expression is strongest in the dorsalmost part of each segment. **B** Stage 14. *Nep2* is expressed in a distinct, segmentally repeated pattern in the epidermis. **C** Stage 14, dorsal view.

A *Neu3* in situ hybridization

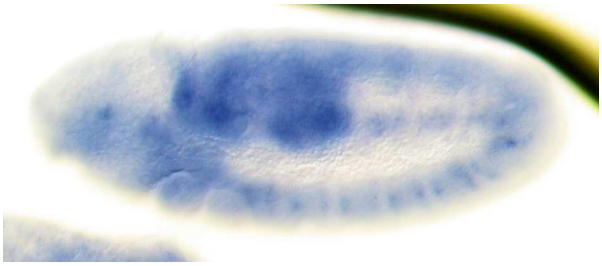

B *Neu3* in situ hybridization

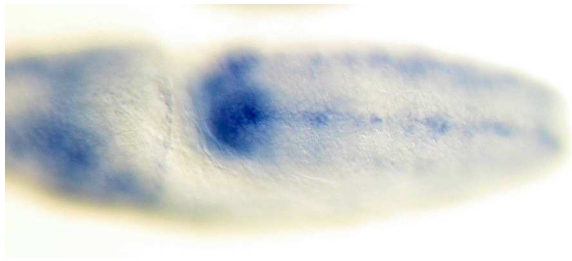

C *Neu3* in situ hybridization

FIGURE A.6. Antisense-RNA-*in situ* hybridisations against *Neuroectoderm-expressed 3 (Neu3)*, also known as *Meltrin*, using the cDNA RE23052. *Neu3* was selected for analysis by David Breier (BREIER 2009) for beeing potentially relevant for myogenesis as an ADAM protein; it one of the two *Drosophila* orthologues of the mammalian ADAM12.

The expression in anterior and posterior structures is somewhat doubtful, as *in situ* hybridizations with a Sense-RNA probe made from the same cDNA show a similar pattern (not shown). Since the time this experiment was conducted, the quality/ identity of the RE23052 cDNA has been challenged. **A** Stage 11. *Neu3* is expressed segmentally in what might be the ventral nerve chord, and in some anterior and posterior structures. **B** Stage 11, dorsolateral view. *Neu3* expression is visible in narrow, segmentally structured stripes lateral to the area of the ventral nerve chord, close to the epidermis. **C** Stage 13. *Neu3* is expressed in segmental domains towards the ventral side of the embryo, possibly part of the mesoderm or the ventral nerve chord. There also seems to be expression in the pharynx and other anterior and posterior structures.

A *Neu3* in situ hybridization

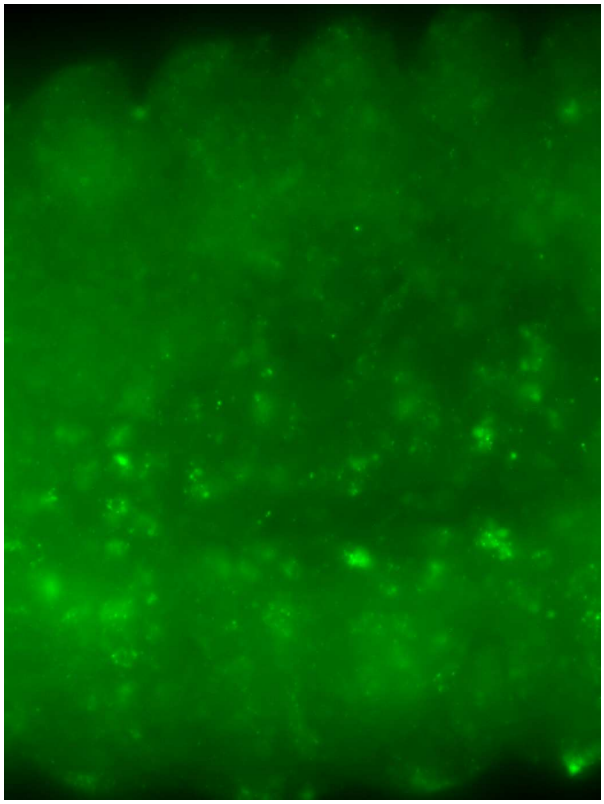

B *Neu3* in situ hybridization, $\alpha - \beta$Gal

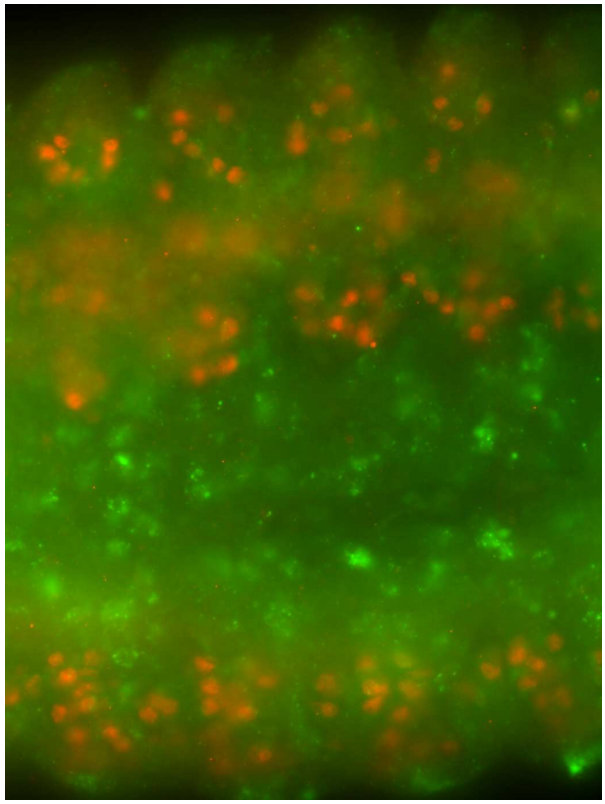

FIGURE A.7. Fluorescent antisense-RNA-*in situ* hybridisations against *Neu3*/ *Meltrin*, using the cDNA RE23052. **A** Stage 12. *Neu3* is expressed in various cells that seem to be part of or closely associated with the ventral nerve chord. There also is a more lateral segmental pattern. **B** The rP298-lacZ marker visualizes the muscle founder cells in red. These do not show *Neu3* expression, but are closely associated with the lateral *Neu3*-expressing cells.

A.2 Mutants and RNAi-knock-downs of candidate genes

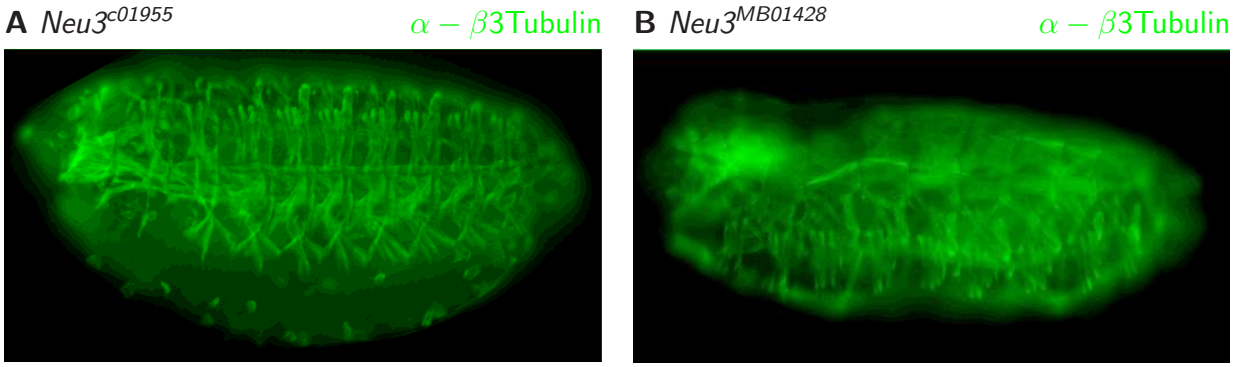

FIGURE A.8. Fluorescent anti-β3Tubulin stains on various mutants of *Neu3*. This metalloprotease, also known as *Meltrin*, is one of two *Drosophila* orthologues of mammalian *ADAM12*. It was selected for analysis because of its mRNA expression pattern, and because of the role *ADAM12* plays in mammalian muscle cell cultures. **A** $Neu3^{c01955}$, a lethal PiggyBac insertion in an intron of *Neu3*. Stage 17, lateral view. The embryo looks like a wild type. **B** $Neu3^{MB01428}$, a lethal Minos insertion in the last, non-coding exon of *Neu3*. Stage 17, dorsolateral view. The shape of the embryo looks altered, but the musculature seems unaffected.

A *Df(3R)BSC714* α- β3Tubulin

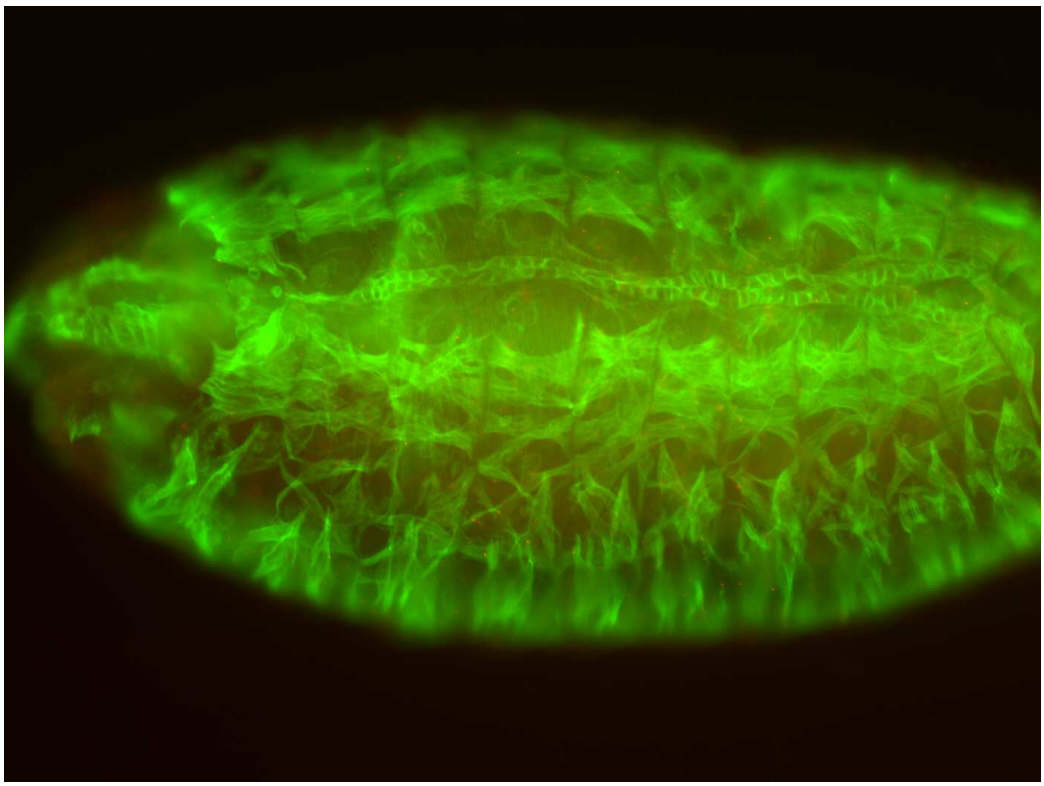

FIGURE A.9. *mind-meld (mmd)* is an orthologue of mammalian ADAM12 and a paralogue of *Meltrin/Neu3* and might take over the latter's functions in a *Neu3* mutant. The deficiency *Df(1)BSC714* (13E14–14A8) covers *mmd* and about 65 other genes. **A** Embryo at about stage 16, dorsolateral view. Somatic musculature and heart appear normal.

A *Acer* α-β3Tubulin **B** *Acer* α-β3Tubulin

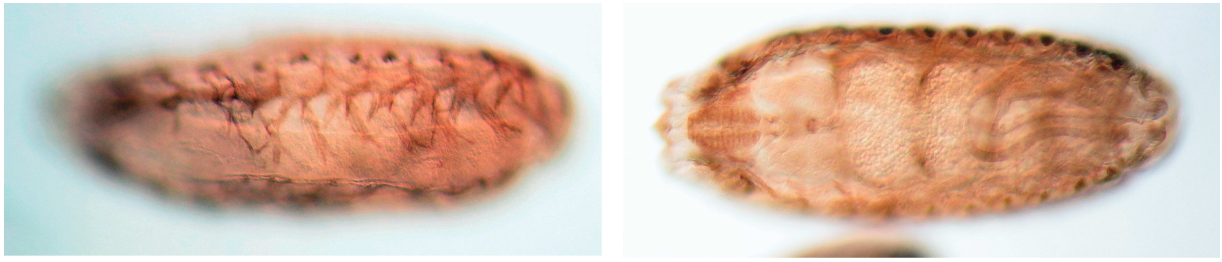

FIGURE A.10. The metalloendopeptidase *Angiotensin-converting enzyme –related (Acer)* is expressed in embryonic cardioblasts and a variety of other tissues. It was selected for further analysis by David Breier (BREIER 2009). CRACKOWER ET AL. 2002 identify $Acer^{k07704}$, a P-element insertion in the 3'-UTR, as embryonic lethal due to a heart defect. However, CARHAN ET AL. 2011 found an *Acer* null allele generated by imprecise excision to be viable. **A** Ventrolateral, stage 16. The anti-β3Tubulin stain shows that the somatic and pharynx musculature are relatively intact in the $Acer^{k07704}$ mutant. **B** Dorsal, stage 16. The gut constrictions are formed normally, implying that the intestinal musculature also is formed.

A *Df(3R)BSC491* α-β3Tubulin **B** *Df(3R)BSC491* α-FasIII

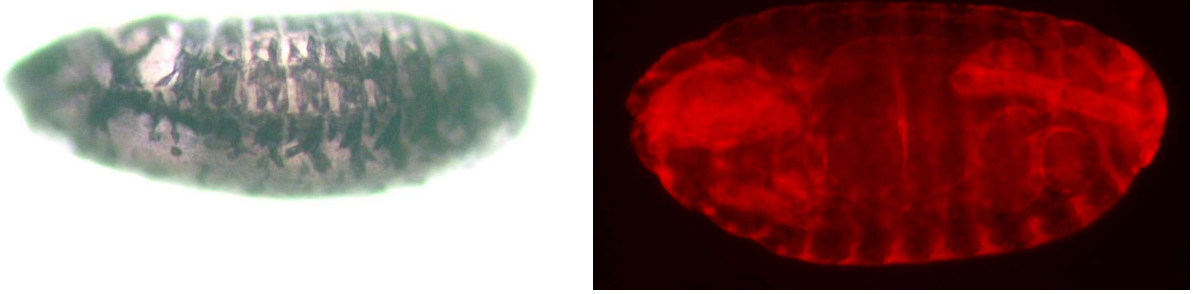

FIGURE A.11. *Spätzle-processing enzyme (SPE)* and its neighbor and putative paralogue *CG18754* are analyzed because of their expression in the embryonic mesoderm: *CG18754* is expressed strongly in the somatic muscle primordia, *SPE* in the fat body (FISHER ET AL. 2012). As secretases with functionality similiar to metalloproteases, they potentially play a role in myogenesis. The deficiency *Df(3R)BSC491* (95A7–95A10) covers *CG18754*, *SPE* and 13 other genes. **A** About stage 15. The musculature appears normal. **B** Stage 16, anti-FasIII stain. The gut appears normal.

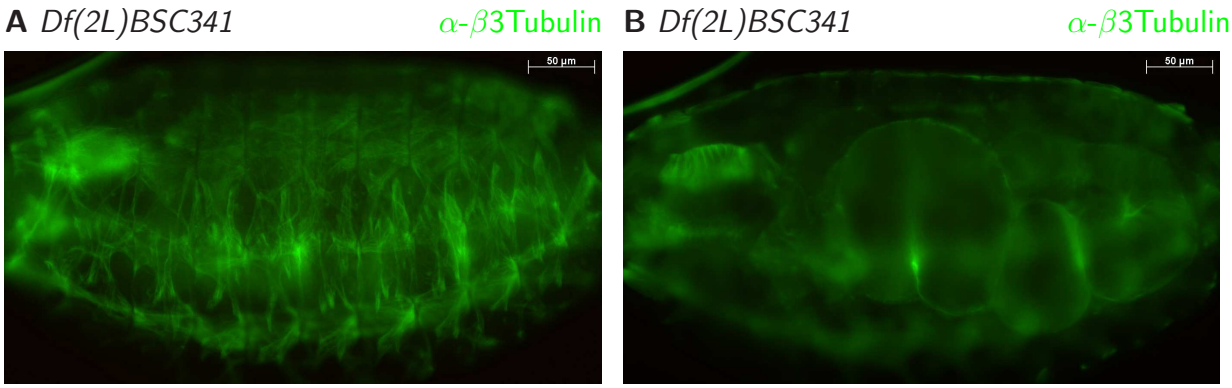

FIGURE A.12. As secretases with functionality similiar to metalloproteases, serine proteases potentially play a role in myogenesis. Inactive proteases like *CG17572* (ROSS ET AL. 2003) can play regulatory roles as competitive inhibitors. The deficiency *Df(2L)BSC341* (37B11–37D3) covers *CG17572* and 45 other genes. **A** Late stage 16. The musculature appears mostly normal. **B** Same embryo, different optical section. The gut constrictions are formed, implying that the visceral musculature is normally developed.

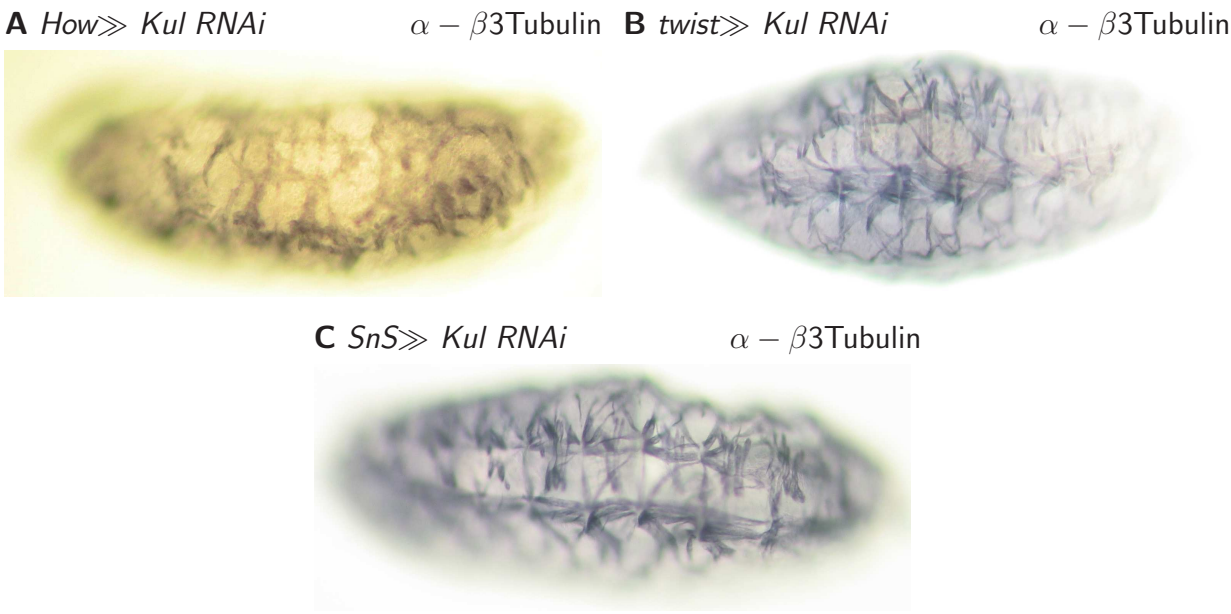

FIGURE A.13. *Kuzbanian-like (Kul)* is one of two *Drosophila* orthologues of the mammalian metalloprotease ADAM10, which among other things cleaves cell adhesion proteins like Cadherins and Ig-Domain proteins in synapses (see f.e. KIM ET AL. 2010). Due to this function of its mammalian orthologue, and due to its mesodermal expression pattern (Detlev Buttgereit, personal communication), *Kul* was selected for further analysis. RNAi knock-down experiments against *Kul*, using the Kul-dsRNA line VDRC 28347 (DIETZL ET AL. 2007), were conducted with various Gal4 drivers. The phenotypes are somewhat variable. **A** Stage 17. *Kul*-RNAi with a *Held-out wings (How)* Gal4-driver can sometimes produce embryos with a disarrayed muscle pattern and reduced muscle mass. **B** Stage 17. *Kul*-RNAi with a *twist* Gal4-driver (TGX). The muscle pattern looks relatively normal; some muscles appear thinner than usual. **C** Stage 17. *Kul*-RNAi with a *Sticks and Stones (SnS)* Gal4-driver. Some muscles are disoriented; many muscles are thinner than usual, verging towards a "mini muscle" phenotype.

A *Df(3R)BSC846* $\alpha - \beta$3Tubulin **B** *Df(3R)01215* $\alpha - \beta$3Tubulin

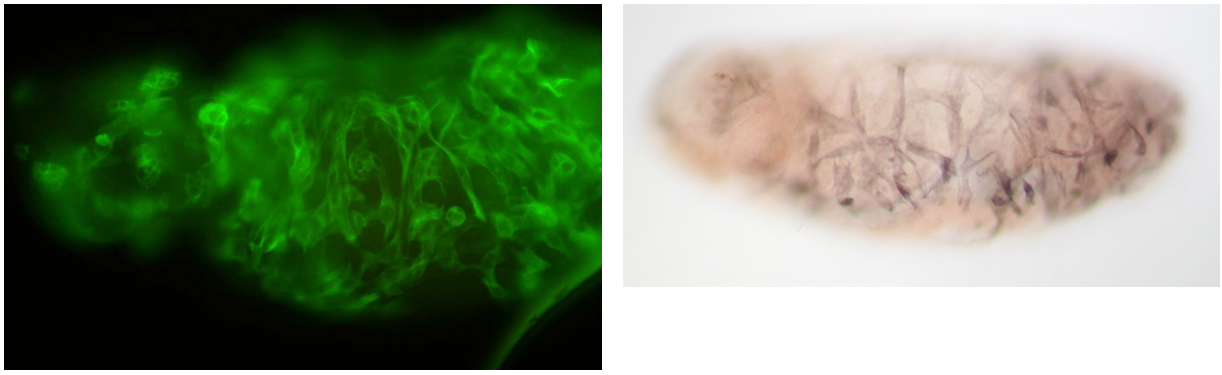

FIGURE A.14. RNAi knock-down experiments against *Kul* have shown light muscle phenotypes, so deficiencies that cover *Kul* are analyzed for their muscle phenotype. **A** Stage 15(?). The deficiency *Df(3R)BSC846* (99A1–99B10) covers *Kul* and about 75 other genes. Its musculature lacks any pattern; many of the β3Tubulin-positive cells are not recognizable as muscle cells. **B** Stage 17(?). The deficiency Df(3R)01215 (99A6–99C1) covers *Kul* and about 80 other genes. The somatic musculature is somewhat reduced in mass; the remaining muscles are disoriented.

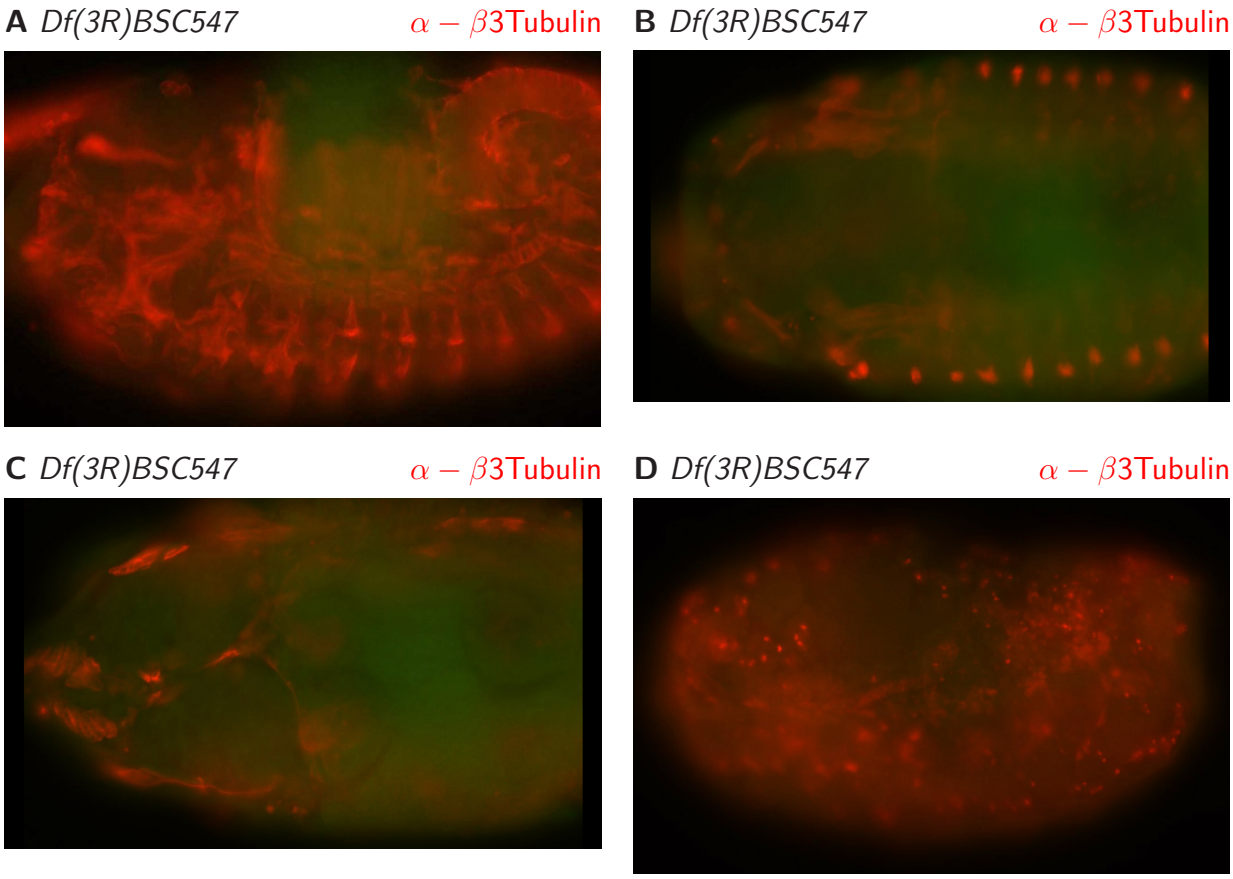

FIGURE A.15. RNAi knock-down experiments against *Kul* have shown light muscle phenotypes, so deficiencies that cover *Kul* are analyzed for their muscle phenotype with an anti-β3Tubulin stain. The deficiency Df(3R)BSC547 covers *Kuzbanian-like (Kul)* and about 45 other genes. The phenotype it shows is extremely variable, with the embryos falling roughly into four categories. **A** Lateral view. The musculature is mostly present, but germ band retraction and/or dorsal closue fail. **B** Dorsal view. Few β3Tubulin-positive structures are visible, and fewer can be identified as muscles. The segmental globular structures might be Bolvig's organs. **C** Dorsal view. The pharynx musculature is present, but most other musculature is missing. **D** Nothing besides the dorsoventral axis is recognizable.

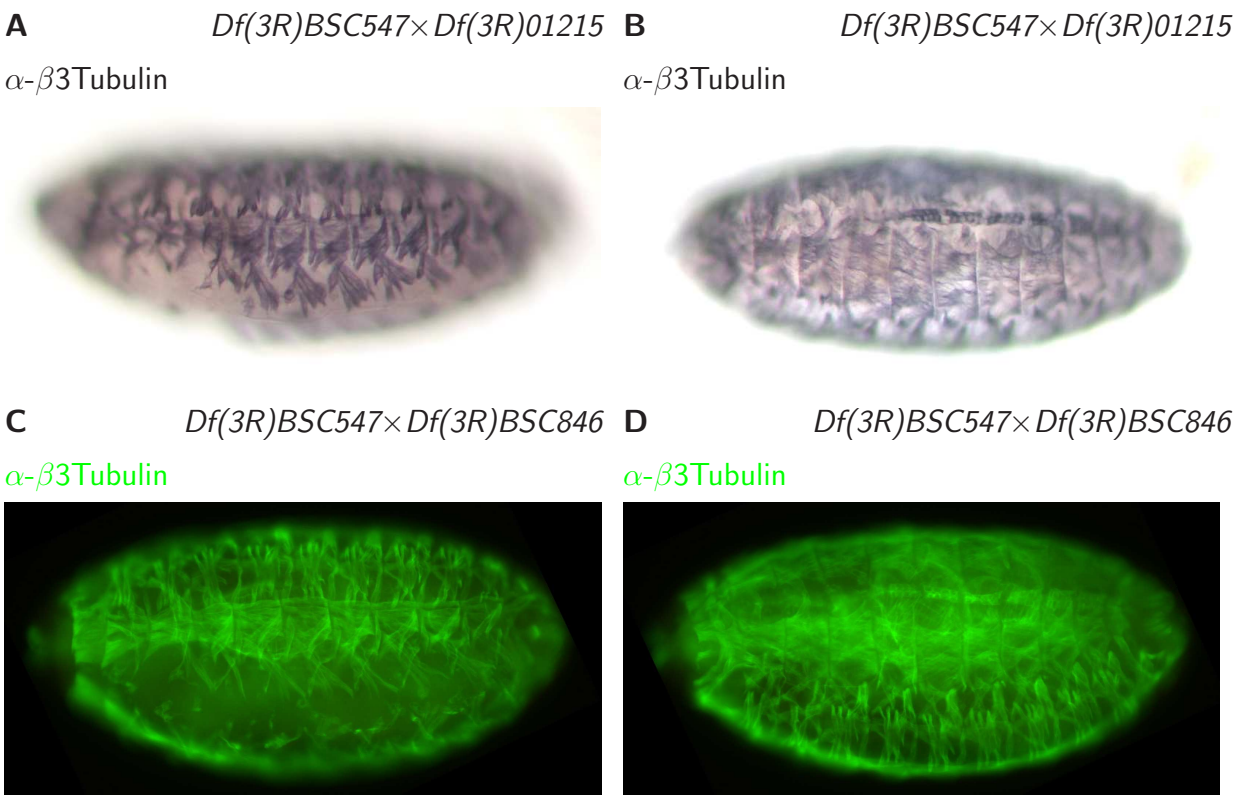

FIGURE A.16. The available deficiencies that cover *Kul* are rather large, deleting a lot of other genes besides *Kul*. Transheterozygous embryos from a crossing of two deficiencies allow to analyze the effect of a smaller deletion. **A** A crossing of the deficiency lines *Df(3R)BSC547* (99B5–99C2) and *Df(3R)01215* (99A6–99C1) yields transheterozygous embryos that are deficient for the chromosomal area 99B5–99C1; this covers *Kul* and about 36 other genes, among them *Cap-D2*. In this lateral view of a stage 16 embryo, the somatic musculature seems normally developed. **B** Same crossing, stage 17, dorsal view. The heart is also normally developed. **C** A crossing of the deficiency lines *Df(3R)BSC547* (99B5–99C2) and *Df(3R)BSC846* (99A1–99B10) yields transheterozygous embryos that are deficient for the chromosomal area 99B5–99B10; this covers *Kul* and about 31 other genes, among them *Cap-D2*. In this stage 17 embryo, the somatic musculature seems normally developed. **D** A different optical section of the same embryo. The heart looks normal.

A *kuz*$^{e29\text{-}4}$ α-β3Tubulin

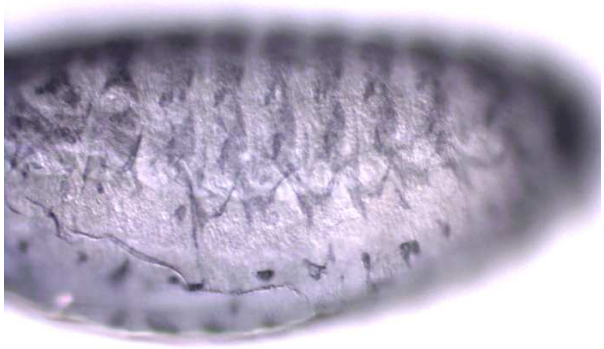

B *kuz*^{3};*Df(3R)BSC846* $\times$ *kuz*^{3};*Df(3R)BSC547*

α-β3Tubulin

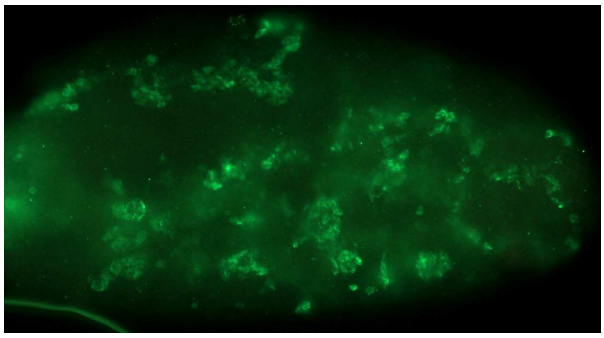

C *kuz*^{3};*Df(3R)BSC846* $\times$ *kuz*^{3};*Df(3R)BSC547*

α-β3Tubulin

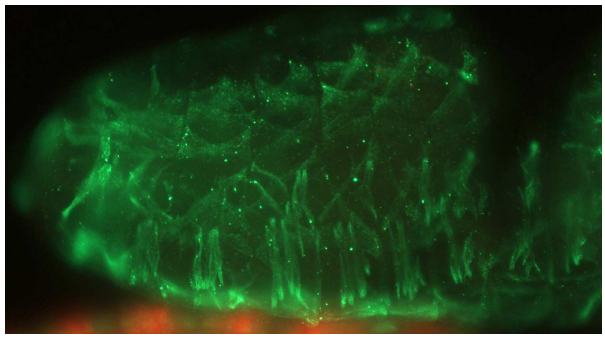

FIGURE A.17. In mammals, the metalloprotease ADAM10 cleaves cell adhesion proteins in synapses (see f.e. KIM ET AL. 2010). This role makes the *Drosophila* orthologues of ADAM10 candidates for a role in myoblast fusion, as this process depends on cell adhesion and involves synapse-like structures. ADAM10 has two *Drosophila* orthologues: *kuzbanian (kuz)* and *Kuzbanian-like (Kul)*. Due to its expression pattern, *kuz* is not a likely candidate for a role in myogenesis; however, metalloproteases often are able to cover for each other, so double mutants might show a phenotype. **A** *kuz*$^{e29\text{-}4}$ is a small deletion that covers the first two exons of *kuz*. The somatic musculature appears to be normally developed. **B** Multiple mutant of *kuz*^{3}, *Kul* and about 31 other genes. *kuz*^{3} is an insertion of a duplicated fragment from the X chromosome into *kuz*; the *Kul* deficiency is a transheterozygous crossing of *Df(3R)BSC846* and *Df(3R)BSC547*. In this embryo, the β3Tubulin-positive cells are not recognizable as muscles. **C** In this stage 16 embryo with the same genotype, the somatic musculature appears mostly normal.

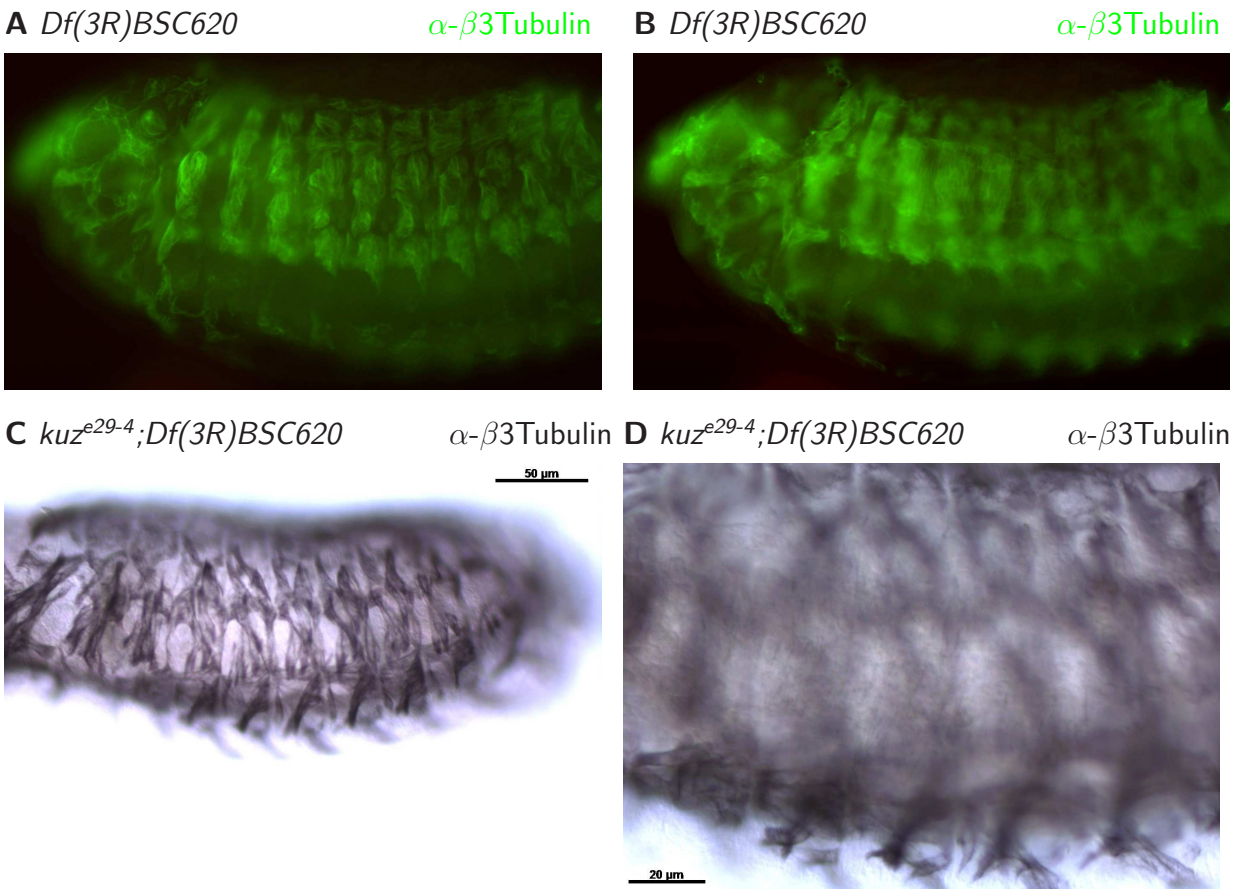

FIGURE A.18. Metalloproteases are a large family of enzymes whose members are often able to functionally replace each other. Because of this, double mutants might show a phenotype where mutations of a single metalloprotease do not. Here, the muscle phenotype of the metalloprotease *tumor necrosis factor alpha—converting enzyme (Tace)* is analyzed with α-β3Tubulin stains. **A** The deficiency *Df(3R)BSC620* (99C5–99D3) covers *Tace* and about 33 other genes. Stage 14. The somatic musculature appears normal. **B** Same embryo, different optical section. The midgut musculature also appears normal. **C** A multiple mutant of $kuz^{e29\text{-}4}$, *Tace* and about 33 other genes. $kuz^{e29\text{-}4}$ is a small deletion that cover the first two exons of *kuz*. Stage 15. The somatic musculature appears normal. **D** Same embryo, higher magnification, different optical section. The circular visceral musculature is present and appears to be normally developed.

A *Df(2R)BSC135* α-β3Tubulin **B** *Df(2R)BSC135* α-β3Tubulin

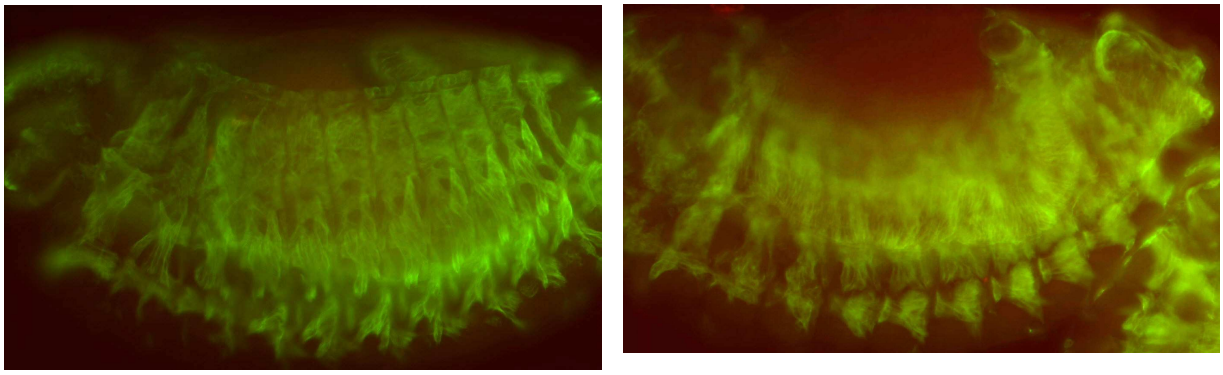

FIGURE A.19. The peptidase *CG9416* is analyzed because of its mesodermal expression pattern. The deficiency *Df(3R)BSC135* (56C11–56D5) covers *CG9416* and about 18 other genes. **A** Stage 15. The somatic musculature is developing normally. **B** Stage 14. The circular visceral musculature is present.

A *Rya-R44F*^{16} α- β3Tubulin

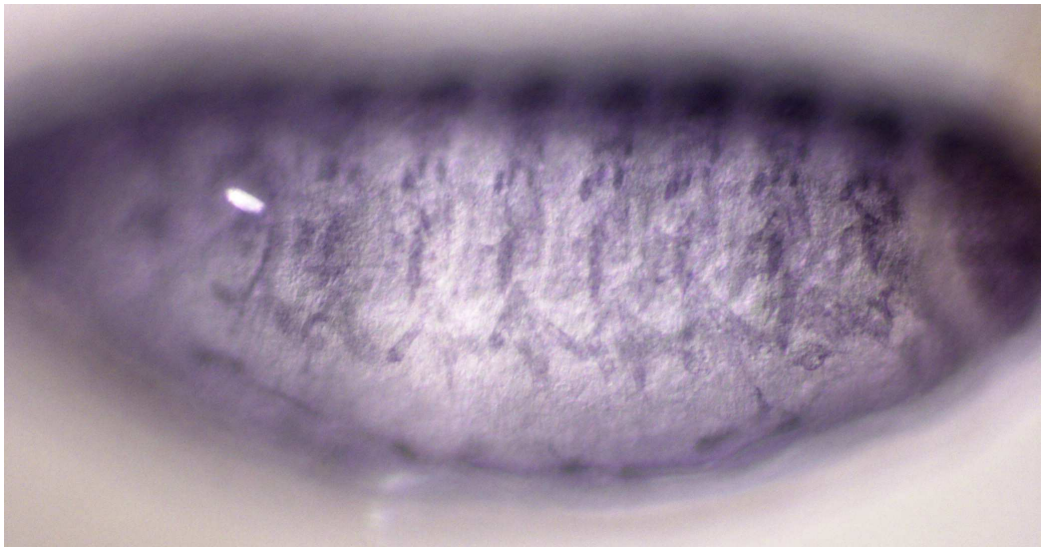

FIGURE A.20. *Ryanodine receptor 44F (Rya-R44F)*, also known as *Ryanodine receptor (RyR)*, is a Calcium channel gene located in chromosomal band 44F, directly downstream of *SnS*. The protein is necessary for muscle contraction (SULLIVAN ET AL. 2000). Many protein components of mature musculature, such as Rols and Titin, also play a role during myogenesis; specifically, the vesicle fusion that occurs during myoblast fusion might be triggered by Rya-R44F controlled Calcium influx. *Rya-R44F* is expressed in myoblasts (HASAN AND ROSBASH 1992).
The mutant *Rya-R44F*^{16} is a jump-out that deletes about 1,8kBP around the first exon. This anti-β3Tubulin stained stage 15 embryo shows a normal somatic musculature.

Appendix B

PCR amplification of the genomic sequence of *barr*

All primer sequences given in 3'–5' direction.

Primers for the upstream half of barr:

barr2F CAT TGC CAT AGT CCA AAG CCT TGG

barr2R GCC AGT GTT GGC AAG AGT CCC

Primers for the downstream half of barr:

barr1F CTC GCA TAT GTA CAG AGT GTA ATC GG

barr1R CGA AGA AGT CAG CGC ATC TGA ATG C

The PCR is conducted in a volume of 25 μl with 0,5 μl of genomic DNA template, 25 pmol of each primer and 1 U of Accuprime DNA polymerase.

Thermocycling sequence:

5 min 94°C

Repeat 3×:

1 min 94°C

2 min 60°C

2 min 68°C

Repeat 35×:

30 s 94°C

30 s 60°C

2 min 68°C

Appendix C

Embryonic developmental stages according to the Atlas of Drosophila Development

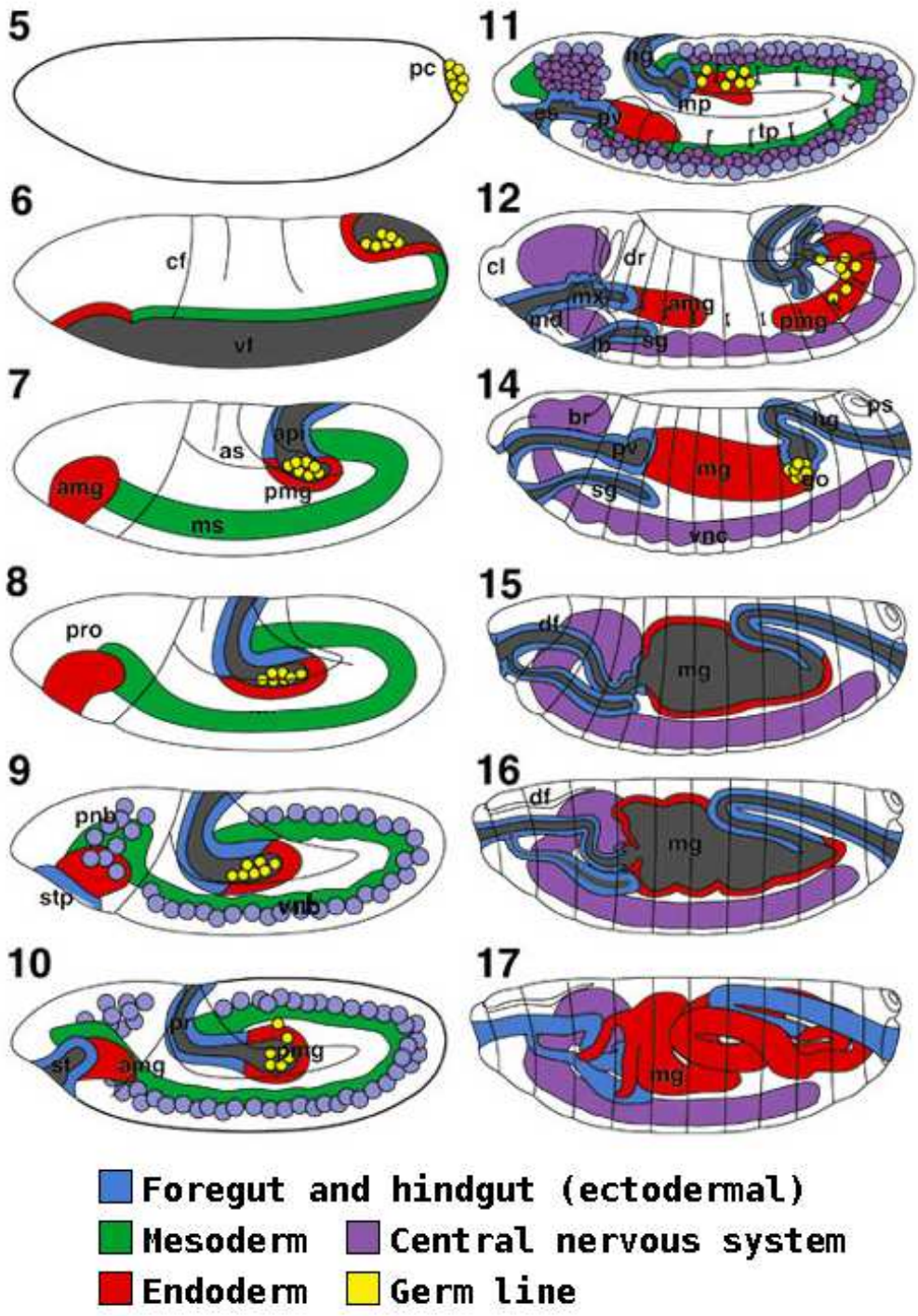

FIGURE C.1. Schematic representation of stages 5 to 17 of *D. melanogaster* embryonic development according to CAMPOS-ORTEGA AND HARTENSTEIN 1985.
Abbreviations: **amg** Anterior midgut rudiment; **br** brain; **cf** cephalic furrow; **cl** clypeolabrum; **df** dorsal fold; **dr** dorsal ridge; **es** esophagus; **go** gonads; **hg** hindgut; **lb** labial bud; **md** mandibular bud; **mg** midgut; **mp** Malpighian tubules; **mx** maxillary bud; **pc** pole cells; **pmg** posterior midgut rudiment; **pnb** procephalic neuroblasts; **pro** procephalon; **ps** posterior spiracle; **po** proventriculus; **sg** salivary gland; **stp** stomodeal plate; **st** stomodeum; **tp** tracheal pits; **vf** ventral furrow; **vnb** ventral neuroblasts; **vnc** ventral nerve cord.
Modified from HARTENSTEIN 1993.

Appendix D

Abbreviations

D.1 Genetic symbols

ap	*apterous*
asp	*abnormal spindle*
atm (=tefu)	*ataxia telangiectasia mutated*
barr	*barren*
cadN	*cadherin N*
Cap-D2	*Chromosome associated protein D2*
Cap-G	*Chromosome associated protein G*
Cap-H	*Chromosome associated protein H*
CyO	*Curly of Oster*
Cy	*Curly*
da	*daughterless*
Dfd	*Deformed*
dia	*diaphanous*

dpp	*decapentaplegic*
Dr	*Drop*
duf (=kirre)	*dumbfounded*
eve	*even-skipped*
Fab-7	*Frontabdominal-7*
FasIII	*Fasciclin III*
fbl	*fumble*
FM7c	*first chromosome multiply inverted 7c*
fs(1)K10	*female sterile (on first chromosome) K10*
ftz	*fushi tarazu*
glu (=SMC4)	*gluon*
hg	*hindgut*
If	*Irregular facets*
kirre (=duf)	*kin of Irregular Chiasma*
Kr	*Krüppel*
Kul	*Kuzbanian-like*
kuz	*kuzbanian*
l(3)11m-254 (=Medea)	*lethal (on third chromosome) 11m-254*
l(3)7m-62 (=sti)	*lethal (on third chromosome) 7m-62*
lb	*ladybird*
lmd	*lame duck*
l'sc	*lethal of scute*

mcph1	*microcephaly 1*
Mef2	*Myocyte enhancer factor 2*
orc2	*origin recognition complex subunit 2*
ph	*polyhomeotic*
rod	*rough deal*
rols	*rolling pebbles*
rst	*roughest*
Sb	*Stubble*
siz	*schizo (=loner)*
slp	*sloppy-paired*
SMC1	*structural maintainance of chromosomes 1*
SMC2	*structural maintainance of chromosomes 2*
SMC4 (=glu)	*structural maintainance of chromosomes 4*
sns	*sticks and stones*
Sp	*Sternopleural*
sti	*sticky*
TDLZ	*TM3, Sb, Deformed-lacZ*
tefu (=atm)	*telomer fusion*
TFLZ	*TM3, Sb, fushi tarazu-lacZ*
TGX	*twist-Gal4 on X chromosome*
TM2	*Third chromosome multiply inverted 2*
TM3	*Third chromosome multiply inverted 3*

tsr	*twin star*
twi	*twist*
UAS	*Upstream activating sequence*
Ubx	*Ultrabithorax*
vtd	*verthandi*
wasp	*Wiskott-Aldrich syndrome protein*
wg	*wingless*
wip	*Wasp-interacting protein*
w	*white*

D.2 List of species

Caenorhabditis elegans
Drosophila melanogaster
Escherichia coli
Saccharomyces cerevisiae
Schizosaccharomyces pombe
Thermus aquaticus
Xenopus laevis

D.3 List of abbreviations

ADAM	A disintegrin and metalloprotease
ADAM-TS	ADAM - Thrombospondin
bp	base pairs
CID	computed image deconvolution

cns	central nervous system
DAB	3-3-Diaminobenzidine tetrahydrochloride
dd	double distilled
demin.	demineralized
DIC	differential interference contrast
DIG	Digoxigenin
DNA	Deoxyribonucleic acid
dNTP	deoxynucleotide triphosphate
eGFP	enhanced green fluorescent protein
EMS	Ethyl methanesulfonate
et al.	*et alii* (and others)
FuRMAS	Fusion-restricted myogenic adhesive complex
GFP	green fluorescent protein
Ig	Immunoglobin
IgSF	Immunoglobin subfamily
kbp	1000 base pairs
LB	Luria - Bertani
mRNA	messenger ribonucleic acid
n.d.	not determined
OD	optical density
ORF	open reading frame
PCR	polymerase chain reaction

pns	peripheral nervous system
SBM	segmental border muscle
Taq	*Thermus aquaticus*
TEM	transmission electron microscopy
TUNEL	terminal deoxynucleotidyl transferase dUTP nick end labeling
UTR	untranslated region
UV	ultraviolet
v/v	volume of volume
w/v	weight of volume

Bibliography

M. Adams et al. The genome sequence of *Drosophila melanogaster*. *Science*, 287(5461): 2185–95, March 2000. ↑p. 9

A. Akhmedov, C. Frei, M. Tsai-Pflugfelder, B. Kemper, S. Gasser, and R. Jessberger. Structural maintenance of chromosomes protein C-terminal domains bind preferentially to DNA with secondary structure. *The Journal of biological chemistry*, 273(37):24088–94, 1998. ↑p. 33

D. Anderson, A. Losada, H. Erickson, and T. Hirano. Condensin and cohesin display different arm conformations with characteristic hinge angles. *The Journal of cell biology*, 156(3): 419–24, 2002. doi: 10.1083/jcb.200111002. ↑p. 18, 21, 22, 31, 32, 33

K. Anderson and C. Nüsslein-Volhard. Information for the dorsal–ventral pattern of the *Drosophila* embryo is stored as maternal mRNA. *Nature*, 311:223–7, September 1984. ↑p. 11

R. Artero, I. Castanon, and M. Baylies. The immunoglobulin-like protein Hibris functions as a dose-dependent regulator of myoblast fusion and is differentially controlled by Ras and Notch signaling. *Development (Cambridge, England)*, 128(21):4251–64, 2001. ↑p. 11

P. Arumugam, S. Gruber, K. Tanaka, C. Haering, K. Mechtler, and K. Nasmyth. ATP hydrolysis is required for cohesin's association with chromosomes. *Current biology : CB*, 13(22): 1941–53, 2003. ↑p. 34

P. Arumugam, T. Nishino, C. Haering, S. Gruber, and K. Nasmyth. Cohesin's ATPase activity is stimulated by the C-terminal Winged-Helix domain of its kleisin subunit. *Current biology : CB*, 16(20):1998–2008, 2006. doi: 10.1016/j.cub.2006.09.002. ↑p. 34

U. Avirneni-Vadlamudi, K. Galindo, T. Endicott, V. Paulson, S. Cameron, and R. Galindo. *Drosophila* and mammalian models uncover a role for the myoblast fusion gene TANC1 in rhabdomyosarcoma. *The Journal of clinical investigation*, 122(1):403–7, 2012. doi: 10.1172/JCI59877. ↑p. 16

R. Baker and G. Schubiger. Autonomous and nonautonomous Notch functions for embryonic muscle and epidermis development in *Drosophila*. *Development (Cambridge, England)*, 122(2):617–26, 1996. ↑p. 11

F. Bantignies, C. Grimaud, S. Lavrov, M. Gabut, and G. Cavalli. Inheritance of Polycomb-dependent chromosomal interactions in *Drosophila*. *Genes & development*, 17(19):2406–20, 2003. doi: 10.1101/gad.269503. ↑p. 29, 106

M. Bate. The embryonic development of larval muscles in *Drosophila*. *Development (Cambridge, England)*, 110(3):791–804, 1990. ↑p. 13, 14

M. Bate, E. Rushton, and D. Currie. Cells with persistent twist expression are the embryonic precursors of adult muscles in *Drosophila*. *Development (Cambridge, England)*, 113(1): 79–89, 1991. ↑p. 13

C. Bauer, T. Hartl, and G. Bosco. Condensin II promotes the formation of chromosome territories by inducing axial compaction of polyploid interphase chromosomes. *PLoS genetics*, 8(8):e1002873, 2012. doi: 10.1371/journal.pgen.1002873. ↑p. 28

M. Baylies and M. Bate. twist: A myogenic switch in *Drosophila*. *Science (New York, N.Y.)*, 272(5267):1481–4, 1996. ↑p. 11, 55

M. Baylies, M. Bate, and M. Ruiz Gomez. Myogenesis: A view from *Drosophila*. *Cell*, 93(6): 921–7, 1998. ↑p. 12

D. Bazett-Jones, K. Kimura, and T. Hirano. Efficient supercoiling of DNA by a single condensin complex as revealed by electron spectroscopic imaging. *Molecular cell*, 9(6):1183–90, 2002. ↑p. 23

K. Beckett and M. Baylies. 3D analysis of founder cell and fusion competent myoblast arrangements outlines a new model of myoblast fusion. *Developmental biology*, 309(1): 113–25, 2007. doi: 10.1016/j.ydbio.2007.06.024. ↑p. 11

C. Bénard, H. Kébir, S. Takagi, and S. Hekimi. mau-2 acts cell-autonomously to guide axonal migrations in Caenorhabditis elegans. *Development (Cambridge, England)*, 131(23): 5947–58, 2004. doi: 10.1242/dev.01433. ↑p. 36

S. Berger, G. Schäfer, D. Kesper, A. Holz, T. Eriksson, R. Palmer, L. Beck, C. Klämbt, R. Renkawitz-Pohl, and S. Onel. WASP and SCAR have distinct roles in activating the Arp2/3 complex during myoblast fusion. *Journal of cell science*, 121(8):1303–13, 2008. doi: 10.1242/jcs.022269. ↑p. 83

M. Bhat, A. Philp, D. Glover, and H. Bellen. Chromatid segregation at anaphase requires the barren product, a novel chromosome-associated protein that interacts with Topoisomerase II. *Cell*, 87(6):1103–14, 1996. ↑p. 23, 24, 25, 26, 83, 107, 108

R. Birkenbihl and S. Subramani. Cloning and characterization of rad21 an essential gene of Schizosaccharomyces pombe involved in DNA double-strand-break repair. *Nucleic acids research*, 20(24):6605–11, 1992. ↑p. 32

R. Birkenbihl and S. Subramani. The rad21 gene product of Schizosaccharomyces pombe is a nuclear, cell cycle-regulated phosphoprotein. *The Journal of biological chemistry*, 270 (13):7703–11, 1995. ↑p. 32

H. Birnboim and J. Doly. A rapid alkaline extraction procedure for screening recombinant plasmid DNA. *Nucleic acids research*, 7(6):1513–23, 1979. ↑p. 63

J. Boulay, C. Dennefeld, and A. Alberga. The *Drosophila* developmental gene snail encodes a protein with nucleic acid binding fingers. *Nature*, 330:395–8, November 1987. ↑p. 11

B. Bour, M. O'Brien, W. Lockwood, E. Goldstein, R. Bodmer, P. Taghert, S. Abmayr, and H. Nguyen. Drosophila MEF2, a transcription factor that is essential for myogenesis. *Genes & development*, 9(6):730–41, 1995. ↑p. 43

B. Bour, M. Chakravarti, J. West, and S. Abmayr. *Drosophila* SNS, a member of the immunoglobulin superfamily that is essential for myoblast fusion. *Genes & development*, 14(12):1498–511, 2000. ↑p. 11, 14

C. Bourgouin, S. Lundgren, and J. Thomas. Apterous is a *Drosophila* LIM domain gene required for the development of a subset of embryonic muscles. *Neuron*, 9(3):549–61, 1992. ↑p. 109

A. Brand and N. Perrimon. Targeted gene expression as a means of altering cell fates and generating dominant phenotypes. *Development (Cambridge, England)*, 118(2):401–15, 1993. ↑p. 69

D. Breier. A possible involvement of CalpainB in embryonic myogenesis of Drosophila melanogaster. Master's thesis, Philipps-Universität Marburg, 2009. ↑p. 116, 117, 118, 119, 120, 125

J. Broadus, S. Fuerstenberg, and C. Doe. Staufen-dependent localization of prospero mRNA contributes to neuroblast daughter-cell fate. *Nature*, 391(6669):792–5, 1998. doi: 10.1038/35861. ↑p. 104

E. Buff, A. Carmena, S. Gisselbrecht, F. Jiménez, and A. Michelson. Signalling by the *Drosophila* epidermal growth factor receptor is required for the specification and diversification of embryonic muscle progenitors. *Development (Cambridge, England)*, 125 (11):2075–86, 1998. ↑p. 11

J. Buheitel and O. Stemmann. Prophase pathway-dependent removal of cohesin from human chromosomes requires opening of the Smc3-Scc1 gate. *The EMBO journal*, 32(5):666–76, 2013. doi: 10.1038/emboj.2013.7. ↑p. 32, 34

S. Bulchand, S. Menon, S. George, and W. Chia. The intracellular domain of Dumbfounded affects myoblast fusion efficiency and interacts with Rolling pebbles and Loner. *PloS one*, 5(2):e9374, 2010. doi: 10.1371/journal.pone.0009374. ↑p. 14

S. Bullock, D. Zicha, and D. Ish-Horowicz. The *Drosophila* hairy RNA localization signal modulates the kinetics of cytoplasmic mRNA transport. *The EMBO journal*, 22(10): 2484–94, 2003. doi: 10.1093/emboj/cdg230. ↑p. 17, 82

L. Burke, R. Zhang, M. Bartkuhn, V. Tiwari, G. Tavoosidana, S. Kurukuti, C. Weth, J. Leers, N. Galjart, R. Ohlsson, and R. Renkawitz. CTCF binding and higher order chromatin structure of the H19 locus are maintained in mitotic chromatin. *The EMBO journal*, 24 (18):3291–300, 2005. doi: 10.1038/sj.emboj.7600793. ↑p. 36

O. Cabello, E. Eliseeva, W. He, H. Youssoufian, S. Plon, B. Brinkley, and J. Belmont. Cell cycle-dependent expression and nucleolar localization of hCAP-H. *Molecular biology of the cell*, 12(11):3527–37, 2001. ↑p. 27

J. A. Campos-Ortega and V. Hartenstein. *The Embryonic development of Drosophila melanogaster*. Springer-Verlag, Berlin, 1985. ↑p. 137

A. Carhan, K. Tang, C. Shirras, A. Shirras, and R. Isaac. Loss of Angiotensin-converting enzyme-related (ACER) peptidase disrupts night-time sleep in adult *Drosophila melanogaster*. *The Journal of experimental biology*, 214(4):680–6, 2011. doi: 10.1242/jeb.049353. ↑p. 125

A. Carmena, M. Bate, and F. Jiménez. Lethal of scute, a proneural gene, participates in the specification of muscle progenitors during *Drosophila* embryogenesis. *Genes & development*, 9(19):2373–83, 1995. ↑p. 11, 13

A. Carmena, S. Gisselbrecht, J. Harrison, F. Jiménez, and A. Michelson. Combinatorial signaling codes for the progressive determination of cell fates in the *Drosophila* embryonic mesoderm. *Genes & development*, 12(24):3910–22, 1998. ↑p. 11, 13

E. Castellanos, P. Dominguez, and C. Gonzalez. Centrosome dysfunction in *Drosophila* neural stem cells causes tumors that are not due to genome instability. *Current biology : CB*, 18(16):1209–14, 2008. doi: 10.1016/j.cub.2008.07.029. ↑p. 26, 111, 112

K. Chan, M. Roig, B. Hu, F. Beckouët, J. Metson, and K. Nasmyth. Cohesin's DNA exit gate is distinct from its entrance gate and is regulated by acetylation. *Cell*, 150(5):961–74, 2012. doi: 10.1016/j.cell.2012.07.028. ↑p. 32

W. Chao, Y. Murayama, S. MuA+-oz, A. Costa, F. Uhlmann, and M. Singleton. Structural Studies Reveal the Functional Modularity of the Scc2-Scc4 Cohesin Loader. *Cell reports*, 12(5):719–25, 2015. doi: 10.1016/j.celrep.2015.06.071. ↑p. 18

E. Chen and E. Olson. Antisocial, an intracellular adaptor protein, is required for myoblast fusion in *Drosophila*. *Developmental cell*, 1(5):705–15, 2001. ↑p. 14

P. Chetaille, C. Preuss, S. Burkhard, J. Côté, C. Houde, J. Castilloux, J. Piché, N. Gosset, S. Leclerc, F. Wünnemann, M. Thibeault, C. Gagnon, A. Galli, E. Tuck, G. Hickson, N. El Amine, I. Boufaied, E. Lemyre, P. de Santa Barbara, S. Faure, A. Jonzon, M. Cameron, H. Dietz, E. Gallo-McFarlane, D. Benson, C. Moreau, D. Labuda, S. Zhan, Y. Shen, M. Jomphe, S. Jones, J. Bakkers, and G. Andelfinger. Mutations in SGOL1 cause a novel cohesinopathy affecting heart and gut rhythm. *Nature genetics*, 46(11): 1245–9, 2014. doi: 10.1038/ng.3113. ↑p. 38

R. Ciosk, M. Shirayama, A. Shevchenko, T. Tanaka, A. Toth, A. Shevchenko, and K. Nasmyth. Cohesin's binding to chromosomes depends on a separate complex consisting of Scc2 and Scc4 proteins. *Molecular cell*, 5(2):243–54, 2000. ↑p. 18

N. Cobbe, E. Savvidou, and M. Heck. Diverse mitotic and interphase functions of condensins in *Drosophila*. *Genetics*, 172(2):991–1008, 2006. doi: 10.1534/genetics.105.050567. ↑p. 26, 31, 88, 106, 107

P. Coelho, J. Queiroz-Machado, and C. Sunkel. Condensin-dependent localisation of topoisomerase II to an axial chromosomal structure is required for sister chromatid resolution during mitosis. *Journal of cell science*, 116(23):4763–76, 2003. doi: 10.1242/jcs.00799. ↑p. 23, 24, 25

M. Crackower, R. Sarao, G. Oudit, C. Yagil, I. Kozieradzki, S. Scanga, A. Oliveira-dos Santos, J. da Costa, L. Zhang, Y. Pei, J. Scholey, C. Ferrario, A. Manoukian, M. Chappell, P. Backx, Y. Yagil, and J. Penninger. Angiotensin-converting enzyme 2 is an essential regulator of heart function. *Nature*, 417(6891):822–8, 2002. doi: 10.1038/nature00786. ↑p. 125

O. Cuvier and T. Hirano. A role of topoisomerase II in linking DNA replication to chromosome condensation. *The Journal of cell biology*, 160(5):645–55, 2003. doi: 10.1083/jcb.200209023. ↑p. 24, 25

S. Cuylen, J. Metz, and C. Haering. Condensin structures chromosomal DNA through topological links. *Nature structural & molecular biology*, 18(8):894–901, 2011. doi: 10.1038/nsmb.2087. ↑p. 21

R. D'Amato, M. Loughnan, E. Flynn, and J. Folkman. Thalidomide is an inhibitor of angiogenesis. *Proceedings of the National Academy of Sciences of the United States of America*, 91(9):4082–5, 1994. ↑p. 37

C. D'Ambrosio, G. Kelly, K. Shirahige, and F. Uhlmann. Condensin-dependent rDNA decatenation introduces a temporal pattern to chromosome segregation. *Current biology : CB*, 18(14):1084–9, 2008a. doi: 10.1016/j.cub.2008.06.058. ↑p. 25

C. D'Ambrosio, C. Schmidt, Y. Katou, G. Kelly, T. Itoh, K. Shirahige, and F. Uhlmann. Identification of cis-acting sites for condensin loading onto budding yeast chromosomes. *Genes & development*, 22(16):2215–27, 2008b. doi: 10.1101/gad.1675708. ↑p. 21, 27

D. D'Amours, F. Stegmeier, and A. Amon. Cdc14 and condensin control the dissolution of cohesin-independent chromosome linkages at repeated DNA. *Cell*, 117(4):455–69, 2004. ↑p. 25

M. Deardorff, M. Kaur, D. Yaeger, A. Rampuria, S. Korolev, J. Pie, C. Gil-Rodríguez, M. Arnedo, B. Loeys, A. Kline, M. Wilson, K. Lillquist, V. Siu, F. Ramos, A. Musio, L. Jackson, D. Dorsett, and I. Krantz. Mutations in cohesin complex members SMC3 and SMC1A cause a mild variant of cornelia de Lange syndrome with predominant mental retardation. *American journal of human genetics*, 80(3):485–94, 2007. doi: 10.1086/511888. ↑p. 37

K. Dej and A. Spradling. The endocycle controls nurse cell polytene chromosome structure during *Drosophila* oogenesis. *Development (Cambridge, England)*, 126(2):293–303, 1999. ↑p. 28

K. Dej, C. Ahn, and T. Orr-Weaver. Mutations in the *Drosophila* condensin subunit dCAP-G: defining the role of condensin for chromosome condensation in mitosis and gene expression in interphase. *Genetics*, 168(2):895–906, 2004. doi: 10.1534/genetics.104.030908. ↑p. 24, 25, 26, 30, 107, 108

A. Dekanty, L. Barrio, M. Muzzopappa, H. Auer, and M. Milán. Aneuploidy-induced delaminating cells drive tumorigenesis in *Drosophila* epithelia. *Proceedings of the National Academy of Sciences of the United States of America*, 109(50):20549–54, 2012. doi: 10.1073/pnas.1206675109. ↑p. 26, 111, 112

A. Dekanty, L. Barrio, and M. Milán. Contributions of DNA repair, cell cycle checkpoints and cell death to suppressing the DNA damage-induced tumorigenic behavior of *Drosophila* epithelial cells. *Oncogene*, 34(8):978–85, 2015. doi: 10.1038/onc.2014.42. ↑p. 26

S. Denison, E. Käfer, and G. May. Mutation in the bimD gene of Aspergillus nidulans confers a conditional mitotic block and sensitivity to DNA damaging agents. *Genetics*, 134(4):1085–96, 1993. ↑p. 32

R. Dequin, H. Saumweber, and J. Sedat. Proteins shifting from the cytoplasm into the nuclei during early embryogenesis of Drosophila melanogaster. *Developmental biology*, 104(1):37–48, 1984. ↑p. 70

N. Dhanyasi, D. Segal, E. Shimoni, V. Shinder, B. Shilo, K. VijayRaghavan, and E. Schejter. Surface apposition and multiple cell contacts promote myoblast fusion in Drosophila flight muscles. *The Journal of cell biology*, 211(1):191–203, 2015. doi: 10.1083/jcb.201503005. ↑p. 15, 16

G. Dietzl, D. Chen, F. Schnorrer, K. Su, Y. Barinova, M. Fellner, B. Gasser, K. Kinsey, S. Oppel, S. Scheiblauer, A. Couto, V. Marra, K. Keleman, and B. Dickson. A genome-wide transgenic RNAi library for conditional gene inactivation in Drosophila. *Nature*, 448 (7150):151–6, 2007. doi: 10.1038/nature05954. ↑p. 127

S. K. Doberstein, R. D. Fetter, A. Y. Metha, and C. C. Goodman. Genetic analysis of myoblast fusion: *blown fuse* is required for progression beyond the prefusion complex. *J Cell Biol*, 136:1249–1261, 1997. ↑p. 15, 16

D. Dorsett. Cohesin, gene expression and development: Lessons from *Drosophila*. *Chromosome research : an international journal on the molecular, supramolecular and evolutionary aspects of chromosome biology*, 17(2):185–200, 2009. doi: 10.1007/s10577-009-9022-5. ↑p. 35, 88

D. Dorsett, J. Eissenberg, Z. Misulovin, A. Martens, B. Redding, and K. McKim. Effects of sister chromatid cohesion proteins on cut gene expression during wing development in *Drosophila*. *Development (Cambridge, England)*, 132(21):4743–53, 2005. doi: 10.1242/dev.02064. ↑p. 35

C. Dottermusch-Heidel, V. Groth, L. Beck, and S. Önel. The Arf-GEF Schizo/Loner regulates N-cadherin to induce fusion competence of *Drosophila* myoblasts. *Developmental biology*, 368(1):18–27, 2012. doi: 10.1016/j.ydbio.2012.04.031. ↑p. 14

W. Driever and C. Nüsslein-Volhard. A gradient of bicoid protein in *Drosophila* embryos. *Cell*, 54(1):83–93, 1988. ↑p. 104

H. Duan, J. Skeath, and H. Nguyen. *Drosophila* Lame duck, a novel member of the Gli superfamily, acts as a key regulator of myogenesis by controlling fusion-competent myoblast development. *Development (Cambridge, England)*, 128(22):4489–500, 2001. ↑p. 11, 43

I. Duncan. Transvection effects in *Drosophila*. *Annual review of genetics*, 36:521–56, 2002. doi: 10.1146/annurev.genet.36.060402.100441. ↑p. 29

H. Dworak, M. Charles, L. Pellerano, and H. Sink. Characterization of *Drosophila* hibris, a gene related to human nephrin. *Development (Cambridge, England)*, 128(21):4265–76, 2001. ↑p. 11, 14

W. Earnshaw and M. Heck. Localization of topoisomerase II in mitotic chromosomes. *The Journal of cell biology*, 100(5):1716–25, 1985. ↑p. 24

W. Earnshaw and U. Laemmli. Architecture of metaphase chromosomes and chromosome scaffolds. *The Journal of cell biology*, 96(1):84–93, 1983. ↑p. 24

C. Eichinger, A. Kurze, R. Oliveira, and K. Nasmyth. Disengaging the Smc3/kleisin interface releases cohesin from *Drosophila* chromosomes during interphase and mitosis. *The EMBO journal*, 32(5):656–65, 2013. doi: 10.1038/emboj.2012.346. ↑p. 32

B. Estrada, A. Maeland, S. Gisselbrecht, J. Bloor, N. Brown, and A. Michelson. The MARVEL domain protein, Singles Bar, is required for progression past the pre-fusion complex stage of myoblast fusion. *Developmental biology*, 307(2):328–39, 2007. doi: 10.1016/j.ydbio.2007.04.045. ↑p. 16

K. Feng, M. Palfreyman, M. Häsemeyer, A. Talsma, and B. Dickson. Ascending SAG neurons control sexual receptivity of Drosophila females. *Neuron*, 83(1):135–48, 2014. doi: 10.1016/j.neuron.2014.05.017. ↑p. 65

D. Ferrandon, I. Koch, E. Westhof, and C. Nüsslein-Volhard. RNA-RNA interaction is required for the formation of specific bicoid mRNA 3' UTR-STAUFEN ribonucleoprotein particles. *The EMBO journal*, 16(7):1751–8, 1997. doi: 10.1093/emboj/16.7.1751. ↑p. 82

B. Fisher, R. Weiszmann, E. Frise, A. Hammonds, P. Tomancak, A. Beaton, B. Berman, E. Quan, S. Shu, S. Lewis, G. Rubin, C. Barale, E. Laguertas, J. Quinn, A. Ghosh, V. Hartenstein, M. Ashburner, and S. Celniker. BDGP insitu homepage, 2012. URL `http://insitu.fruitfly.org/cgi-bin/ex/insitu.pl`. ↑p. 125

M. Frasch, T. Hoey, C. Rushlow, H. Doyle, and M. Levine. Characterization and localization of the even-skipped protein of Drosophila. *The EMBO journal*, 6(3):749–59, 1987. ↑p. 70

L. Freeman, L. Aragon-Alcaide, and A. Strunnikov. The condensin complex governs chromosome condensation and mitotic transmission of rDNA. *The Journal of cell biology*, 149 (4):811–24, 2000. ↑p. 27

K. Furuya, K. Takahashi, and M. Yanagida. Faithful anaphase is ensured by Mis4, a sister chromatid cohesion molecule required in S phase and not destroyed in G1 phase. *Genes & development*, 12(21):3408–18, 1998. ↑p. 18, 33

R. Gandhi, P. Gillespie, and T. Hirano. Human Wapl is a cohesin-binding protein that promotes sister-chromatid resolution in mitotic prophase. *Current biology : CB*, 16(24):2406–17, 2006. doi: 10.1016/j.cub.2006.10.061. ↑p. 32, 34

S. Gasser, T. Laroche, J. Falquet, E. Boy de la Tour, and U. Laemmli. Metaphase chromosome structure. Involvement of topoisomerase II. *Journal of molecular biology*, 188(4):613–29, 1986. ↑p. 24

M. Gause, Z. Misulovin, A. Bilyeu, and D. Dorsett. Dosage-sensitive regulation of cohesin chromosome binding and dynamics by Nipped-B, Pds5, and Wapl. *Molecular and cellular biology*, 30(20):4940–51, 2010. doi: 10.1128/MCB.00642-10. ↑p. 35

C. Georgias, M. Wasser, and U. Hinz. A basic-helix-loop-helix protein expressed in precursors of *Drosophila* longitudinal visceral muscles. *Mechanisms of development*, 69(1–2):115–24, 1997. ↑p. 78

D. Gerlich, T. Hirota, B. Koch, J. Peters, and J. Ellenberg. Condensin I stabilizes chromosomes mechanically through a dynamic interaction in live cells. *Current biology : CB*, 16(4): 333–44, 2006. doi: 10.1016/j.cub.2005.12.040. ↑p. 24, 35

E. Glynn, P. Megee, H. Yu, C. Mistrot, E. Unal, D. Koshland, J. DeRisi, and J. Gerton. Genome-wide mapping of the cohesin complex in the yeast Saccharomyces cerevisiae. *PLoS biology*, 2(9):E259, 2004. doi: 10.1371/journal.pbio.0020259. ↑p. 35

D. Gogendeau, K. Siudeja, D. Gambarotto, C. Pennetier, A. Bardin, and R. Basto. Aneuploidy causes premature differentiation of neural and intestinal stem cells. *Nature communications*, 6:8894, 2015. doi: 10.1038/ncomms9894. ↑p. 26

K. Gosling, L. Makaroff, A. Theodoratos, Y. Kim, B. Whittle, L. Rui, H. Wu, N. Hong, G. Kennedy, J. Fritz, A. Yates, C. Goodnow, and A. Fahrer. A mutation in a chromosome condensin II subunit, kleisin beta, specifically disrupts T cell development. *Proceedings of the National Academy of Sciences of the United States of America*, 104(30):12445–50, 2007. doi: 10.1073/pnas.0704870104. ↑p. 31

J. Gottesfeld and D. Forbes. Mitotic repression of the transcriptional machinery. *Trends in biochemical sciences*, 22(6):197–202, 1997. ↑p. 30

L. Gramates, S. Marygold, G. dos Santos, J.-M. Urbano, G. Antonazzo, B. Matthews, A. Rey, C. Tabone, M. Crosby, D. Emmert, K. Falls, J. Goodman, Y. Hu, L. Ponting, A. Schroeder, V. Strelets, J. Thurmond, P. Zhou, and the FlyBase Consortium. FlyBase at 25: Looking to the future, 2017. URL `http://flybase.org`. ↑p. 51

S. Gruber, C. Haering, and K. Nasmyth. Chromosomal cohesin forms a ring. *Cell*, 112(6): 765–77, 2003. ↑p. 18, 32, 33

S. Gruber, P. Arumugam, Y. Katou, D. Kuglitsch, W. Helmhart, K. Shirahige, and K. Nasmyth. Evidence that loading of cohesin onto chromosomes involves opening of its SMC hinge. *Cell*, 127(3):523–37, 2006. doi: 10.1016/j.cell.2006.08.048. ↑p. 34

V. Guacci, D. Koshland, and A. Strunnikov. A direct link between sister chromatid cohesion and chromosome condensation revealed through the analysis of MCD1 in S. cerevisiae. *Cell*, 91(1):47–57, 1997. ↑p. 32

O. Hachet and A. Ephrussi. Splicing of oskar RNA in the nucleus is coupled to its cytoplasmic localization. *Nature*, 428(6986):959–63, 2004. doi: 10.1038/nature02521. ↑p. 82

C. Haering, J. Löwe, A. Hochwagen, and K. Nasmyth. Molecular architecture of SMC proteins and the yeast cohesin complex. *Molecular cell*, 9(4):773–88, 2002. ↑p. 18, 31

C. Haering, A. Farcas, P. Arumugam, J. Metson, and K. Nasmyth. The cohesin ring concatenates sister DNA molecules. *Nature*, 454(7202):297–301, 2008. doi: 10.1038/nature07098. ↑p. 32

R. Haeusler, M. Pratt-Hyatt, P. Good, T. Gipson, and D. Engelke. Clustering of yeast tRNA genes is mediated by specific association of condensin with tRNA gene transcription complexes. *Genes & development*, 22(16):2204–14, 2008. doi: 10.1101/gad.1675908. ↑p. 27

K. Hagstrom, V. Holmes, N. Cozzarelli, and B. Meyer. C. elegans condensin promotes mitotic chromosome architecture, centromere organization, and sister chromatid segregation during mitosis and meiosis. *Genes & development*, 16(6):729–42, 2002. doi: 10.1101/gad.968302. ↑p. 24, 25

G. Hallson, M. Syrzycka, S. Beck, J. Kennison, D. Dorsett, S. Page, S. Hunter, R. Keall, W. Warren, H. Brock, D. Sinclair, and B. Honda. The *Drosophila* cohesin subunit Rad21 is a trithorax group (trxG) protein. *Proceedings of the National Academy of Sciences of the United States of America*, 105(34):12405–10, 2008. doi: 10.1073/pnas.0801698105. ↑p. 88

M. Ham, T. Takakuwa, N. Rahadiani, K. Tresnasari, H. Nakajima, and K. Aozasa. Condensin mutations and abnormal chromosomal structures in pyothorax-associated lymphoma. *Cancer science*, 98(7):1041–7, 2007. doi: 10.1111/j.1349-7006.2007.00500.x. ↑p. 31

J. Hamp, A. Löwer, C. Dottermusch-Heidel, L. Beck, B. Moussian, M. Flötenmeyer, and S. Anel. Drosophila Kette coordinates myoblast junction dissolution and the ratio of Scar-to-WASp during myoblast fusion. *Journal of cell science*, 129(18):3426–36, 2016. doi: 10.1242/jcs.175638. ↑p. 15, 16

K. Hara, G. Zheng, Q. Qu, H. Liu, Z. Ouyang, Z. Chen, D. Tomchick, and H. Yu. Structure of cohesin subcomplex pinpoints direct shugoshin-Wapl antagonism in centromeric cohesion. *Nature structural & molecular biology*, 21(10):864–70, 2014. doi: 10.1038/nsmb.2880. ↑p. 32

V. Hartenstein. Atlas of Drosophila Development. In M. Bate and A. M. Arias, editors, *The Development of Drosophila melanogaster*. Cold Spring Harbor Laboratory Press, New York, 1993. URL `http://www.sdbonline.org/sites/fly/atlas/00atlas.htm`. ↑p. 108, 137

T. Hartl, H. Smith, and G. Bosco. Chromosome alignment and transvection are antagonized by condensin II. *Science (New York, N.Y.)*, 322(5906):1384–7, 2008. doi: 10.1126/science.1164216. ↑p. 28, 29

T. Hartman, K. Stead, D. Koshland, and V. Guacci. Pds5p is an essential chromosomal protein required for both sister chromatid cohesion and condensation in Saccharomyces cerevisiae. *The Journal of cell biology*, 151(3):613–26, 2000. ↑p. 32

E. Hartswood, J. Brodie, G. Vendra, I. Davis, and D. Finnegan. RNA:RNA interaction can enhance RNA localization in *Drosophila* oocytes. *RNA (New York, N.Y.)*, 18(4):729–37, 2012. doi: 10.1261/rna.026674.111. ↑p. 82

G. Hasan and M. Rosbash. *Drosophila* homologs of two mammalian intracellular Ca(2+)-release channels: identification and expression patterns of the inositol 1,4,5-triphosphate and the ryanodine receptor genes. *Development (Cambridge, England)*, 116(4):967–75, 1992. ↑p. 133

S. Herzog, S. Nagarkar Jaiswal, E. Urban, A. Riemer, S. Fischer, and S. Heidmann. Functional dissection of the *Drosophila melanogaster* condensin subunit Cap-G reveals its exclusive association with condensin I. *PLoS genetics*, 9(4):e1003463, 2013. doi: 10.1371/journal.pgen.1003463. ↑p. 23

T. Hirano. Condensins: organizing and segregating the genome. *Current biology : CB*, 15(7): R265–75, 2005. doi: 10.1016/j.cub.2005.03.037. ↑p. 18, 23

T. Hirano and T. Mitchison. A heterodimeric coiled-coil protein required for mitotic chromosome condensation in vitro. *Cell*, 79(3):449–58, 1994. ↑p. 18, 31

T. Hirano, R. Kobayashi, and M. Hirano. Condensins, chromosome condensation protein complexes containing XCAP-C, XCAP-E and a Xenopus homolog of the *Drosophila* Barren protein. *Cell*, 89(4):511–21, 1997. ↑p. 18, 21, 31

Y. Hiraoka, A. Dernburg, S. Parmelee, M. Rykowski, D. Agard, and J. Sedat. The onset of homologous chromosome pairing during *Drosophila melanogaster* embryogenesis. *The Journal of cell biology*, 120(3):591–600, 1993. ↑p. 27

T. Hirota, D. Gerlich, B. Koch, J. Ellenberg, and J. Peters. Distinct functions of condensin I and II in mitotic chromosome assembly. *Journal of cell science*, 117(26):6435–45, 2004. doi: 10.1242/jcs.01604. ↑p. 24

J. Horsfield, S. Anagnostou, J. Hu, K. Cho, R. Geisler, G. Lieschke, K. Crosier, and P. Crosier. Cohesin-dependent regulation of Runx genes. *Development (Cambridge, England)*, 134 (14):2639–49, 2007. doi: 10.1242/dev.002485. ↑p. 36

D. Hudson, P. Vagnarelli, R. Gassmann, and W. Earnshaw. Condensin is required for non-histone protein assembly and structural integrity of vertebrate mitotic chromosomes. *Developmental cell*, 5(2):323–36, 2003. ↑p. 24, 25

T. Hummel, K. Schimmelpfeng, and C. Klämbt. Commissure formation in the embryonic CNS of *Drosophila*. *Dev. Biol.*, 209:381–398, 1999a. ↑p. 53, 83

T. Hummel, K. Schimmelpfeng, and C. Klämbt. Commissure formation in the embryonic CNS of *Drosophila*. *Development*, 126:771–779, 1999b. ↑p. 53, 83

A. Ismat, C. Schaub, I. Reim, K. Kirchner, D. Schultheis, and M. Frasch. HLH54F is required for the specification and migration of longitudinal gut muscle founders from the caudal mesoderm of *Drosophila*. *Development (Cambridge, England)*, 137(18):3107–17, 2010. doi: 10.1242/dev.046573. ↑p. 52, 78

D. Ivanov and K. Nasmyth. A topological interaction between cohesin rings and a circular minichromosome. *Cell*, 122(6):849–60, 2005. doi: 10.1016/j.cell.2005.07.018. ↑p. 18

D. Ivanov, A. Schleiffer, F. Eisenhaber, K. Mechtler, C. Haering, and K. Nasmyth. Eco1 is a novel acetyltransferase that can acetylate proteins involved in cohesion. *Current biology : CB*, 12(4):323–8, 2002. ↑p. 34

O. Iwasaki, A. Tanaka, H. Tanizawa, S. Grewal, and K. Noma. Centromeric localization of dispersed Pol III genes in fission yeast. *Molecular biology of the cell*, 21(2):254–65, 2010. doi: 10.1091/mbc.E09-09-0790. ↑p. 27

O. Iwasaki, H. Tanizawa, K. Kim, Y. Yokoyama, C. Corcoran, A. Tanaka, E. Skordalakes, L. Showe, and K. Noma. Interaction between TBP and Condensin Drives the Organization and Faithful Segregation of Mitotic Chromosomes. *Molecular cell*, 59(5):755–67, 2015. doi: 10.1016/j.molcel.2015.07.007. ↑p. 27, 30

M. Jacobs. Herstellung eines Reportergenkonstruktes zur Überprüfung der Bedeutung des *rolling pebbles*-mRNA-Trailers für die Transkriptlokalisation in Myoblasten und Kartierung der Myogenese-relevanten Mutation auf dem E831-Chromosom von *Drosophila melanogaster*. Diplomarbeit, 2006. Philipps-Universität Marburg. ↑p. 18, 78, 83

T. Jagla, F. Bellard, Y. Lutz, G. Dretzen, M. Bellard, and K. Jagla. ladybird determines cell fate decisions during diversification of Drosophila somatic muscles. *Development (Cambridge, England)*, 125(18):3699–708, 1998. ↑p. 91

H. Jambor, C. Brunel, and A. Ephrussi. Dimerization of oskar 3' UTRs promotes hitchhiking for RNA localization in the *Drosophila* oocyte. *RNA (New York, N.Y.)*, 17(12):2049–57, 2011. doi: 10.1261/rna.2686411. ↑p. 82

E. Joyce, B. Williams, T. Xie, and C. Wu. Identification of genes that promote or antagonize somatic homolog pairing using a high-throughput FISH-based screen. *PLoS genetics*, 8 (5):e1002667, 2012. doi: 10.1371/journal.pgen.1002667. ↑p. 27

E. Joyce, N. Apostolopoulos, B. Beliveau, and C. Wu. Germline progenitors escape the widespread phenomenon of homolog pairing during *Drosophila* development. *PLoS genetics*, 9(12):e1004013, 2013. doi: 10.1371/journal.pgen.1004013. ↑p. 27

S. Kaitna, P. Pasierbek, M. Jantsch, J. Loidl, and M. Glotzer. The aurora B kinase AIR-2 regulates kinetochores during mitosis and is required for separation of homologous Chromosomes during meiosis. *Current biology : CB*, 12(10):798–812, 2002. ↑p. 24

M. Kaur, C. DeScipio, J. McCallum, D. Yaeger, M. Devoto, L. Jackson, N. Spinner, and I. Krantz. Precocious sister chromatid separation (PSCS) in Cornelia de Lange syndrome. *American journal of medical genetics. Part A*, 138(1):27–31, 2005. doi: 10.1002/ajmg.a.30919. ↑p. 37

D. Kesper. Die Analyse der cis-Regulation des *rols*-Gens und die Beteiligung von Rols7 am Aufbau eines podosomenähnlichen adhäsiven Komplexes (PILMAC), der eine zentrale Rolle in der Myoblastenfusion bei *Drosophila melanogaster* einnimmt. Dissertation zur Erlangung des Doktorgrades, 2005. Philipps-Universität Marburg. ↑p. 17, 77, 78, 79

D. Kesper, C. Stute, D. Buttgereit, N. Kreisköther, S. Vishnu, K. Fischbach, and R. Renkawitz-Pohl. Myoblast fusion in *Drosophila melanogaster* is mediated through a fusion-restricted myogenic-adhesive structure (FuRMAS). *Developmental dynamics : an official publication of the American Association of Anatomists*, 236(2):404–15, 2007. doi: 10.1002/dvdy.21035. ↑p. 14, 15

W. Kibbe. OligoCalc: an online oligonucleotide properties calculator. *Nucleic acids research*, 35:W43–6, 2007. doi: 10.1093/nar/gkm234. ↑p. 51

J. Kim, C. Lilliehook, A. Dudak, J. Prox, P. Saftig, H. Federoff, and S. Lim. Activity-dependent alpha-cleavage of nectin-1 is mediated by a disintegrin and metalloprotease 10 (ADAM10). *The Journal of biological chemistry*, 285(30):22919–26, 2010. doi: 10.1074/jbc.M110.126649. ↑p. 127, 131

J. Kim, T. Zhang, N. Wong, N. Davidson, J. Maksimovic, A. Oshlack, W. Earnshaw, P. Kalitsis, and D. Hudson. Condensin I associates with structural and gene regulatory regions in vertebrate chromosomes. *Nature communications*, 4:2537, 2013. doi: 10.1038/ncomms3537. ↑p. 30

S. Kim, K. Shilagardi, S. Zhang, S. Hong, K. Sens, J. Bo, G. Gonzalez, and E. Chen. A critical function for the actin cytoskeleton in targeted exocytosis of prefusion vesicles during myoblast fusion. *Developmental cell*, 12(4):571–86, 2007. doi: 10.1016/j.devcel.2007.02.019. ↑p. 14

K. Kimura, M. Hirano, R. Kobayashi, and T. Hirano. Phosphorylation and activation of 13S condensin by Cdc2 in vitro. *Science (New York, N.Y.)*, 282(5388):487–90, 1998. ↑p. 23

K. Kimura, V. Rybenkov, N. Crisona, T. Hirano, and N. Cozzarelli. 13S condensin actively reconfigures DNA by introducing global positive writhe: implications for chromosome condensation. *Cell*, 98(2):239–48, 1999. ↑p. 23

T. Kitajima, T. Sakuno, K. Ishiguro, S. Iemura, T. Natsume, S. Kawashima, and Y. Watanabe. Shugoshin collaborates with protein phosphatase 2A to protect cohesin. *Nature*, 441 (7089):46–52, 2006. doi: 10.1038/nature04663. ↑p. 32

K. Kocherlakota, J. Wu, J. McDermott, and S. Abmayr. Analysis of the cell adhesion molecule sticks-and-stones reveals multiple redundant functional domains, protein-interaction motifs and phosphorylated tyrosines that direct myoblast fusion in *Drosophila melanogaster*. *Genetics*, 178(3):1371–83, 2008. doi: 10.1534/genetics.107.083808. ↑p. 54

I. Krantz, J. McCallum, C. DeScipio, M. Kaur, L. Gillis, D. Yaeger, L. Jukofsky, N. Wasserman, A. Bottani, C. Morris, M. Nowaczyk, H. Toriello, M. Bamshad, J. Carey, E. Rappaport, S. Kawauchi, A. Lander, A. Calof, H. Li, M. Devoto, and L. Jackson. Cornelia de Lange syndrome is caused by mutations in NIPBL, the human homolog of *Drosophila melanogaster* Nipped-B. *Nature genetics*, 36(6):631–5, 2004. doi: 10.1038/ng1364. ↑p. 37

N. Kreisköther, N. Reichert, D. Buttgereit, A. Hertenstein, K. Fischbach, and R. Renkawitz-Pohl. *Drosophila* rolling pebbles colocalises and putatively interacts with alpha-Actinin and the Sls isoform Zormin in the Z-discs of the sarcomere and with Dumbfounded/Kirre, alpha-Actinin and Zormin in the terminal Z-discs. *Journal of muscle research and cell motility*, 27(1):93–106, 2006. doi: 10.1007/s10974-006-9060-y. ↑p. 16

S. Kueng, B. Hegemann, B. Peters, J. Lipp, A. Schleiffer, K. Mechtler, and J. Peters. Wapl controls the dynamic association of cohesin with chromatin. *Cell*, 127(5):955–67, 2006. doi: 10.1016/j.cell.2006.09.040. ↑p. 32, 34

I. Kulemzina, M. Schumacher, V. Verma, J. Reiter, J. Metzler, A. Failla, C. Lanz, V. Sreedharan, G. Rätsch, and D. Ivanov. Cohesin rings devoid of Scc3 and Pds5 maintain their stable association with the DNA. *PLoS genetics*, 8(8):e1002856, 2012. doi: 10.1371/journal.pgen.1002856. ↑p. 32

T. Kusch and R. Reuter. Functions for *Drosophila* brachyenteron and forkhead in mesoderm specification and cell signalling. *Development (Cambridge, England)*, 126(18):3991–4003, 1999. ↑p. 78

A. Lafont, J. Song, and S. Rankin. Sororin cooperates with the acetyltransferase Eco2 to ensure DNA replication-dependent sister chromatid cohesion. *Proceedings of the National Academy of Sciences of the United States of America*, 107(47):20364–9, 2010. doi: 10.1073/pnas.1011069107. ↑p. 32, 34

A. Lammens, A. Schele, and K. Hopfner. Structural biochemistry of ATP-driven dimerization and DNA-stimulated activation of SMC ATPases. *Current biology : CB*, 14(19):1778–82, 2004. doi: 10.1016/j.cub.2004.09.044. ↑p. 34

V. Larionov, T. Karpova, N. Kouprina, and G. Jouravleva. A mutant of Saccharomyces cerevisiae with impaired maintenance of centromeric plasmids. *Current genetics*, 10 (1):15–20, 1985. ↑p. 18

M. Lawrence, P. Stojanov, C. Mermel, J. Robinson, L. Garraway, T. Golub, M. Meyerson, S. Gabriel, E. Lander, and G. Getz. Discovery and saturation analysis of cancer genes across 21 tumour types. *Nature*, 505(7484):495–501, 2014. doi: 10.1038/nature12912. ↑p. 38

E. Lécuyer, H. Yoshida, N. Parthasarathy, C. Alm, T. Babak, T. Cerovina, T. Hughes, P. Tomancak, and H. Krause. Global analysis of mRNA localization reveals a prominent role in organizing cellular architecture and function. *Cell*, 131(1):174–87, 2007. doi: 10.1016/j.cell.2007.08.003. ↑p. 105

E. Lécuyer, A. Necakov, L. Cáceres, and H. Krause. High-resolution fluorescent in situ hybridization of *Drosophila* embryos and tissues. *CSH protocols*, 2008:pdb.prot5019, 2008. ↑p. 74, 77

J. Lee and T. Orr-Weaver. The molecular basis of sister-chromatid cohesion. *Annual review of cell and developmental biology*, 17:753–77, 2001. doi: 10.1146/annurev.cellbio.17.1.753. ↑p. 34, 88

D. Leiss, U. Hinz, A. Gasch, R. Mertz, and R. Renkawitz-Pohl. Beta 3 tubulin expression characterizes the differentiating mesodermal germ layer during *Drosophila* embryogenesis. *Development (Cambridge, England)*, 104(4):525–31, 1988. ↑p. 43

A. Lengronne, Y. Katou, S. Mori, S. Yokobayashi, G. Kelly, T. Itoh, Y. Watanabe, K. Shirahige, and F. Uhlmann. Cohesin relocation from sites of chromosomal loading to places of convergent transcription. *Nature*, 430(6999):573–8, 2004. doi: 10.1038/nature02742. ↑p. 35

M. Leptin and B. Grunewald. Cell shape changes during gastrulation in *Drosophila*. *Development (Cambridge, England)*, 110(1):73–84, 1990. ↑p. 11

C. Lewis and U. Laemmli. Higher order metaphase chromosome structure: evidence for metalloprotein interactions. *Cell*, 29(1):171–81, 1982. ↑p. 24

P. Li, X. Yang, M. Wasser, Y. Cai, and W. Chia. Inscuteable and Staufen mediate asymmetric localization and segregation of prospero RNA during *Drosophila* neuroblast cell divisions. *Cell*, 90(3):437–47, 1997. ↑p. 104

B. Lilly, S. Galewsky, A. Firulli, R. Schulz, and E. Olson. D-MEF2: a MADS box transcription factor expressed in differentiating mesoderm and muscle cell lineages during *Drosophila* embryogenesis. *Proceedings of the National Academy of Sciences of the United States of America*, 91(12):5662–6, 1994. ↑p. 11

D. L. Lindsley and G. G. Zimm. *The Genome of Drosophila melanogaster*. Academic Press, San Diego, 1992. ↑p. 65

A. Losada. Cohesin in cancer: chromosome segregation and beyond. *Nature reviews. Cancer*, 14(6):389–93, 2014. doi: 10.1038/nrc3743. ↑p. 38

A. Losada, M. Hirano, and T. Hirano. Identification of Xenopus SMC protein complexes required for sister chromatid cohesion. *Genes & development*, 12(13):1986–97, 1998. ↑p. 18, 34

A. Losada, T. Yokochi, R. Kobayashi, and T. Hirano. Identification and characterization of SA/Scc3p subunits in the Xenopus and human cohesin complexes. *The Journal of cell biology*, 150(3):405–16, 2000. ↑p. 32

R. Lupo, A. Breiling, M. Bianchi, and V. Orlando. *Drosophila* chromosome condensation proteins Topoisomerase II and Barren colocalize with Polycomb and maintain Fab-7 PRE silencing. *Molecular cell*, 7(1):127–36, 2001. ↑p. 29, 106

P. MacDonald. bicoid mRNA localization signal: phylogenetic conservation of function and RNA secondary structure. *Development (Cambridge, England)*, 110(1):161–71, 1990. ↑p. 17

P. Macdonald and G. Struhl. cis-acting sequences responsible for anterior localization of bicoid mRNA in *Drosophila* embryos. *Nature*, 336(6199):595–8, 1988. doi: 10.1038/336595a0. ↑p. 17

K. Maeshima and U. Laemmli. A two-step scaffolding model for mitotic chromosome assembly. *Developmental cell*, 4(4):467–80, 2003. ↑p. 24

T. Maqbool and K. Jagla. Genetic control of muscle development: learning from *Drosophila*. *Journal of muscle research and cell motility*, 28(7–8):397–407, 2007. doi: 10.1007/s10974-008-9133-1. ↑p. 10

R. Massarwa, S. Carmon, B. Shilo, and E. Schejter. WIP/WASp-based actin-polymerization machinery is essential for myoblast fusion in *Drosophila*. *Developmental cell*, 12(4): 557–69, 2007. doi: 10.1016/j.devcel.2007.01.016. ↑p. 14

J. Mc Intyre, E. Muller, S. Weitzer, B. Snydsman, T. Davis, and F. Uhlmann. In vivo analysis of cohesin architecture using FRET in the budding yeast Saccharomyces cerevisiae. *The EMBO journal*, 26(16):3783–93, 2007. doi: 10.1038/sj.emboj.7601793. ↑p. 32, 33

T. Melby, C. Ciampaglio, G. Briscoe, and H. Erickson. The symmetrical structure of structural maintenance of chromosomes (SMC) and MukB proteins: long, antiparallel coiled coils, folded at a flexible hinge. *The Journal of cell biology*, 142(6):1595–604, 1998. ↑p. 18

S. Menon and W. Chia. *Drosophila* rolling pebbles: a multidomain protein required for myoblast fusion that recruits D-Titin in response to the myoblast attractant Dumbfounded. *Developmental cell*, 1(5):691–703, 2001. ↑p. 14, 54, 100, 104, 109

S. Menon, Z. Osman, K. Chenchill, and W. Chia. A positive feedback loop between Dumbfounded and Rolling pebbles leads to myotube enlargement in *Drosophila*. *The Journal of cell biology*, 169(6):909–20, 2005. doi: 10.1083/jcb.200501126. ↑p. 104

C. Metz. Chromosome studies on the Diptera. II. The paired association of chromosomes in the Diptera, and its significance. *Journal of Experimental Zoology*, 21(2):213–279, 1916. doi: 10.1002/jez.1400210204. ↑p. 27

C. Michaelis, R. Ciosk, and K. Nasmyth. Cohesins: chromosomal proteins that prevent premature separation of sister chromatids. *Cell*, 91(1):35–45, 1997. ↑p. 18, 32, 33

Z. Misulovin, Y. Schwartz, X. Li, T. Kahn, M. Gause, S. MacArthur, J. Fay, M. Eisen, V. Pirrotta, M. Biggin, and D. Dorsett. Association of cohesin and Nipped-B with transcriptionally active regions of the *Drosophila melanogaster* genome. *Chromosoma*, 117(1): 89–102, 2008. doi: 10.1007/s00412-007-0129-1. ↑p. 35

C. Moore, C. Parkin, Y. Bidet, and P. Ingham. A role for the Myoblast city homologues Dock1 and Dock5 and the adaptor proteins Crk and Crk-like in zebrafish myoblast fusion. *Development (Cambridge, England)*, 134(17):3145–53, 2007. doi: 10.1242/dev.001214. ↑p. 10

K. Mullis, F. Faloona, S. Scharf, R. Saiki, G. Horn, and H. Erlich. Specific enzymatic amplification of DNA in vitro: the polymerase chain reaction. *Cold Spring Harbor symposia on quantitative biology*, 51(1):263–73, 1986. ↑p. 57

A. Musio, A. Selicorni, M. Focarelli, C. Gervasini, D. Milani, S. Russo, P. Vezzoni, and L. Larizza. X-linked Cornelia de Lange syndrome owing to SMC1L1 mutations. *Nature genetics*, 38(5):528–30, 2006. doi: 10.1038/ng1779. ↑p. 37

E. Myers, G. Sutton, A. Delcher, I. Dew, D. Fasulo, M. Flanigan, S. Kravitz, C. Mobarry, K. Reinert, K. Remington, E. Anson, R. Bolanos, H. Chou, C. Jordan, A. Halpern, S. Lonardi, E. Beasley, R. Brandon, L. Chen, P. Dunn, Z. Lai, Y. Liang, D. Nusskern, M. Zhan, Q. Zhang, X. Zheng, G. Rubin, M. Adams, and J. Venter. A whole-genome assembly of *Drosophila*. *Science (New York, N.Y.)*, 287(5461):2196–204, 2000. ↑p. 9

N. Nakazawa, K. Sajiki, X. Xu, A. Villar-Briones, O. Arakawa, and M. Yanagida. RNA pol II transcript abundance controls condensin accumulation at mitotically up-regulated and heat-shock-inducible genes in fission yeast. *Genes to cells : devoted to molecular & cellular mechanisms*, 20(6):481–99, 2015. doi: 10.1111/gtc.12239. ↑p. 27, 30

R. Nativio, K. Wendt, Y. Ito, J. Huddleston, S. Uribe-Lewis, K. Woodfine, C. Krueger, W. Reik, J. Peters, and A. Murrell. Cohesin is required for higher-order chromatin conformation at the imprinted IGF2-H19 locus. *PLoS genetics*, 5(11):e1000739, 2009. doi: 10.1371/journal.pgen.1000739. ↑p. 36

H. Nguyen, R. Bodmer, S. Abmayr, J. McDermott, and N. Spoerel. D-mef2: a *Drosophila* mesoderm-specific MADS box-containing gene with a biphasic expression profile during embryogenesis. *Proceedings of the National Academy of Sciences of the United States of America*, 91(16):7520–4, 1994. ↑p. 11

T. Nishiyama, R. Ladurner, J. Schmitz, E. Kreidl, A. Schleiffer, V. Bhaskara, M. Bando, K. Shirahige, A. Hyman, K. Mechtler, and J. Peters. Sororin mediates sister chromatid cohesion by antagonizing Wapl. *Cell*, 143(5):737–49, 2010. doi: 10.1016/j.cell.2010.10.031. ↑p. 32, 34

K. Noma, H. Cam, R. Maraia, and S. Grewal. A role for TFIIIC transcription factor complex in genome organization. *Cell*, 125(5):859–72, 2006. doi: 10.1016/j.cell.2006.04.028. ↑p. 27

A. Nose, T. Isshiki, and M. Takeichi. Regional specification of muscle progenitors in *Drosophila*: the role of the msh homeobox gene. *Development (Cambridge, England)*, 125(2):215–23, 1998. ↑p. 54, 77

S. Notarnicola, M. McIntosh, and K. Wise. A Mycoplasma hyorhinis protein with sequence similarities to nucleotide-binding enzymes. *Gene*, 97(1):77–85, 1991. ↑p. 18

M. Ocampo-Hafalla and F. Uhlmann. Cohesin loading and sliding. *Journal of cell science*, 124 (5):685–91, 2011. doi: 10.1242/jcs.073866. ↑p. 35

R. Oliveira, S. Heidmann, and C. Sunkel. Condensin I binds chromatin early in prophase and displays a highly dynamic association with *Drosophila* mitotic chromosomes. *Chromosoma*, 116(3):259–74, 2007. doi: 10.1007/s00412-007-0097-5. ↑p. 55, 96

S. Önel and R. Renkawitz-Pohl. FuRMAS: triggering myoblast fusion in *Drosophila*. *Developmental dynamics : an official publication of the American Association of Anatomists*, 238(6):1513–25, 2009. doi: 10.1002/dvdy.21961. ↑p. 15

S. Önel, M. Rust, R. Jacob, and R. Renkawitz-Pohl. Tethering membrane fusion: common and different players in myoblasts and at the synapse. *Journal of neurogenetics*, 28(3): 302–15, 2014. doi: 10.3109/01677063.2014.936014. ↑p. 15

T. Ono, A. Losada, M. Hirano, M. Myers, A. Neuwald, and T. Hirano. Differential contributions of condensin I and condensin II to mitotic chromosome architecture in vertebrate cells. *Cell*, 115(1):109–21, 2003. ↑p. 21, 24

T. Ono, Y. Fang, D. Spector, and T. Hirano. Spatial and temporal regulation of Condensins I and II in mitotic chromosome assembly in human cells. *Molecular biology of the cell*, 15 (7):3296–308, 2004. doi: 10.1091/mbc.E04-03-0242. ↑p. 24

O. Orgil, H. Mor, A. Matityahu, and I. Onn. Identification of a region in the coiled-coil domain of Smc3 that is essential for cohesin activity. *Nucleic acids research*, 44(13):6309–17, 2016. doi: 10.1093/nar/gkw539. ↑p. 38

X. Pan, M. Papasani, Y. Hao, M. Calamito, F. Wei, W. Quinn Iii, A. Basu, J. Wang, S. Hodawadekar, K. Zaprazna, H. Liu, Y. Shi, D. Allman, M. Cancro, and M. Atchison. YY1 controls Igk repertoire and B-cell development, and localizes with condensin on the Igk locus. *The EMBO journal*, 32(8):1168–82, 2013. doi: 10.1038/emboj.2013.66. ↑p. 30

S. Panizza, T. Tanaka, A. Hochwagen, F. Eisenhaber, and K. Nasmyth. Pds5 cooperates with cohesin in maintaining sister chromatid cohesion. *Current Biology*, 10(24):1557–64, 2000. ↑p. 32

V. Parelho, S. Hadjur, M. Spivakov, M. Leleu, S. Sauer, H. Gregson, A. Jarmuz, C. Canzonetta, Z. Webster, T. Nesterova, B. Cobb, K. Yokomori, N. Dillon, L. Aragon, A. Fisher, and M. Merkenschlager. Cohesins functionally associate with CTCF on mammalian chromosome arms. *Cell*, 132(3):422–33, 2008. doi: 10.1016/j.cell.2008.01.011. ↑p. 35, 36

N. Patel, P. Snow, and C. Goodman. Characterization and cloning of fasciclin III: a glycoprotein expressed on a subset of neurons and axon pathways in Drosophila. *Cell*, 48(6):975–88, 1987. ↑p. 44

A. Pauli, F. Althoff, R. Oliveira, S. Heidmann, O. Schuldiner, C. Lehner, B. Dickson, and K. Nasmyth. Cell-type-specific TEV protease cleavage reveals cohesin functions in *Drosophila* neurons. *Developmental cell*, 14(2):239–51, 2008. doi: 10.1016/j.devcel.2007.12.009. ↑p. 35, 88, 111

A. Pauli, J. van Bemmel, R. Oliveira, T. Itoh, K. Shirahige, B. van Steensel, and K. Nasmyth. A direct role for cohesin in gene regulation and ecdysone response in *Drosophila* salivary glands. *Current biology : CB*, 20(20):1787–98, 2010. doi: 10.1016/j.cub.2010.09.006. ↑p. 36, 88

S. Percival, H. Thomas, A. Amsterdam, A. Carroll, J. Lees, H. Yost, and J. Parant. Variations in dysfunction of sister chromatid cohesion in esco2 mutant zebrafish reflect the phenotypic diversity of Roberts syndrome. *Disease models & mechanisms*, 8(8):941–55, 2015. doi: 10.1242/dmm.019059. ↑p. 34

A. Philp. Mitotic sister-chromatid separation: what Drosophila mutants can tell us. *Trends in cell biology*, 8(4):150, 1998. ↑p. 88

G. Ranganayakulu, D. Elliott, R. Harvey, and E. Olson. Divergent roles for NK-2 class homeobox genes in cardiogenesis in flies and mice. *Development (Cambridge, England)*, 125 (16):3037–48, 1998. ↑p. 54

S. Rankin, N. Ayad, and M. Kirschner. Sororin, a substrate of the anaphase-promoting complex, is required for sister chromatid cohesion in vertebrates. *Molecular cell*, 18(2):185–200, 2005. doi: 10.1016/j.molcel.2005.03.017. ↑p. 32

A. Rau, D. Buttgereit, A. Holz, R. Fetter, S. Doberstein, A. Paululat, N. Staudt, J. Skeath, A. Michelson, and R. Renkawitz-Pohl. rolling pebbles (rols) is required in *Drosophila* muscle precursors for recruitment of myoblasts for fusion. *Development (Cambridge, England)*, 128(24):5061–73, 2001. ↑p. 14, 17

J. Rawlings, M. Gatzka, P. Thomas, and J. Ihle. Chromatin condensation via the condensin II complex is required for peripheral T-cell quiescence. *The EMBO journal*, 30(2):263–76, 2011. doi: 10.1038/emboj.2010.314. ↑p. 31

N. Reichert. Entwicklung von Myotuben bei Drosophila melanogaster: Analyse zweier EMS induzierter Mutanten und Protein-Protein Wechselwirkungen zwischen Rolling Pebbles und weiteren fusions-relevaten Proteinen. Dissertation zur Erlangung des Doktorgrades, 2004. Philipps-Universität Marburg. ↑p. 83

I. Reim and M. Frasch. The Dorsocross T-box genes are key components of the regulatory network controlling early cardiogenesis in *Drosophila*. *Development (Cambridge, England)*, 132(22):4911–25, 2005. doi: 10.1242/dev.02077. ↑p. 55

B. Richardson, K. Beckett, S. Nowak, and M. Baylies. SCAR/WAVE and Arp2/3 are crucial for cytoskeletal remodeling at the site of myoblast fusion. *Development (Cambridge, England)*, 134(24):4357–67, 2007. doi: 10.1242/dev.010678. ↑p. 14

V. Riechmann, U. Irion, R. Wilson, R. Grosskortenhaus, and M. Leptin. Control of cell fates and segmentation in the *Drosophila* mesoderm. *Development (Cambridge, England)*, 124(15):2915–22, 1997. ↑p. 11, 12

R. Rollins, P. Morcillo, and D. Dorsett. Nipped-B, a *Drosophila* homologue of chromosomal adherins, participates in activation by remote enhancers in the cut and Ultrabithorax genes. *Genetics*, 152(2):577–93, 1999. ↑p. 35

J. Ross, H. Jiang, M. Kanost, and Y. Wang. Serine proteases and their homologs in the *Drosophila melanogaster* genome: an initial analysis of sequence conservation and phylogenetic relationships. *Gene*, 304:117–31, 2003. ↑p. 126

B. Rowland, M. Roig, T. Nishino, A. Kurze, P. Uluocak, A. Mishra, F. Beckouët, P. Underwood, J. Metson, R. Imre, K. Mechtler, V. Katis, and K. Nasmyth. Building sister chromatid

cohesion: smc3 acetylation counteracts an antiestablishment activity. *Molecular cell*, 33 (6):763–74, 2009. doi: 10.1016/j.molcel.2009.02.028. ↑p. 34

G. Rubin and A. Spradling. Genetic transformation of *Drosophila* with transposable element vectors. *Science (New York, N.Y.)*, 218(4570):348–53, 1982. ↑p. 9, 67

E. Rubio, D. Reiss, P. Welcsh, C. Disteche, G. Filippova, N. Baliga, R. Aebersold, J. Ranish, and A. Krumm. CTCF physically links cohesin to chromatin. *Proceedings of the National Academy of Sciences of the United States of America*, 105(24):8309–14, 2008. doi: 10.1073/pnas.0801273105. ↑p. 36

A. Rudolf, D. Buttgereit, M. Jacobs, G. Wolfstetter, D. Kesper, M. Pütz, S. Berger, R. Renkawitz-Pohl, A. Holz, and S. Önel. Distinct genetic programs guide *Drosophila* circular and longitudinal visceral myoblast fusion. *BMC cell biology*, 15:27, 2014. doi: 10.1186/1471-2121-15-27. ↑p. 104

M. Ruiz-Gómez, S. Romani, C. Hartmann, H. Jäckle, and M. Bate. Specific muscle identities are regulated by Kruppel during *Drosophila* embryogenesis. *Development (Cambridge, England)*, 124(17):3407–14, 1997. ↑p. 13, 91

M. Ruiz-Gómez, N. Coutts, A. Price, M. Taylor, and M. Bate. *Drosophila* dumbfounded: a myoblast attractant essential for fusion. *Cell*, 102(2):189–98, 2000. ↑p. 14

J. Rusconi and V. Corbin. Evidence for a novel Notch pathway required for muscle precursor selection in *Drosophila*. *Mechanisms of development*, 79(1–2):39–50, 1998. ↑p. 11

E. Rushton, R. Drysdale, S. Abmayr, A. Michelson, and M. Bate. Mutations in a novel gene, myoblast city, provide evidence in support of the founder cell hypothesis for *Drosophila* muscle development. *Development (Cambridge, England)*, 121(7):1979–88, 1995. ↑p. 13

R. Saiki, D. Gelfand, S. Stoffel, S. Scharf, R. Higuchi, G. Horn, K. Mullis, and H. Erlich. Primer-directed enzymatic amplification of DNA with a thermostable DNA polymerase. *Science (New York, N.Y.)*, 239(4839):487–91, 1988. ↑p. 57

N. Saitoh, I. Goldberg, E. Wood, and W. Earnshaw. ScII: an abundant chromosome scaffold protein is a member of a family of putative ATPases with an unusual predicted tertiary structure. *The Journal of cell biology*, 127(2):303–18, 1994. ↑p. 18, 21

Y. Saka, T. Sutani, Y. Yamashita, S. Saitoh, M. Takeuchi, Y. Nakaseko, and M. Yanagida. Fission yeast cut3 and cut14, members of a ubiquitous protein family, are required for chromosome condensation and segregation in mitosis. *The EMBO journal*, 13(20):4938–52, 1994. ↑p. 18, 24

A. Sakai, K. Hizume, T. Sutani, K. Takeyasu, and M. Yanagida. Condensin but not cohesin SMC heterodimer induces DNA reannealing through protein-protein assembly. *The EMBO journal*, 22(11):2764–75, 2003. doi: 10.1093/emboj/cdg247. ↑p. 21, 23, 33

C. Saunders and R. Cohen. The role of oocyte transcription, the 5'UTR, and translation repression and derepression in *Drosophila* gurken mRNA and protein localization. *Molecular cell*, 3(1):43–54, 1999. ↑p. 17

C. Schaaf, Z. Misulovin, G. Sahota, A. Siddiqui, Y. Schwartz, T. Kahn, V. Pirrotta, M. Gause, and D. Dorsett. Regulation of the *Drosophila* Enhancer of split and invected-engrailed gene complexes by sister chromatid cohesion proteins. *PloS one*, 4(7):e6202, 2009. doi: 10.1371/journal.pone.0006202. ↑p. 35, 88

G. Schäfer, S. Weber, A. Holz, S. Bogdan, S. Schumacher, A. Müller, R. Renkawitz-Pohl, and S. Önel. The Wiskott-Aldrich syndrome protein (WASP) is essential for myoblast fusion in *Drosophila*. *Developmental biology*, 304(2):664–74, 2007. doi: 10.1016/j.ydbio.2007.01.015. ↑p. 14, 83

A. Schleiffer, S. Kaitna, S. Maurer-Stroh, M. Glotzer, K. Nasmyth, and F. Eisenhaber. Kleisins: a superfamily of bacterial and eukaryotic SMC protein partners. *Molecular cell*, 11(3):571–5, 2003. ↑p. 18

D. Schmidt, P. Schwalie, C. Ross-Innes, A. Hurtado, G. Brown, J. Carroll, P. Flicek, and D. Odom. A CTCF-independent role for cohesin in tissue-specific transcription. *Genome research*, 20(5):578–88, 2010. doi: 10.1101/gr.100479.109. ↑p. 36

J. Schmitz, E. Watrin, P. Lénárt, K. Mechtler, and J. Peters. Sororin is required for stable binding of cohesin to chromatin and for sister chromatid cohesion in interphase. *Current biology : CB*, 17(7):630–6, 2007. doi: 10.1016/j.cub.2007.02.029. ↑p. 32

O. Schuldiner, D. Berdnik, J. Levy, J. Wu, D. Luginbuhl, A. Gontang, and L. Luo. piggyBac-based mosaic screen identifies a postmitotic function for cohesin in regulating developmental axon pruning. *Developmental cell*, 14(2):227–38, 2008. doi: 10.1016/j.devcel.2007.11.001. ↑p. 36

B. Schüle, A. Oviedo, K. Johnston, S. Pai, and U. Francke. Inactivating mutations in ESCO2 cause SC phocomelia and Roberts syndrome: no phenotype-genotype correlation. *American journal of human genetics*, 77(6):1117–28, 2005. doi: 10.1086/498695. ↑p. 37

K. Schuster, B. Leeke, M. Meier, Y. Wang, T. Newman, S. Burgess, and J. Horsfield. A neural crest origin for cohesinopathy heart defects. *Human molecular genetics*, 24(24):7005–16, 2015. doi: 10.1093/hmg/ddv402. ↑p. 36

K. Sens, S. Zhang, P. Jin, R. Duan, G. Zhang, F. Luo, L. Parachini, and E. Chen. An invasive podosome-like structure promotes fusion pore formation during myoblast fusion. *The Journal of cell biology*, 191(5):1013–27, 2010. doi: 10.1083/jcb.201006006. ↑p. 15, 16

T. Serano and R. Cohen. A small predicted stem-loop structure mediates oocyte localization of *Drosophila* K10 mRNA. *Development (Cambridge, England)*, 121(11):3809–18, 1995. ↑p. 17

K. Shilagardi, S. Li, F. Luo, F. Marikar, R. Duan, P. Jin, J. Kim, K. Murnen, and E. Chen. Actin-propelled invasive membrane protrusions promote fusogenic protein engagement during cell-cell fusion. *Science (New York, N.Y.)*, 340(6130):359–63, 2013. doi: 10.1126/science.1234781. ↑p. 16

K. Shintomi and T. Hirano. Releasing cohesin from chromosome arms in early mitosis: opposing actions of Wapl-Pds5 and Sgo1. *Genes & development*, 23(18):2224–36, 2009. doi: 10.1101/gad.1844309. ↑p. 32, 34

P. Simpson. Maternal-Zygotic Gene Interactions during Formation of the Dorsoventral Pattern in *Drosophila* Embryos. *Genetics*, 105(3):615–32, 1983. ↑p. 11

R. Skibbens, L. Corson, D. Koshland, and P. Hieter. Ctf7p is essential for sister chromatid cohesion and links mitotic chromosome structure to the DNA replication machinery. *Genes & development*, 13(3):307–19, 1999. ↑p. 34

V. Sollars, X. Lu, L. Xiao, X. Wang, M. Garfinkel, and D. Ruden. Evidence for an epigenetic mechanism by which Hsp90 acts as a capacitor for morphological evolution. *Nature genetics*, 33(1):70–4, 2003. doi: 10.1038/ng1067. ↑p. 35

D. Solomon, J. Kim, and T. Waldman. Cohesin gene mutations in tumorigenesis: from discovery to clinical significance. *BMB reports*, 47(6):299–310, 2014. ↑p. 38

M. Somma, B. Fasulo, G. Siriaco, and G. Cenci. Chromosome condensation defects in barren RNA-interfered *Drosophila* cells. *Genetics*, 165(3):1607–11, 2003. ↑p. 24

A. Spradling and G. Rubin. Transposition of cloned P elements into *Drosophila* germ line chromosomes. *Science (New York, N.Y.)*, 218(4570):341–7, 1982. ↑p. 9, 67

B. Srinivas, J. Woo, W. Leong, and S. Roy. A conserved molecular pathway mediates myoblast fusion in insects and vertebrates. *Nature genetics*, 39(6):781–6, 2007. doi: 10.1038/ng2055. ↑p. 10

S. Steffensen, P. Coelho, N. Cobbe, S. Vass, M. Costa, B. Hassan, S. Prokopenko, H. Bellen, M. Heck, and C. Sunkel. A role for *Drosophila* SMC4 in the resolution of sister chromatids in mitosis. *Current biology : CB*, 11(5):295–307, 2001. ↑p. 24, 25

N. Stevens. A study of the germ cells of certain Diptera, with reference to the heterochromosomes and phenomena of synapsis. *Journal of Experimental Zoology*, 5:359–374, 1908. ↑p. 27

T. Strick, T. Kawaguchi, and T. Hirano. Real-time detection of single-molecule DNA compaction by condensin I. *Current biology : CB*, 14(10):874–80, 2004. doi: 10.1016/j.cub.2004.04.038. ↑p. 23

M. Strünkelnberg, B. Bonengel, L. Moda, A. Hertenstein, H. de Couet, R. Ramos, and K. Fischbach. rst and its paralogue kirre act redundantly during embryonic muscle development in *Drosophila*. *Development (Cambridge, England)*, 128(21):4229–39, 2001. ↑p. 14

A. Strunnikov. One-hit wonders of genomic instability. *Cell division*, 5(1):15, 2010. doi: 10.1186/1747-1028-5-15. ↑p. 26, 31, 38

A. Strunnikov, V. Larionov, and D. Koshland. SMC1: an essential yeast gene encoding a putative head-rod-tail protein is required for nuclear division and defines a new ubiquitous protein family. *The Journal of cell biology*, 123(6):1635–48, 1993. ↑p. 18

A. Strunnikov, E. Hogan, and D. Koshland. SMC2, a Saccharomyces cerevisiae gene essential for chromosome segregation and condensation, defines a subgroup within the SMC family. *Genes & development*, 9(5):587–99, 1995. ↑p. 18, 24, 25

K. Sullivan, K. Scott, C. Zuker, and G. Rubin. The ryanodine receptor is essential for larval development in *Drosophila melanogaster*. *Proceedings of the National Academy of Sciences of the United States of America*, 97(11):5942–7, 2000. doi: 10.1073/pnas.110145997. ↑p. 133

T. Sutani and M. Yanagida. DNA renaturation activity of the SMC complex implicated in chromosome condensation. *Nature*, 388(6644):798–801, 1997. doi: 10.1038/42062. ↑p. 23

T. Sutani, T. Yuasa, T. Tomonaga, N. Dohmae, K. Takio, and M. Yanagida. Fission yeast condensin complex: essential roles of non-SMC subunits for condensation and Cdc2 phosphorylation of Cut3/SMC4. *Genes & development*, 13(17):2271–83, 1999. ↑p. 24

T. Sutani, T. Kawaguchi, R. Kanno, T. Itoh, and K. Shirahige. Budding yeast Wpl1(Rad61)-Pds5 complex counteracts sister chromatid cohesion-establishing reaction. *Current biology : CB*, 19(6):492–7, 2009. doi: 10.1016/j.cub.2009.01.062. ↑p. 34

S. Takagi, C. Bénard, J. Pak, D. Livingstone, and S. Hekimi. Cellular and axonal migrations are misguided along both body axes in the maternal-effect mau-2 mutants of Caenorhabditis elegans. *Development (Cambridge, England)*, 124(24):5115–26, 1997. ↑p. 36

G. Thio, R. Ray, G. Barcelo, and T. Schüpbach. Localization of gurken RNA in *Drosophila* oogenesis requires elements in the 5' and 3' regions of the transcript. *Developmental biology*, 221(2):435–46, 2000. doi: 10.1006/dbio.2000.9690. ↑p. 17

B. Thisse, C. Stoetzel, C. Gorostiza-Thisse, and F. Perrin-Schmitt. Sequence of the twist gene and nuclear localization of its protein in endomesodermal cells of early *Drosophila* embryos. *The EMBO journal*, 7(7):2175–83, 1988. ↑p. 11

V. Tixier, L. Bataillé, and K. Jagla. Diversification of muscle types: recent insights from *Drosophila*. *Experimental cell research*, 316(18):3019–27, 2010. doi: 10.1016/j.yexcr.2010.07.013. ↑p. 11, 13

D. Tomkins and J. Sisken. Abnormalities in the cell-division cycle in Roberts syndrome fibroblasts: a cellular basis for the phenotypic characteristics? *American journal of human genetics*, 36(6):1332–40, 1984. ↑p. 37

B. Tomson, D. D'Amours, B. Adamson, L. Aragon, and A. Amon. Ribosomal DNA transcription-dependent processes interfere with chromosome segregation. *Molecular and cellular biology*, 26(16):6239–47, 2006. doi: 10.1128/MCB.00693-06. ↑p. 25

E. Tonkin, T. Wang, S. Lisgo, M. Bamshad, and T. Strachan. NIPBL, encoding a homolog of fungal Scc2-type sister chromatid cohesion proteins and fly Nipped-B, is mutated in Cornelia de Lange syndrome. *Nature genetics*, 36(6):636–41, 2004. doi: 10.1038/ng1363. ↑p. 37

A. Tóth, R. Ciosk, F. Uhlmann, M. Galova, A. Schleiffer, and K. Nasmyth. Yeast cohesin complex requires a conserved protein, Eco1p(Ctf7), to establish cohesion between sister chromatids during DNA replication. *Genes & development*, 13(3):320–33, 1999. ↑p. 18, 32, 33, 34

M. Trimborn, D. Schindler, H. Neitzel, and T. Hirano. Misregulated chromosome condensation in MCPH1 primary microcephaly is mediated by condensin II. *Cell cycle (Georgetown, Tex.)*, 5(3):322–6, 2006. ↑p. 31

F. Uhlmann, D. Wernic, M. Poupart, E. Koonin, and K. Nasmyth. Cleavage of cohesin by the CD clan protease separin triggers anaphase in yeast. *Cell*, 103(3):375–86, 2000. ↑p. 34

R. Uzbekov, E. Timirbulatova, E. Watrin, F. Cubizolles, D. Ogereau, P. Gulak, V. Legagneux, V. Polyakov, K. Le Guellec, and I. Kireev. Nucleolar association of pEg7 and XCAP-E, two members of Xenopus laevis condensin complex in interphase cells. *Journal of cell science*, 116(9):1667–78, 2003. ↑p. 27

V. Van De Bor, E. Hartswood, C. Jones, D. Finnegan, and I. Davis. gurken and the I factor retrotransposon RNAs share common localization signals and machinery. *Developmental cell*, 9(1):51–62, 2005. doi: 10.1016/j.devcel.2005.04.012. ↑p. 17

N. Vargesson. Thalidomide-induced teratogenesis: history and mechanisms. *Birth defects research. Part C, Embryo today : reviews*, 105(2):140–56, 2015. doi: 10.1002/bdrc.21096. ↑p. 37

H. Vega, Q. Waisfisz, M. Gordillo, N. Sakai, I. Yanagihara, M. Yamada, D. van Gosliga, H. Kayserili, C. Xu, K. Ozono, E. Jabs, K. Inui, and H. Joenje. Roberts syndrome is caused by mutations in ESCO2, a human homolog of yeast ECO1 that is essential for the establishment of sister chromatid cohesion. *Nature genetics*, 37(5):468–70, 2005. doi: 10.1038/ng1548. ↑p. 37

F. Verná, R. Gandhi, M. Goldberg, and M. Gatti. Genetic and molecular analysis of wings apart-like (wapl), a gene controlling heterochromatin organization in *Drosophila melanogaster*. *Genetics*, 154(4):1693–710, 2000. ↑p. 32

I. Waizenegger, S. Hauf, A. Meinke, and J. Peters. Two distinct pathways remove mammalian cohesin from chromosome arms in prophase and from centromeres in anaphase. *Cell*, 103(3):399–410, 2000. ↑p. 34

M. Wakelam. The fusion of myoblasts. *The Biochemical journal*, 228(1):1–12, 1985. ↑p. 10

B. Wang, P. Butylin, and A. Strunnikov. Condensin function in mitotic nucleolar segregation is regulated by rDNA transcription. *Cell cycle (Georgetown, Tex.)*, 5(19):2260–7, 2006. doi: 10.4161/cc.5.19.3292. ↑p. 25

X. Wang and W. Dai. Shugoshin, a guardian for sister chromatid segregation. *Experimental cell research*, 310(1):1–9, 2005. doi: 10.1016/j.yexcr.2005.07.018. ↑p. 32

E. Watrin, A. Schleiffer, K. Tanaka, F. Eisenhaber, K. Nasmyth, and J. Peters. Human Scc4 is required for cohesin binding to chromatin, sister-chromatid cohesion, and mitotic progression. *Current biology : CB*, 16(9):863–74, 2006. doi: 10.1016/j.cub.2006.03.049. ↑p. 18, 33

K. Weigmann, R. Klapper, T. Strasser, C. Rickert, G. Technau, H. Jäckle, W. Janning, and C. Klämbt. FlyMove - a new way to look at development of *Drosophila*, 2003. URL `http://flymove.uni-muenster.de`. ↑p. 51, 108

S. Weitzer, C. Lehane, and F. Uhlmann. A model for ATP hydrolysis-dependent binding of cohesin to DNA. *Current biology : CB*, 13(22):1930–40, 2003. ↑p. 34

J. Wells, T. Gligoris, K. Nasmyth, and J. Marsh. Evolution of condensin and cohesin complexes driven by replacement of Kite by Hawk proteins. *Current biology : CB*, 27(1):R17–R18, 2017. doi: 10.1016/j.cub.2016.11.050. ↑p. 18

K. Wendt, K. Yoshida, T. Itoh, M. Bando, B. Koch, E. Schirghuber, S. Tsutsumi, G. Nagae, K. Ishihara, T. Mishiro, K. Yahata, F. Imamoto, H. Aburatani, M. Nakao, N. Imamoto, K. Maeshima, K. Shirahige, and J. Peters. Cohesin mediates transcriptional insulation by CCCTC-binding factor. *Nature*, 451(7180):796–801, 2008. doi: 10.1038/nature06634. ↑p. 36

H. Xing, D. Wilkerson, C. Mayhew, E. Lubert, H. Skaggs, M. Goodson, Y. Hong, O. Park-Sarge, and K. Sarge. Mechanism of hsp70i gene bookmarking. *Science (New York, N.Y.)*, 307(5708):421–3, 2005. doi: 10.1126/science.1106478. ↑p. 30

H. Xing, N. Vanderford, and K. Sarge. The TBP-PP2A mitotic complex bookmarks genes by preventing condensin action. *Nature cell biology*, 10(11):1318–23, 2008. doi: 10.1038/ncb1790. ↑p. 30, 107

D. Yamashita, K. Shintomi, T. Ono, I. Gavvovidis, D. Schindler, H. Neitzel, M. Trimborn, and T. Hirano. MCPH1 regulates chromosome condensation and shaping as a composite modulator of condensin II. *The Journal of cell biology*, 194(6):841–54, 2011. doi: 10.1083/jcb.201106141. ↑p. 31

F. Yeong, H. Hombauer, K. Wendt, T. Hirota, I. Mudrak, K. Mechtler, T. Loregger, A. Marchler-Bauer, K. Tanaka, J. Peters, and E. Ogris. Identification of a subunit of a novel Kleisin-beta/SMC complex as a potential substrate of protein phosphatase 2A. *Current biology : CB*, 13(23):2058–64, 2003. ↑p. 21

S. Yoshimura, K. Hizume, A. Murakami, T. Sutani, K. Takeyasu, and M. Yanagida. Condensin architecture and interaction with DNA: regulatory non-SMC subunits bind to the head of SMC heterodimer. *Current biology : CB*, 12(6):508–13, 2002. ↑p. 18, 21, 23, 33

J. Zhang, X. Shi, Y. Li, B. Kim, J. Jia, Z. Huang, T. Yang, X. Fu, S. Jung, Y. Wang, P. Zhang, S. Kim, X. Pan, and J. Qin. Acetylation of Smc3 by Eco1 is required for S phase sister chromatid cohesion in both human and yeast. *Molecular cell*, 31(1):143–51, 2008. doi: 10.1016/j.molcel.2008.06.006. ↑p. 34

R. Zhang, L. Burke, J. Rasko, V. Lobanenkov, and R. Renkawitz. Dynamic association of the mammalian insulator protein CTCF with centrosomes and the midbody. *Experimental cell research*, 294(1):86–93, 2004. doi: 10.1016/j.yexcr.2003.11.015. ↑p. 36

Acknowledgements

This work would not have been possible without:

- Prof. Dr. Renate Renkawitz-Pohl, the supervisor and reviewer of this thesis, who conceived part of the presented projects and made this thesis possible with having me in her research group
- Prof. Dr. Christian Bökel, the second reviewer of this thesis
- Dr. Detlev Buttgereit, who planned the early stages of the projects presented in this thesis, helped out with advice in countless cases and made the PCR experiments possible with his suggestions
- Dörthe Kesper, on whose work on *rols* mine is based
- Nina Reichert, who conducted an initial analysis of the mutant E831, laying the foundations for my work on Condensin
- Dr. Stefan Heidmann, who sent me his barr-eGFP rescue construct fly stocks, which became a key stone for this study
- Prof. Dr. Hugo Bellen and Karen Schulze, who generously sent me the anti-Barr antibody described in the groundbreaking work of Bhat et al.
- Prof. Dr. Benny Shilo and Shari Carmon, who generously sent me the anti-Kul antibody and Kul-HA rescue construct generated in their laboratory
- Ruth Hyland, always willing to help with advice on fly work, who conducted the microinjections for this study
- Sabina Huhn, Nadine Müller, Ljubinka Cigoja, Angela Zimmer and our other technicians, who keep the lab running

- Inge Simon, who cooks tons of culture media and cleans millions of laboratory dishes
- Katja Gessner, whose organisational work is indispensable, and whose seminars on image processing and graphical design helped me to create the figures in this thesis and so many other things
- Christina, Susanne, Roxane and Christiana, who provided advice in countless meetings
- Andreas, Angela, Bettina, Birgit, Bridlin, Carina, David, Detlev's Angels Jessi, Chrissi and Anja, Ina, Kathi, Katja L., Lisa, Loreen, Maik, Martin, Michael, Nicola, Nina, Silke, Sophie, Stefanie, Stephan, Susanne B., Tatjana, Tim, Verena, Zeynep,
  whose advice, support and companionship were an invaluable help and whose names evoke fond memories upon writing
- Monika and Peter, who unintentionally raised me to be a biologist
- Angelika, Erich and Effi, who gracefully put up with all my moanings
- the many people whom I probably forgot to mention here
- my mentor, commander, friend, therapist and cat Tori

To all of them go my deepest thanks.

Stocks obtained from the Bloomington Drosophila Stock Center (NIH P40OD018537) were used in this study.
Additional transgenic fly stocks were obtained from the Vienna Drosophila Resource Center (VDRC, `www.vdrc.at`).
This work was supported by the DFG grant RE628/15-2.

Erklärung

Ich versichere, dass ich meine Dissertation

Intracellular *rols7* mRNA localization and the importance of Barren for mitosis in the embryonic myogenesis of *Drosophila melanogaster*

selbständig, ohne unerlaubte Hilfe angefertigt und mich dabei keiner anderen als der von mir ausdrücklich angegebenen Quellen und Hilfen bedient habe.

Die vorliegende Dissertation wurde in ihrer jetzigen oder einer ähnlichen Form noch bei keiner anderen Hochschule eingereicht und hat noch keinen sonstigen Prüfungszwecken gedient.

Marburg, den Matthias Philipp Florian Jacobs

Akademischer Werdegang

— Diese Seiten enthalten persönliche Daten und sind deshalb nicht Teil der Online-Publikation —